POLITECNICO DI MILANO

Scuola di Ingegneria Industriale e dell'Informazione

Dipartimento di Ingegneria Energetica

In collaborazione con:

UNIVERSITY OF WATERLOO

Department of Mechanical and Mechatronics Engineering

FIVE HOLE PRESSURE PROBE FOR LOCAL INFLOW STUDY ON A HORIZONTAL AXIS WIND TURBINE

Relatore: Prof. Paolo SILVA

Co-Relatore: Prof. David A. JOHNSON

Tesi di Laurea Magistrale di:

Andrea Moscardi, matr. 800757

Anno Accademico 2013/2014

Acknowledgements

Extended Summary

Lo scopo della tesi era quello di investigare le possibili metodologie da usare per la determinazione delle caratteristiche di afflusso locali alla pala di una turbina eolica ad asse orizzontale di piccola taglia (3m di diametro). L'applicabilità di una sonda di pressione multi foro è stata studiata per questo scopo, vedere sezione 2.1 per spiegazione dettagliata dei principi di funzionamento della sonda.

L'importanza dello studio è legata alla fase di progettazione delle turbine eoliche ad asse orizzontale. Queste sono generalmente progettate con un approccio 2D e stazionario, tuttavia, è stato dimostrato, come le reali condizioni di afflusso alla pala durante l'operazione della turbina siano altamente 3D e non stazionarie. Sufficienti misurazioni sperimentali non sono disponibili per creare e validare modelli aerodinamici per predire gli effetti di tali condizioni di afflusso 3D sulla struttura della turbina stessa.

E' risaputo che in condizioni operative una turbina eolica è soggetta, per la maggior parte del tempo, ai cosiddetti "yaw loads", gli "yaw loads" sono qualsiasi situazione in cui la pala incontra una velocità e direzione di afflusso non uniforme durante la sua rotazione, vedi Figure 0.1 per tipici esempi di "yaw loads". Questo risulta in carichi variabili, che, presentano usualmente una frequenza uguale a quella di rotazione del rotore della turbina. Gli "yaw loads" devono essere considerati durante la fase di progetto siccome gli sforzi sulla struttura della turbina eolica possono risultare essere molto differenti rispetto a quelli predetti con il tradizionale metodo 2D BEM (Blade Element Momentum). Per questo, dei larghi margini di sicurezza vengono di solito impiegati, risultando in un maggiore impiego di materiali, che quindi si rispecchia in costi più elevati.

Gli obiettivi principali del lavoro di tesi possono essere essenzialmente riassunti in due punti:

- Primo, studiare la sonda di Pitot a cinque fori come una possibile soluzione per determinare le condizioni locali di incidenza del flusso d'aria, calibrare sperimentalmente lo strumento e determinare le migliori pratiche per l'applicazione di questo a una turbina eolica di piccola taglia.

- Secondo, progettare una nuova sezione di pala e il sistema di acquisizione dei dati, installare la sonda a cinque fori sulla pala usando la nuova sezione e testare il corretto funzionamento di tutta la strumentazione installata sull'apparato sperimentale, il tutto mantenendosi in un budget il più contenuto possibile.

Calibrazione della sonda

La calibrazione della sonda di Pitot a cinque fori è stata portata a termine con successo sotto tutti i suoi aspetti.

Per effettuare questa fase del progetto è stato necessario progettare e costruire un apposito sistema di posizionamento a due assi, vedi Figure 3.3. Questo apparato permette di posizionare con precisione la sonda sul piano orizzontale e verticale mentre la punta di questa è mantenuta in una posizione costante durante tutta la procedura di calibrazione. Per semplificare il posizionamento della sonda e al tempo stesso minimizzare i tempi di costruzione del sistema di posizionamento è stato deciso di muovere manualmente la sonda sul piano orizzontale, mentre sul piano verticale questa viene posizionata mediante un motore stepper controllato automaticamente con un microcontrollore Arduino.

Al fine di calibrare con accuratezza la sonda, considerando la tabella di marcia molto serrata, sono state prese alcune decisioni per quanto riguarda le condizioni di calibrazione. Come riportato in letteratura (1) (2), il numero di Reynolds ha una piccola influenza sulla calibrazione della sonda, questa influenza può essere minimizzata effettuando la calibrazione allo stesso numero di Reynolds che ci si aspetta di incontrare durante l'effettivo impiego della sonda, per questo la calibrazione è stata effettuata a un unico numero di Reynolds (risultante da una velocità dell'aria durante la calibrazione di 29 m/s). La sonda è stata posizionata in numerose combinazioni di angoli verticali e orizzontali compresi in un range di ±45° con intervalli di 5° tra una posizione e la successiva, questo forma una matrice quadrata di combinazioni di angoli a cui la sonda è stata mossa, Figure 3.1. A causa dell'elevata turbolenza presente nella galleria del vento usata per la calibrazione un alto numero di misurazioni ha dovuto essere rilevato in ogni punto della griglia di calibrazione, questo numero è stato determinato studiando la deviazione standard cumulata di una popolazione di 1000 misurazioni effettuate in diverse posizioni della griglia, 400 sembra essere il numero oltre il quale la deviazione standard si stabilizza a un livello costante, vedere Figure 3.2. Il setup temporaneo della piccola galleria del vento usata per la calibrazione presenta un gomito di 90° a circa 2.8 m a monte dell'efflusso, durante l'analisi dei dati di calibrazione si è scoperto che questo gomito genera una deviazione negativa di 4°

dall'assialità sul piano orizzontale, la correzione di questa deviazione è stata applicata durante la post analisi dei dati.

I dati raccolti durante la calibrazione sono stati analizzati sia visivamente che numericamente e nessuna particolare anomalia è stata riscontrata. La ricerca del miglior metodo per interpolare i dati tra i vari punti di calibrazione ha condotto alla scelta di usare l'interpolazione cubica invece dell'interpolazione polinomiale di quarto grado e dell'interpolazione lineare diretta.

Tre diversi metodi, che necessitano la determinazione di coefficienti di pressione adimensionali, sono stati presi in analisi, vedere sezione 2.1. Un'analisi dell'errore sperimentale ha mostrato che i coefficienti di pressione multi-zona permettono di ottenere risultati più accurati rispetto agli approcci mono-zona ed NREL. L'errore è stato quantificato in 0.3° sul piano verticale, 1° sul piano orizzontale (errore più elevato dovuto al sistema di posizionamento manuale e con più bassa risoluzione) e 0.3% per quanto riguarda la determinazione della velocità, Figure 3.22.

Questo approccio presenta due ulteriori vantaggi rispetto agli altri metodi. In primo luogo permette di estendere il range degli angoli misurabili fino a ±70° rispetto ai ±30°dei coefficienti di pressione mono-zona, questo perché esclude dalla creazione di questi ultimi il foro che si trova sottovento, dove avviene la separazione del flusso, vedere sezione 3.4.2. In secondo luogo rende non più necessario usare la pressione statica del flusso come pressione di riferimento per le misurazioni effettuate con i trasduttori di pressione differenziali collegati ai cinque fori della sonda, basta che questi siano tutti riferiti a un qualsiasi medesimo livello di pressione. Questo è un grosso miglioramento rispetto alla configurazione usata per l'esperimento NREL, dove un complesso sistema di tubazioni era stato realizzato al fine di portare la pressione statica della galleria del vento fino al rotore per essere usata come riferimento, per dettagli vedere sezione 4.4.2.

Sistema di acquisizione dati

L'applicazione di una sonda di Pitot a cinque fori alla pala di una turbina eolica di piccola taglia ha richiesto lo sviluppo di un apposito sistema di acquisizione dei dati. Gli ostacoli principali erano il limitato spazio disponibile e il fatto che non ci fosse la possibilità di una connessione cablata tra il rotore della turbina e il computer principale posizionato nella sala di controllo della galleria del vento. Entrambi questi problemi sono stati risolti con successo. Maggiori dettagli sulla progettazione e la costruzione di questo sistema si possono trovare in sezione 2.3.

L'impossibilità di una comunicazione cablata è stata risolta grazie alla scelta di trasmettere i dati via Bluetooth tra la strumentazione di acquisizione dati sul

rotore e il computer principale. Il Bluetooth si è rivelato una scelta vincente, economica e relativamente facile da implementare.

Le limitazioni spaziali sono state risolte facendo un'accurata selezione dei componenti più minuti disponibili sul mercato che rispettassero le caratteristiche di accuratezza necessarie per un sistema di acquisizione di dati sperimentali. Il risultato di questa selezione è un sistema di acquisizione dati di dimensioni molto contenute, lunghezza 20cm, larghezza 7 cm e spessore minore di 1,5 cm. Questo sistema comprende 5 trasduttori di pressione allocati su un circuito stampato, un chip per la conversione del segnale da analogico a digitale, un microcontrollore Arduino, un sistema di alimentazione autonomo basato su una batteria da 9V, una micro SD per il backup dei dati raccolti e un ricetrasmettitore Bluetooth per inviarli a computer principale.

Lo stesso sistema di acquisizione dei dati che è stato usato per la calibrazione è stato poi installato sul rotore della turbina, questo per ottenere il massimo livello di accuratezza possibile.

Il prezzo complessivo di tutta la strumentazione impiegata per il sistema di acquisizione dei dati è rimasto sotto i 400 CAD (dollari Canadesi), circa 300 €.

Installazione sull'apparato sperimentale

La strumentazione ha successivamente dovuto essere installata sull'apparato sperimentale al fine di essere usata per determinare le condizioni locali da afflusso alla pala. Grazie alla modularità del design della pala solo una delle cinque sezioni che la compongono ha dovuto essere radicalmente ridisegnata. Questa nuova sezione ha dovuto rispettare una serie di stringenti richieste, elencate in seguito.

La nuova sezione della pala è stata progettata in modo che la strumentazione di acquisizione dati posizionata al suo interno fosse facilmente accessibile per poter apportare eventuali piccole modifiche o riparazioni. L'interferenza con il flusso d'aria è stata minimizzata posizionando tutta la strumentazione all'interno del profilo alare, con l'unica eccezione della sonda di Pitot a cinque fori, la cui estremità si trova a una distanza pari a una corda dal bordo di ingresso del profilo. La sezione di pala può essere facilmente installata e rimossa dall'apparato sperimentale ed è stata progettata per non interferire con le misurazioni degli estensimetri ne danneggiarli durante la sua installazione, essendo questi posizionati sul supporto centrale della pala.

Un requisito fondamentale della nuova sezione è la solidità strutturale, necessaria in un ambiente caratterizzato da elevate forze centrifughe e vibrazioni. Questa è stata ottenuta grazie a una ragnatela di sottili supporti interni e dotando il

coperchio di accesso alla strumentazione di tre pilastri di supporto, questi svolgono inoltre la funzione di fissare saldamente il coperchio al resto della pala grazie e sei viti accessibili dalla parte inferiore del profilo, vedere Figure 4.11 e Figure 4.12.

Un design così complesso è stato possibile solo grazie alla stampa 3D, questa si è dimostrata essere la tecnica di prototipazione rapida più adatta per un modello di così elevata complessità.

La sola nuova sezione di pala non era sufficiente a supportare la sonda di Pitot a cinque fori in un ambiente caratterizzato da elevate forze centrifughe e vibrazioni. La sonda di pressione è stata così collegata direttamente al supporto centrale della pala grazie a un sistema di ancoraggio appositamente progettato, vedere Figure 4.14. Questo inclina la sonda a un angolo di 15° rispetto alla corda del profilo, questo è l'angolo d'attacco nominale nella posizione radiale di installazione della sonda, calcolato con una velocità del vento di 8.5 m/s, la velocità media che si intende usare durante i test.

Test

In ultima fase una serie di test è stata effettuata con lo scopo di verificare il corretto funzionamento del sistema e come questo risponda alle severe condizioni dei test a cui sarà sottoposto.

Per prima cosa è stato verificato l'effetto della forza centrifuga e delle vibrazioni sui trasduttori di pressione, l'effetto della forza centrifuga, a 200 RPM, influenza la misurazione della pressione di meno di 1/1000 della misurazione stessa, mentre non è stato riscontrato nessun effetto evidente generato dalle vibrazioni dell'apparato sperimentale sulla deviazione standard della popolazione di dati acquisita, vedere Figure 4.21. Siccome la presa per la pressione di riferimento per i trasduttori differenziali è posizionata nell'hub del rotore, questa pressione è aumentata dalla forza centrifuga che agisce sull'aria presente all'interno del sistema di tubazioni. Questo effetto è stato quantificato essere nell'ordine dei 210 Pa a 200 RPM e può leggermente variare a causa di fattori quali la densità dell'aria e la posizione radiale della sonda. La correzione di questo effetto è stata considerata durante l'analisi dei dati con MatLab™.

Questa fase dei test è inoltre stata di fondamentale importanza per verificare la tenuta strutturale del nuovo design della sezione di pala e il corretto funzionamento del sistema di acquisizione dati. Nessun problema è stato riscontrato nel sistema di misura dopo questa serie di test, le pressioni provenienti dai cinque fori della sonda sono state regolarmente misurate e trasmesse al computer centrale. L'acquisizione dei dati trasmessi al computer principale è stata

effettuata con LabView™, questo software è stato usato per coordinare la lettura delle pressioni con la posizione della pala e in prospettiva potrà essere implementato per raccogliere altre misurazioni quali quelle relative agli sforzi o alla coppia generata.

Una seconda serie di test è stata successivamente effettuata con lo scopo di misurare effettivamente le condizioni di afflusso locale dell'aria alla pala della turbina in condizioni di "yaw loads", questo è lo scopo finale per cui tutta la strumentazione è stata progettata e costruita. I risultati ottenuti in condizioni di "yaw loads" sono stati valutati rispetto a quelli ottenuti con la turbina allineata alla direzione principale del vento. Come ci si aspettava le misurazioni mostrano un andamento periodicamente oscillatorio delle condizioni di afflusso, il periodo di questa oscillazione è effettivamente corrispondente con quello di rotazione della pala, vedere sezione 5.2.4 e 5.2.5. Un'ulteriore conferma del buon funzionamento è stata ottenuta confrontando queste misurazioni con delle misurazioni simili trovate nella letteratura accademica, queste mostrano lo stesso tipo di andamento oscillatorio.

E' quindi possibile concludere che la strumentazione progettata e costruita, che comprende la sonda di Pitot a cinque fori, gli strumenti per la sua calibrazione, il sistema di acquisizione dati, la nuova sezione della pala e i codici per l'analisi dei dati, è in grado di caratterizzare con successo le condizioni afflusso locale dell'aria alla pala di una turbina eolica, quindi tutti gli obiettivi inizialmente preposti sono stati portati a termine con successo.

Index

Abstract

Understanding local inflow conditions to a wind turbine blade can help predict loads on the turbine. Those are generally designed with 2D steady approach, however the real wind conditions are highly 3D and unsteady. Detailed measurements do not exist for validating aerodynamic models. The aim of this theoretical and experimental study is to build, calibrate, install and test a five hole pressure probe system to be used to retrieve these measurements. Wind tunnel calibration of the five hole pressure probe has been successfully carried out, thanks to the partly automated traversing system built, over a ±45° range, with 5°.steps. Error analysis showed that the multi-zone pressure coefficient data reduction approach is the most suitable for wind turbine application. This not only extends the measurable local inflow angles up to ±70°, furthermore it accepts any reference pressure for differential pressure readings. A new data acquisition system and wind turbine blade section had to be developed. Space limitation resulted in a custom built DAQ of very contained dimensions, this included, among others, 5 pressure transducers on a printed circuit board, a 16 bit analog to digital converter chip, Arduino microcontroller, and a Bluetooth transreceiver to transmit the data to the main computer. The new blade section was designed and 3D-printed in a way that the DAQ instrumentation could be easily accessed and, at the same time, to have an acceptable structural solidity. A series of test was conducted on the test rig (a 3m diameter wind turbine positioned in a large scale wind tunnel at the University of Waterloo) in order to assess the correct functioning of the probe system. As expected, the inflow measurement performed, while the turbine was under yawed conditions, showed a periodically oscillating inflow vector, the period of this variation was the same as the period of the rotor's rotation.

Keywords

Sommario

Capire le condizioni locali di afflusso alla pala di una turbina eolica aiuta a prevedere gli sforzi agenti sulla stessa. Queste sono generalmente progettate con approcci 2D e stazionari, anche se le reali condizioni del vento sul campo sono 3D e variabili. Misurazioni dettagliate non esistono per la creazione e validazione di modelli aerodinamici. Lo scopo di questo lavoro è di costruire, calibrare, installare e testare un sistema di sonda di pressione a cinque fori che sarà usato per ottenere queste misurazioni. La calibrazione in galleria del vento di questo strumento è stata portata a termine con successo, grazie al sistema di posizionamento parzialmente automatizzato costruito, su un range di ±45° con steps di 5°. Un analisi degli errori ha dimostrato che il sistema di riduzione dati basato sull'approccio multi-zona è il più indicato per l'applicazione a turbine eoliche, questo estende gli angoli di afflusso misurabili fino a ±70°, inoltre accetta qualsiasi pressione di riferimento per le misurazioni. Un nuovo sistema di acquisizione dati e una nuova sezione della pala sono stati contestualmente sviluppati. Limitazioni nello spazio disponibile hanno costretto a ricorrere a un sistema di acquisizioni dati appositamente costruito, questo include, tra l'altro, 5 trasduttori di pressione alloggiati su un circuito stampato, un chip per la conversione analogico digitale da 16 bit, un microcontrollore Arduino e un trasmettitore Bluetooth per inviare i dati al computer principale. La nuove sezione della pala è stata progettata e stampata in 3D in maniera tale da rendere facilmente accessibile la strumentazione al suo interno e allo stesso tempo per essere strutturalmente solida. Una serie di test è stata condotta sull'apparato sperimentale (una turbine di 3 m di diametro posizionata in una galleria del vento di grossa taglia) per testare il corretto funzionamento della sonda e dei sistemi correlati. Come previsto le misurazioni condotte quando la turbina presentava un angolo di imbardata mostrano un vettore di afflusso locale dell'aria con variazioni periodiche, il periodo di queste variazioni è lo stesso che quello della rotazione del rotore.

Keywords

Energia eolica, Turbine eoliche ad asse orizzontale, Sonda di pressione a cinque fori, Condizioni di afflusso locale alla pala.

Introduction

Understanding local inflow conditions to a wind turbine blade can help study and predict loads on the turbine's structure, that are caused by different flow phenomena, this is of fundamental importance during the turbine's design stage.

Motivations and objectives

Wind turbines are generally designed with 2D steady approach, then the predictions are verified in wind tunnel testing, since numerical approaches are too complicated as an infinite number of situation should be simulated. However the wind around the turbine blades in field operation condition is 3D and unsteady. Sufficient field measurement is not available in order to create and validate new aerodynamic models to predict the effects on this 3Dimensional flow field on the turbine structure.

In field operation conditions a wind turbine operates for the majority of the time under yaw loads, a yaw load is any situation when the blade experiences a non-uniform inflow velocity and direction during its rotation. This yawed condition can be the result of various situations, for example in case of horizontal or vertical wind shear, or when the turbine is not perfectly aligned with the wind direction, this happens very often because it is impossible to be always following the changing wind direction.

These yaw loads are cyclic and have a frequency that is usually the same as the rotational speed of the blade. They must be kept into account during the design phase as the loads on the wind turbine structure can result to be very different than the loads estimated with 2D BEM methods, and therefore adequate safety parameters must be adopted.

Previous studies performed by the Wind Energy Group (1) have demonstrated that periodically oscillating inflow condition radically influence lift and drag

coefficients of the considered airfoils. It is therefore reasonable to expect that loads on the wind turbine will vary greatly due to oscillating local inflow conditions.

The aim of the experimentation presented in this document is to build, calibrate, install and test a system to be used to characterize the local inflow conditions on a wind turbine blade, in order to be able to correlate these inflow conditions with the dynamically changing loads on the turbine's structure.
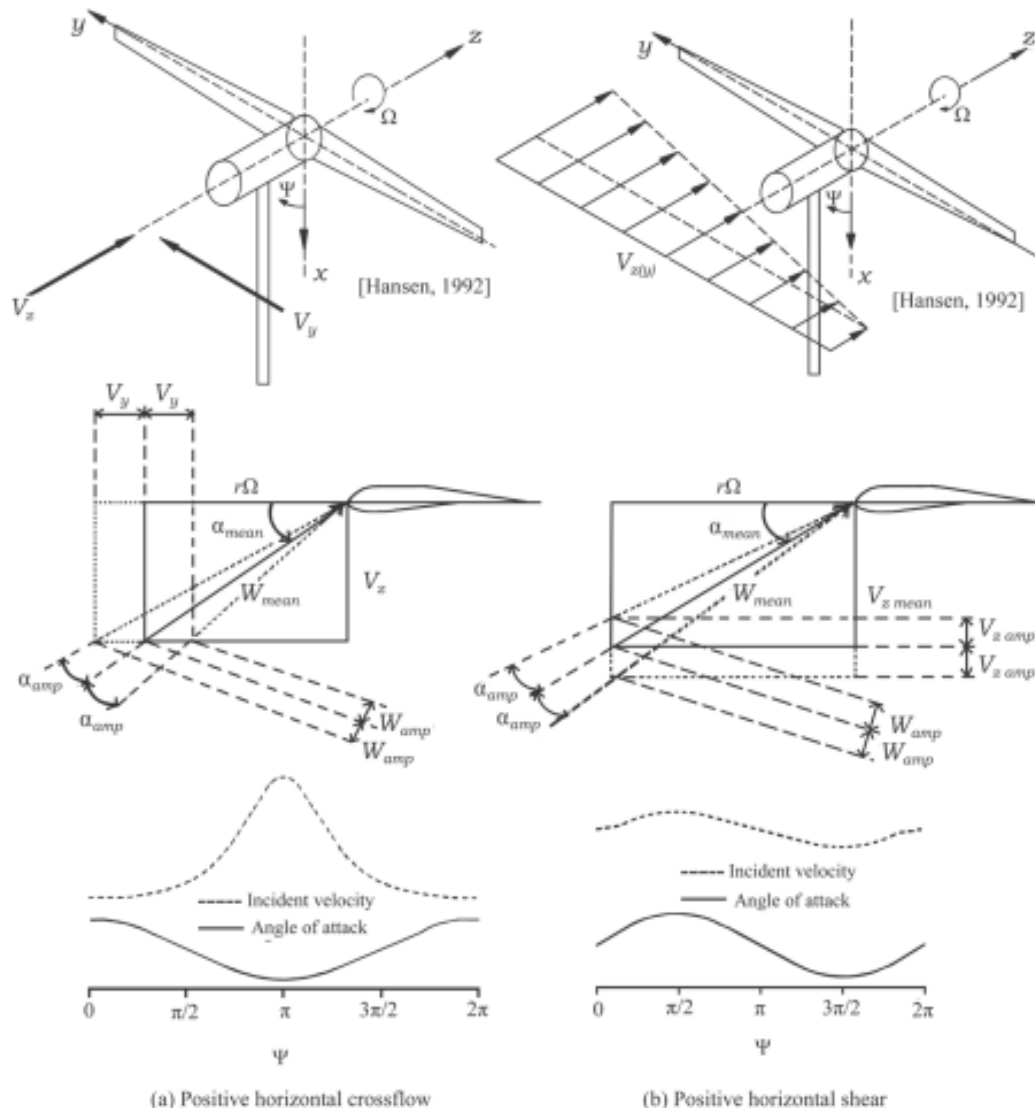
Figure 0.1 Examples of yaw loads conditions (1).

This is part of a larger series of tests carried out by the Wind Energy Group at the University of Waterloo, whose scope is to provide sufficient data for the validation of models to be employed for the prediction of loads and performance of a wind turbine in different operational conditions.

After the instrumentation will be built and calibrated, study of local inflow conditions will be performed in a large scale wind tunnel, the FireLab, located at the University of Waterloo, the instrumentation will be installed on a custom built 3m diameter wind turbine. Both yawed and non-yawed operational conditions will be tested in order to assess the difference between yaw loads compared to the design operational condition.

It is not certain that sufficiently detailed measurements exist for validating aerodynamic models against the actual 3D, unsteady flow. Complexity of the flow on the wind turbine blade makes it fundamental to make more data available for a broad range of experimental conditions.

The instrument that is proved to be more suitable for this kind of experiment is the five hole pressure probe, this, measuring dynamic pressure, allows to determine both instantaneous velocity and angles of the incident flow.

Outline

This thesis covers three main phases. First the study on five hole pressure probes and its calibration method, second the installation of a five hole pressure probe on a small scale wind turbines blade and third the collection of preliminary data to assess the correct functioning of the instrument. The thesis is laid out into six main chapters, starts with this introduction followed by:

- **Chapter 1 Background and**

  After a brief introduction on wind energy, the energy scenario in general and a literature review, it discusses the theory for the operation of the five hole pressure probe and it's calibration, then the selected data acquisition apparatus is explained in detail, finally probe calibration apparatus and procedure are laid out.

- **Chapter 2 Analysis of calibration results**
  Discusses the results obtained during five hole pressure probe calibration and best practice for application of this instrument on the small scale wind turbine test rig.

- **Chapter 3 Experimental setup**
  Describes the wind tunnel facility used for the study and the small scale wind turbine test rig. Design choices for installation of the probe on the turbine are explained in detail along with the necessary data acquisition setup.

- **Chapter 4 Results**

Discusses the results obtained during the campaign of preliminary data acquisition oriented to assess the correct functioning of the five hole pressure probe and the related equipment.

Chapter 1   Background and literature review

Multi Hole Pressure Probes (MHPP) extend the theory of Pitot Tube to extrapolate the characteristics of a flow to more than one dimension. A typical MHPP consists of three or more holes on the measuring tip arranged in a specific pattern. This allows the instrument to measure the direction of the flow in addition to its magnitude. Three holes arranged in a line allow the pressure probes to measure the velocity vector in two dimensions. More holes, for example five in a cross formation, allow the measurement of the three-dimensional velocity vector.

1.1 Background

1.1.1 World Energy Scenario

Humans need energy, often more then we think. Behind everything we consume and use in our everyday life there is energy, from electronic devices to the food we eat and the table we dine on, everything is built up on energy.

The growth of the world population and the everyday increasing demand for new goods to consume, results in a monstrous trend for the global energy request.

As it can be observed in the **Errore. L'origine riferimento non è stata trovata.** electricity generation has almost quadruplicated over the past 40 years (2), with an increasing number of people asking for the more versatile form of energy that is electricity, and this trend is set to keep this pace in the future, according to BP (3), the Total Primary Energy Supply, TPES will increase by 41% in 2035 with developing countries, China and India on top, leading the growth.

Pollution and global warming are becoming a strong concern, and the world is interrogating itself over finding more sustainable ways to meet the ever growing request for energy. Renewable energies are starting to cover a considerable share of the demand as it can be seen in the chart below.

Hydroelectric power is slowly growing around the word, but the capacity is starting to be saturated especially in Europe and North America, where most of the existing plants have been built during the past century. Therefore it comes to newer renewable energies to take up the challenge of reducing the emissions of pollutants and carbon dioxide due to the usage of fossil fuel.
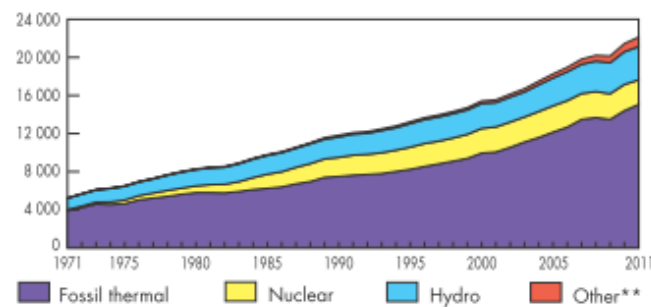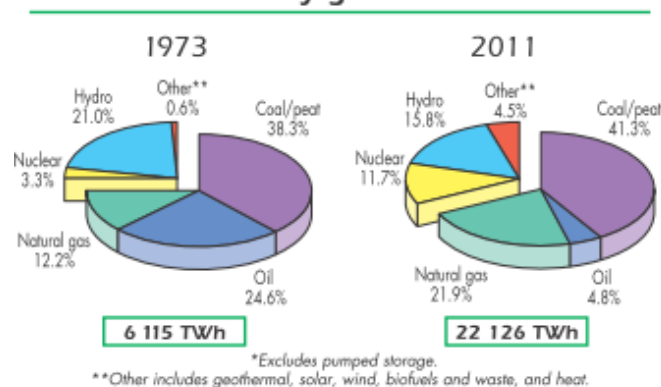
Figure 1.1 Word electricity generation from 1971 to 2011 by fuel **(2)**.

1.1.2 Growth of wind energy

Renewable energies have seen a stunning growth over the past decade, and they will surely keep the same trend into the near, as government all over the world are pushing a lot for their development. For example in 2009 the European union has set the goal of raising the share of EU energy consumption produced with renewable energy to 20%. This has given a huge push to the market with a consequently more attention and resources invested on research and develop on renewable energies.

Renewable energies present numerous challenges, they are more costly that fossil fuel technologies, they present a lower energy density and, probably the biggest of

all, they are intermittent and unpredictable, especially in the case of solar and wind, and this makes them unfit to satisfy the base load.

In this scenario wind energy is one of the fastest growing energy markets, this field has progressively moved towards larger machines designed to give a more stable output. The best wind conditions can be found where there are no obstacles and the wind can grow strong and stable. This is why the progress in this technology is moving toward larger offshore wind turbine.
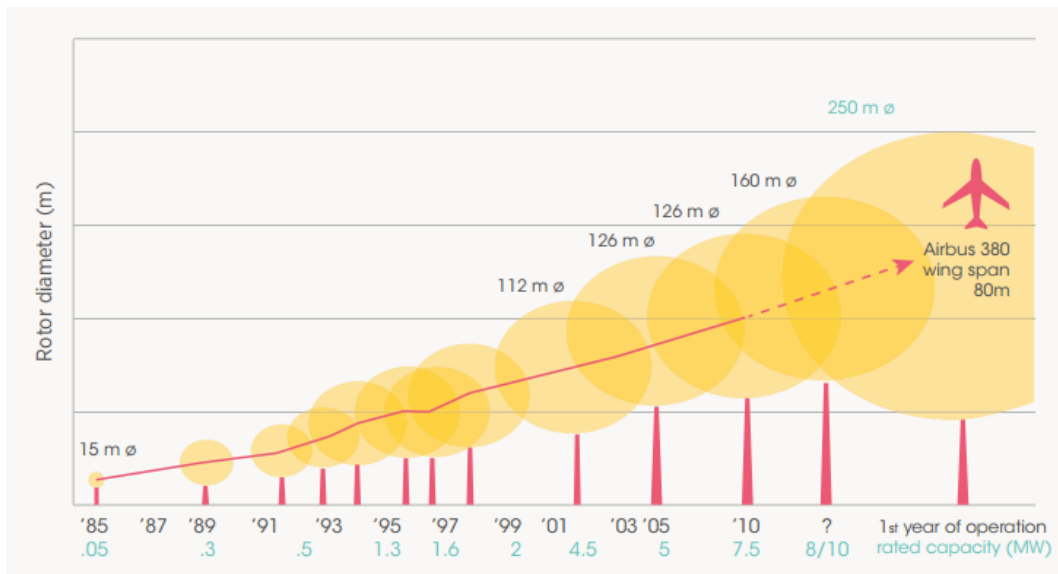
Figure 1.2 Increasing wind turbine size **(4)**.

Designing these machines presents many new challenges, larger turbines means higher stresses, and being able to predict those stresses is crucial to design and build machines capable of enduring even the harshest environmental conditions.

1.2 Wind turbine components and conventions

Horizontal axis wind turbine (HAWT) are the most common kind of design for modern wind turbines. In this configuration the axis of the rotational axis of the blade is parallel to the ground.

Figure 1.3 shows a HAWT main components.
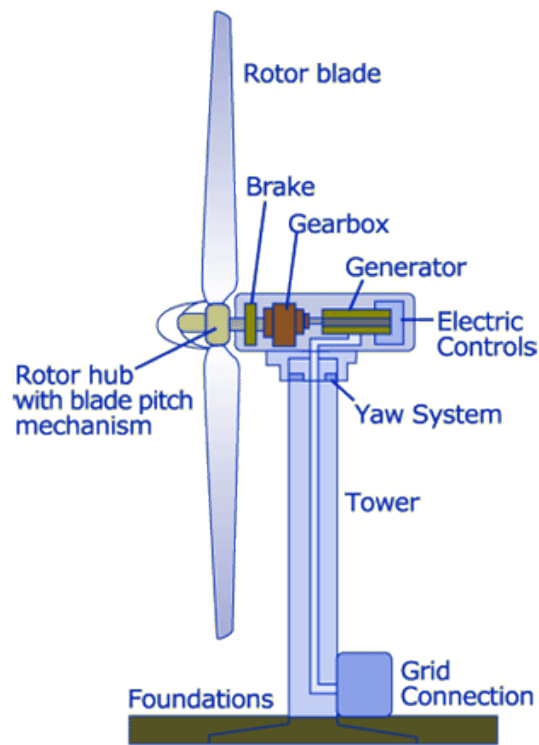
Figure 1.3 HAWT main parts **(5)**.
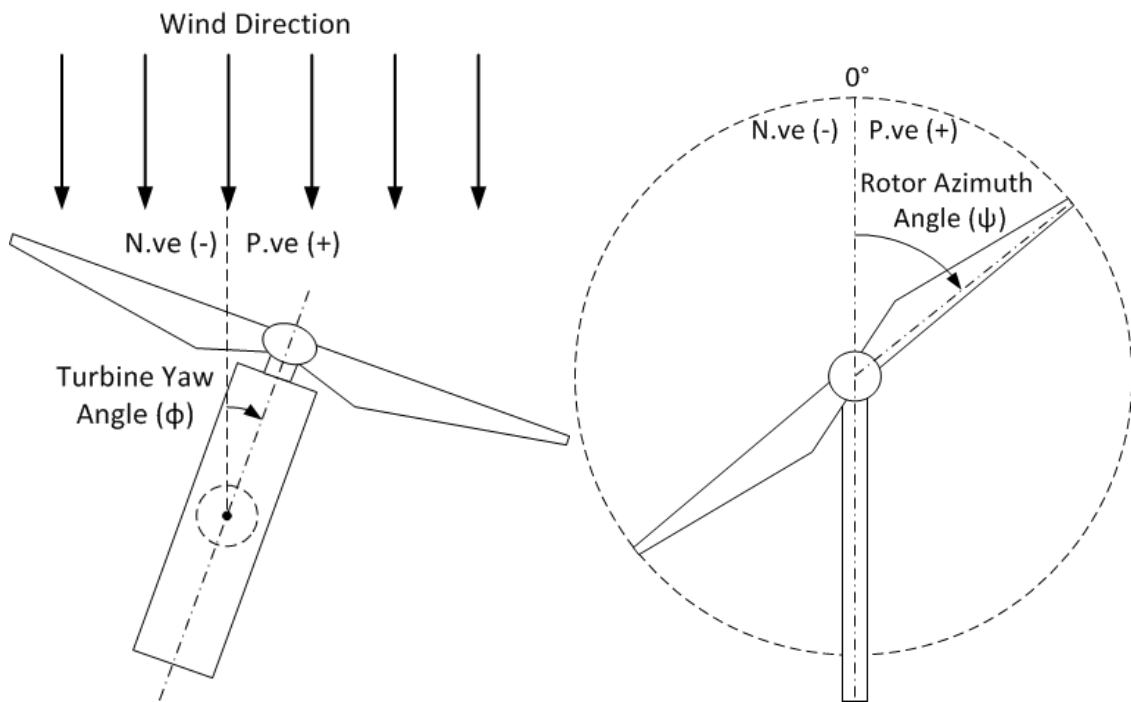
Figure 1.4 Wind turbine angle conventions, seen from the top (left), seen from the front (right).

Figure 1.4 shows the wind turbine angles conventions used in this work. On the left yaw angle (φ) is shown, this expresses the misalignment between the rotor's axis of rotation and the wind main direction, on the right blade azimuth angle (ψ) is shown.
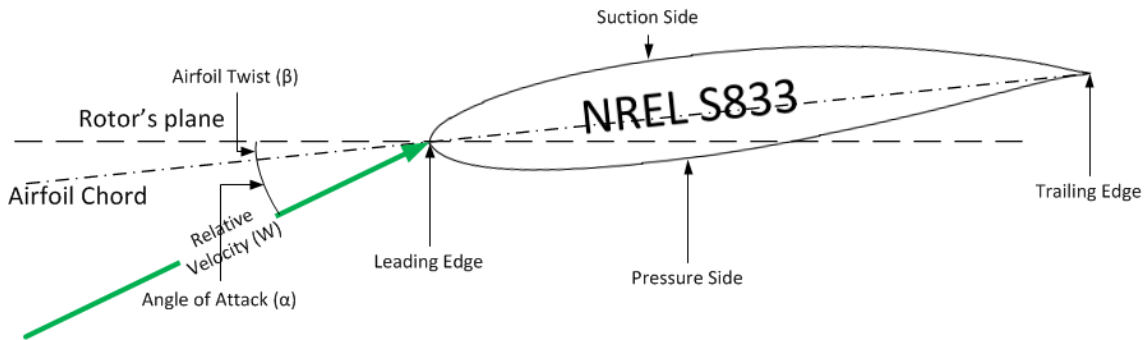
Figure 1.5 Airfoil terminology and angle conventions.

Figure 1.5 show the NREL S833 with terminology used and angle conventions.

1.3 Wind turbine local inflow condition characterization

In the past years some other experiments have aimed to characterize the local inflow conditions to the wind turbine blade.

1.3.1 Field experiments

A few cases of local inflow condition determination on medium and large scale wind turbine operating on the field have been found during the bibliographic research.

For example Maeda and Kawabuchi (6) have instrumented a 10m diameter wind turbine with a five hole pressure probe to determine local inflow angle and dynamic pressure to the blade. Their aim was to investigate how the normal force acting on the turbine structure changes in yawed conditions compared to non-yawed conditions.

Another contribution to this evolving field of study comes from the combined work of DTU (Technical University of Denmark), Siemens and Vestas (7), their aim was to carry out a number of coordinated measurements on full scale MW size rotors to provide insights on aerodynamics and aero-acoustic issues. They instrumented a 3.6 MW wind turbine with five hole pressure probe and used this instrument to measure local inflow conditions.

Figure 1.6 Multi hole pressure probe on 3.6MW size wind turbine **(7)**.

However, field measurement does not allow to easily correlate inflow condition to loads on the turbine structure, due to the always changing meteorological conditions. Data obtained in wind gallery testing allows to have complete control on the turbine's working conditions.

1.3.2 The NREL Unsteady Aerodynamic Experiment

The first and most notable attempt to perform this kind of study was the Unsteady Aerodynamic Experiment (UAE) conducted by the US National Renewable Energy Lab (NREL) between 1987 and 1996. The data collected during this test is without doubt the major contributions to the community working on wind turbine aerodynamics and is often still used as a reference to validate models and predict Horizontal Axes Wind Turbine's (HAWT) behaviours.

For their testing they used a 10m diameter wind turbineWind tunnel testing provided the opportunity to fully control the inflow conditions and therefore to separate the effects due to inflow anomalies to the effect due to strictly operate in a 3-D environment. The wind tunnel chosen for their testing was the NASA wind tunnel at the Ames Research Center in California, This wind tunnel section is 24.4 m high and 36.6 m wide (8).

Differential pressure probe or multi hole pressure probe were found to posses all the necessary characteristics to characterize local inflow conditions: fast response, wide angle range and high sensitivity.

In this work different approaches to the use of multi-hole pressure probe will be comparatively evaluated in order to assess the best practice for the application of this instrument on small scale horizontal axis wind turbine.

1.4 Pitot-Static tube functioning principle

The Pitot Static Tube is a flow meter that is used to measure the velocity of a fluid in a specific point in the flow. The Pitot Static tube measures pressure, this is then converted into a velocity in accordance with fluid theory.

The Pitot Static Tube, invented by Henri Pitot in 1732, measures velocity by converting the kinetic energy of the flow into potential energy. At the stagnation point of the probe, total pressure is measured by one large hole. Static pressure of the flow is also measured by a series of static pressure ports that are drilled on the side of the probe and must be perpendicular to the direction of the flow for a correct reading.
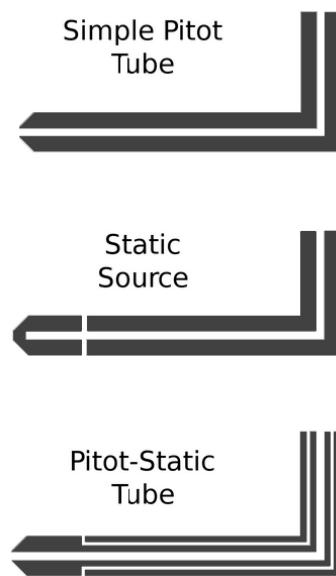
Figure 1.7 Different types of Pitot tubes used to measure pressures

The difference between the two measured pressures, total and static, corresponds to the dynamic pressure of the flow. This pressure difference is then converted into the fluid velocity depending on the particular flow regime that the Pitot Tube is measuring.

Bernoulli's equation can be applied to incompressible flows, when the velocity is less than 0.3 times its sonic velocity. This equation gives the correlation between

dynamic pressure and flow velocity along a streamline given that the local value of density of the medium is known.
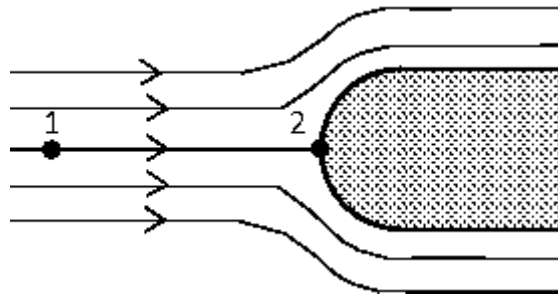
Figure 1.8 Streamlines of incident flow to a Pitot tube

Applied at two different points along the same streamline Bernoulli's equation yields that the energy of the flow at those two points is constant:

$$\frac{v_1^2}{2g}+z_1+\frac{p_1}{\rho g}=\frac{v_2^2}{2g}+z_2+\frac{p_2}{\rho g}$$

Eq. 1.1

Point 2 is the stagnation point, where $v = 0$, point 1 is a point upwind of the instrument laying on the same streamline as the stagnation point. Given that $z_1 = z_2$, we have:

$$\frac{v_1^2}{2g}+\frac{p_1}{\rho g}=\frac{p_2}{\rho g}$$

Eq. 1.2

Therefore:

$$v_1=\sqrt{\frac{2(p_2-p_1)}{\rho}}=\sqrt{\frac{2(p_{total}-p_{static})}{\rho}}$$

Eq. 1.3

Pitot Static tubes have many advantages when it comes to measure flow velocity, they are of very simple construction, easy-to-use and inexpensive pieces of equipments, but they have the huge limitation that the probe must be aligned with the flow. In order to obtain good result any misalignment should not exceed ±5° (9).

For this reason a simple Pitot-Static tube is not enough to measure the characteristics of a highly unstable and 3-Dimensional flow, like the inflow conditions to a HAWT.

Chapter 2   Five hole pressure probe and DAQ

2.1 Five Hole Pressure Probe

Different techniques have been taken into consideration for the scope of characterizing the local inflow conditions to a wind turbine blade during its operation, including flow angle flags and other devices. After a meticulous evaluation the decision was taken to use a 5 hole pressure probe.

Five holes pressure probes come in different shapes and configurations. Due to its availability in the lab, for this experiment we chose to use a probe composed of an array of 5 different tubes lying on two perpendicular planes and tightly packed together in the shape of a cross, with the intersection between the two planes passing through the center tube.

Figure 2.1 Close-up of the five hole pressure probe tip used for the experiment.

As it can be seen in the Figure 2.1, the Five Holes Pitot tube is machined so that the inlet of the four outer tubes form an angle with the axis of the probe. It is easy to understand that since the tubes inlet have different orientation, when the instrument is inserted into a flow, each one of the 5 tube will senses a different dynamic pressure level. Of course the tube that will measure the highest pressure is the one whose inlet is closest to be perpendicular to the flow.

Multi hole pressure probes can be used in two different configurations, nulling and non-nulling (10) mode.

The nulling technique is the most simple when it comes to data analysis. In this case the probe is mounted on a traversing system with 5 degrees of freedom, It is then moved and rotated until its axis is parallel to the flow, this means that the center hole is measuring the stagnation pressure, while the pressures at the four outer tubes are equal. This technique has the considerable disadvantage that it needs a complex traversing system, also, this method uses time, since the probe must be moved until the four outer holes are measuring the same pressure. Therefore it is not indicated to characterize highly dynamic or turbulent flows, like the case of this experiment.

The non-nulling technique allows the determination of the direction and magnitude of the flow with respect to the coordinates of the probe's axis, every particular combination of the five measured pressures corresponds to one pitch, yaw and velocity situation. Since the multi hole pressure probe doesn't need to be moved during data acquisition this approach is particularly indicated for application where limited space is available and when fast data acquisition rate is required, like the case of a rotating blade of a wind turbine; therefore this is the approach that will be used during this experiment. On the other hand this method requires to perform an extensive calibration of the probe, since each situation of pressures must be associated to a flow direction and magnitude during the calibration stage.

As mentioned above the characteristics of the flow can be inferred from the correlations established between the pressures measured at the five holes. It is apparent that the calibration characteristics must include data that accounts for pressure change on both pitch and yaw plane, and also the difference between the measured and true local total and static pressure (11). It is commonly accepted that the best way to express these relationships is to make them independent of velocity and a function of the flow angularity only.
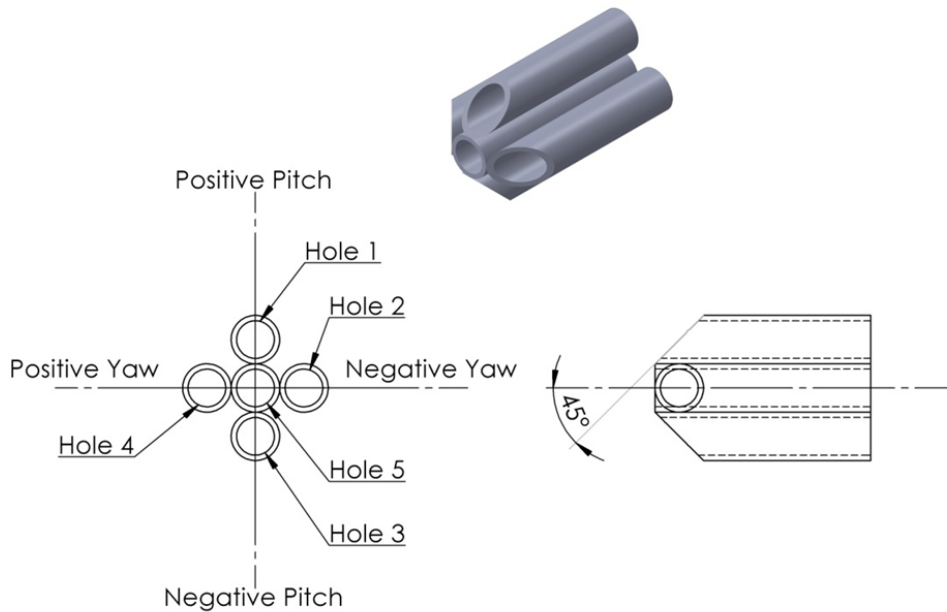
Figure 2.2 Details of the five hole pressure probe tip and angle conventions (image on the left seen from the front).

Krause an Dudzinsky (12), pioneers of this flow measurement technique, were the first to introduce pressure normalization. Without normalization knowing the stream's total and static pressure was required in order to determine the flow direction, that is surely impossible in the case of the rotating blade of a wind turbine. They found that the best way to normalize the pressures is to use the difference between the centre hole pressure and the average value of the pressures measured by the four outer holes:

$$p_5 - \frac{1}{4}(p_1 + p_2 + p_3 + p_4)$$ <div style="text-align:right">**Eq. 2.1**</div>

Three different sets of pressure coefficient will be tested and analyzed for wind turbine inflow characterization application during this experimentation.

The fist one is the one that was used during the NREL unsteady aerodynamics experiment (13). They used as a normalization parameter the free stream dynamic pressure of the flow incident to the probe, defining three dimensionless pressure coefficients.

The centre hole pressure coefficient:

$$Cp_c = \frac{p_5 - p_\infty}{q_\infty}$$

<div align="right">Eq. 2.2</div>

Where p_∞ is the free stream static pressure and $q_\infty = \frac{1}{2}\rho_\infty V_\infty$ is the free stream dynamic pressure.

The pitch and yaw pressure coefficients are defined as:

$$Cp_p = \frac{p_1 - p_3}{q_\infty}$$

<div align="right">Eq. 2.3</div>

$$Cp_y = \frac{p_2 - p_4}{q_\infty}$$

<div align="right">Eq. 2.4</div>

The second set of pressure coefficients analyzed is the one introduced by Krause an Dudzinsky in 1969 (12), as said, the first data analysis technique to include pressure normalization. This can be considered the basic set of pressure coefficients since all literature on multi hole pressure probe uses this coefficients or a slight variation of Them. Four different pressure coefficients are defined:

The pitch and yaw pressure coefficient, used to determine the flow direction:

$$Cp_p = \frac{p_1 - p_3}{p_5 - \bar{p}}$$

<div align="right">Eq. 2.5</div>

$$Cp_y = \frac{p_2 - p_4}{p_5 - \bar{p}}$$

<div align="right">Eq. 2.6</div>

Where $\bar{p} = \frac{1}{4}(p_1 + p_2 + p_3 + p_4)$ is the average value of the pressures measured by the four outer holes.

The total and static pressure coefficients, used to determine the velocity of the flow:

$$Cp_{total} = \frac{p_5 - p_{total}}{p_5 - \bar{p}}$$

<div align="right">Eq. 2.7</div>

$$Cp_{static} = \frac{\bar{p} - p_{static}}{p_5 - \bar{p}}$$

<div align="right">Eq. 2.8</div>

Lastly a variation of the Krause an Dudzinsky (12) pressure coefficients has been analyzed, this variation employs the so called sectoring scheme, a technique that allows to extend the functioning range of the multi hole pressure probe.

As it was observed by Zillac (14), the flow on the lee side of the pressure probe begins to separate at high flow angles. The sectoring scheme, first proposed by Gallington (15), aims to solve this problem. Based on the hole that is sensing the highest pressure, a combination of holes where the flow is not detached is used to define the pressure coefficients. This means that when the probe is almost parallel to the flow, hole number 5 is measuring the highest pressure, the set of pressure coefficients is the same as the one presented by Krause an Dudzinsky. When, for example, hole number 1, an outer hole, is measuring the highest pressure, the reading from hole number 3, opposite to number 1, is ignored in the creation of the pressure coefficient.

Table 2.1 Multi-zone set of pressure coefficients.

Zone 5	Zone 4	Zone 3	Zone 2	Zone 1
$\bar{p} = \dfrac{(p_1 + p_2 + p_3 + p_4)}{4}$	$\bar{p} = \dfrac{(p_1 + p_3 + p_5)}{3}$	$\bar{p} = \dfrac{(p_2 + p_4 + p_5)}{3}$	$\bar{p} = \dfrac{(p_1 + p_3 + p_5)}{3}$	$\bar{p} = \dfrac{(p_2 + p_4 + p_5)}{3}$
$Cp_p = \dfrac{p_1 - p_3}{p_5 - \bar{p}}$	$Cp_p = \dfrac{p_1 - p_3}{p_4 - \bar{p}}$	$Cp_p = \dfrac{p_5 - p_3}{p_3 - \bar{p}}$	$Cp_p = \dfrac{p_1 - p_3}{p_2 - \bar{p}}$	$Cp_p = \dfrac{p_1 - p_5}{p_1 - \bar{p}}$
$Cp_y = \dfrac{p_2 - p_4}{p_5 - \bar{p}}$	$Cp_y = \dfrac{p_5 - p_4}{p_4 - \bar{p}}$	$Cp_y = \dfrac{p_2 - p_4}{p_3 - \bar{p}}$	$Cp_y = \dfrac{p_2 - p_5}{p_2 - \bar{p}}$	$Cp_y = \dfrac{p_2 - p_4}{p_1 - \bar{p}}$
$Cp_{total} = \dfrac{p_5 - p_{total}}{p_5 - \bar{p}}$	$Cp_{total} = \dfrac{p_4 - p_{total}}{p_4 - \bar{p}}$	$Cp_{total} = \dfrac{p_3 - p_{total}}{p_3 - \bar{p}}$	$Cp_{total} = \dfrac{p_2 - p_{total}}{p_2 - \bar{p}}$	$Cp_{total} = \dfrac{p_1 - p_{total}}{p_1 - \bar{p}}$
$Cp_{static} = \dfrac{\bar{p} - p_{static}}{p_5 - \bar{p}}$	$Cp_{static} = \dfrac{\bar{p} - p_{static}}{p_4 - \bar{p}}$	$Cp_{static} = \dfrac{\bar{p} - p_{static}}{p_3 - \bar{p}}$	$Cp_{static} = \dfrac{\bar{p} - p_{static}}{p_2 - \bar{p}}$	$Cp_{static} = \dfrac{\bar{p} - p_{static}}{p_1 - \bar{p}}$

The correlations between pressures at the five holes of the probe cannot be determined with an analytical procedure nor with CFD simulation. This is mainly due to possible imperfections during manufacturing stage, therefore, using a 5 hole pressure probe means performing a long experimental calibration procedure.

2.2 Calibration of a five hole pressure probe

Precise calibration is crucial to obtaining good readings from a multi hole pressure probe. In a few words, the goal of calibration is to establish a correlation between the 5 measured pressures, and the directional pressure coefficients obtained from them, and the flow angles and total pressure coefficient and static pressure coefficients.

The calibration procedure consists in inserting the probe in a known axial flow field, typically an open-jet wind tunnel, and then varying its pitch and yaw of over a matrix of angles which exceeds the angularity expected in the flow field to be measured. The five pressures from the probe, static and total pressure of the flow are measured and stored at each position of this grid for subsequent data analysis and the creation of the pressure coefficients.

The spacing of the matrix of angle to which the probe must be moved to needs to be chosen carefully. A lower spacing means better accuracy, but, on the other hand, the increasing number of positions that the probe must be moved to requires much more time spent on calibration.

### 2.2.1 Effects of Reynolds number

Effects of Reynolds number on the performance of a multi hole pressure probe have been widely investigated in academic literature.

Zillac (14) explains that the effects due to the Reynolds number are certainly present but they are small compared to other effects, like errors in readings.

Treaser and Yocum (11) more specifically say that pitch, yaw and total pressure coefficient are basically unaffected by the Reynolds number, however there is a measurable change in the static pressure coefficient. This means that the measurement of the flow angularity is does not present considerable errors (due to the influence of the Reynolds number), while the measurement of velocity presented a maximum error of 2.8% over the investigated Reynolds number range. Since this error is small, one possible solution to bypass this problem is to perform the calibration at the expected Reynolds number that will be encountered during experimentation, so the result can be considered accurate if the Reynolds number remains close enough to the calibration value.
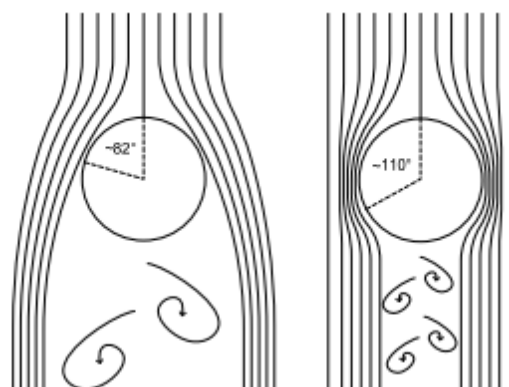
Figure 2.3 Cross flow over a cylinder in a situation of laminar (left) and turbulent (right) flow regime **(16)**.
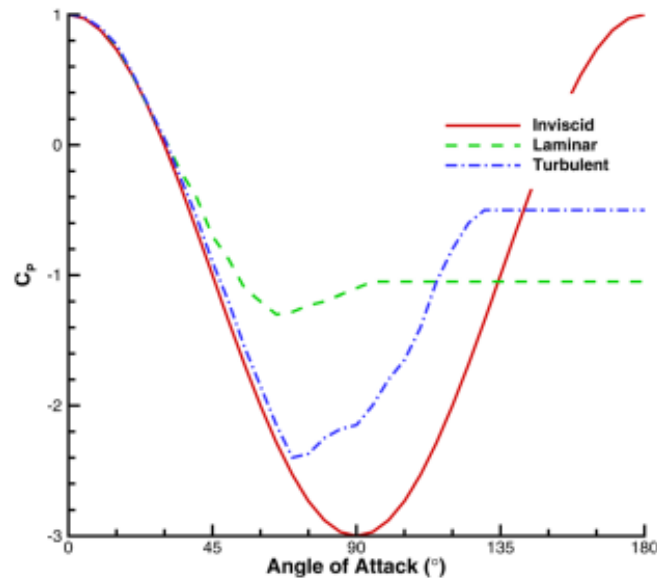
Figure 2.4 Pressure distribution of the cross flow over a cylinder **(16)**.

Krause (12) confirms the goodness of this solution and adds that the influence of Reynolds number is higher at higher angle of incidence and lower Reynolds number. The reason for this can be easily explained thinking about the separation of cross flow over a cylinder, in the Figure 1.7 it can be clearly identified the difference in flow separation angle between laminar flow (lower Reynolds number) and turbulent flow (higher Reynolds number), when the flow regime is turbulent the separation of the flow happens at a much higher angle then when it is laminar. This is why the highest error is at low Reynolds number and high angle of incidence.

In conclusion Reynolds number certainly has some influence on the performance of the multi hole pressure probe, especially at high angle of incidence, however this influence can be considered small enough to calibrate the probe at a single Reynolds number.

2.2.2 Other parameters

Mach number also has an influence on the response of a multi hole pressure probe. To account for this effects Gerner (17) defined a compressibility coefficient that becomes a third independent variable in the calibration procedure.

$$C_{M,n} = \frac{P_n - \bar{P}_n}{P_n}$$

Eq. 2.9

This coefficient was proposed to physically represent the ratio between an approximation of the dynamic pressure and an approximation of the total pressure.

There is no need to define this compressibility coefficients for low speed flow, below 0.3 of mach number, this is the case of this HAWT study.

Turbulence can also greatly affect the response of a multi hole pressure probe, this is particularly important because, since pressure is proportional to the square of the flow velocity, highly turbulent flows can have effect on the calibration data when it is time averaged. Also fast changes in the flow direction due to turbulence can result in a non linear response of the probe.

2.3 Data Acquisition Apparatus

For accuracy reasons the Data Acquisition System that was used to perform the instrument's calibration is the same that will be used during the experimental measurement campaign, this allows to avoid problems that could come from using different materials, like for example using different pressure transducers that present slightly different calibration curves.

Designing and adapting the Data Acquisition System (DAQ) for the five hole pressure probe to work on a small wind turbine presents numerous challenges.

First, finding a way to fit all the devices necessary for data acquisition, in such a confined space such as the blade of a small horizontal axis wind turbine, means not being able to use conventional plug and play devices.

The second problem comes from the fact that the instrumentation will located on a rotating support, this means that, since no slip ring was installed on the test rig, data transmission between the data acquisition system and the computer that controls the test rig has to be performed wirelessly. This same problem affects the power supply to the DAQ.

Lastly the DAQ must be able to correctly work in an environment that is subject to high centrifugal forces and high frequency vibrations.

All the above factors, and a limited budget had, to be considered during the design stage.

2.3.1 The Five Hole Pressure Probe

The five hole pressure probe used in the present study is constituted of an array of tightly packed stainless steel tubes. The tubes are arranged in the shape of a cross,

so that the pressure measured by each couple of opposite tubes, has the main function to sense the pressure difference on the pitch or the yaw plane as shown in the figure.

The five tubes have an exterior diameter of 1mm, the five tubes were bonded together with soft solder at about 2 tip diameter downwind of the probe's tip, as shown in Figure 2.1. The extremity of each one of the four outer tubes were machined to form an angle of 45° between the tube's inlet and the axis of the probe. The five tubes are then inserted into a ½" diameter brass tube through a collar, five 1/8" stainless steel tubes are connected on the other side of the collar, as it can be observed in Figure 2.5, both sides of the collar are sealed to be airtight using epoxy resin. The brass tube gives structural solidity to the instrument and a support for its installation on both the calibration device and the wind turbine blade.
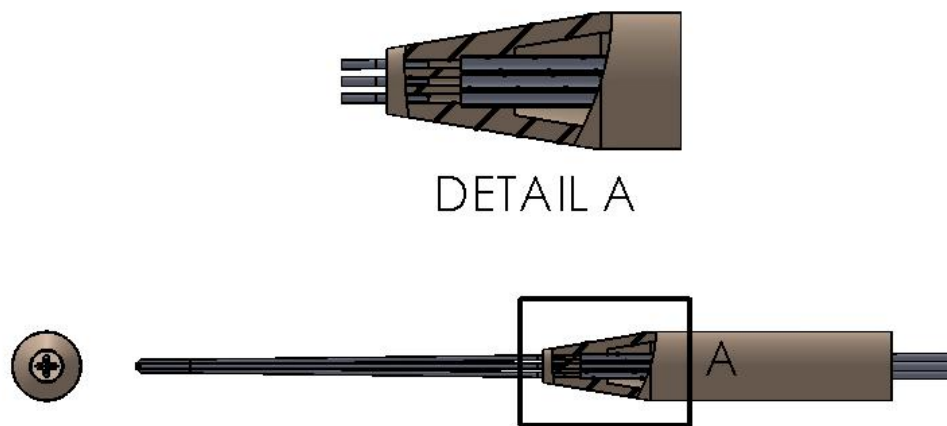
**Figure 2.5** Detailed five hole pressure probe design.

The probe was already present at the fluid lab at the University of Waterloo and finding data about its origin was impossible. From its characteristics and the fact that is a very rudimental and easy to build design it is possible to think that it was likely machined in house at the university's machine shop some years back.

Five silicone tubes are connected to the tubes to the far side of the probe and then to the 5 pressure transducers.

2.3.2 Pressure Transducers

Various models of pressure transducers were comparatively evaluated for five hole pressure probe application, ultimately, keeping in mind the space limitations

and required pressure rage, Honeywell HSCDRRN005NDAA5 (18) pressure transducers.
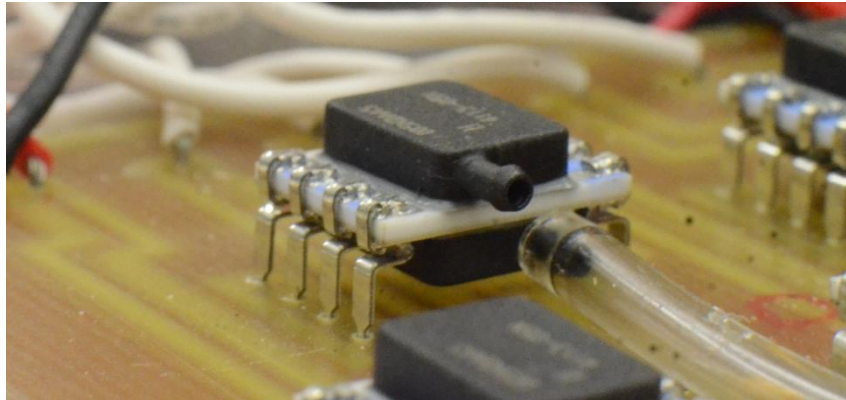
Figure 2.6 HSCDRRN005NDAA5 pressure transducer.

This model is a differential pressure transducer with a range of ±5 in of water (1245 Pa), this particular pressure range was chosen after an rough estimation of the possible local inflow conditions that will happen once the instrument is installed on the wind turbine blade.

Considering that the initial intention was to install the five hole pressure probe at a location about 1m from the hub, that the rotor's maximum speed is 200 RPM and the maximum wind speed in the wind tunnel is around 13 m/s, this means that the estimated maximum local inflow wind speed is 24.65 m/s, corresponding to a dynamic pressure a slightly below 400 Pa.

Since the accuracy specifications for the pressure transducers are given at the full scale range it is important for the expected pressure to be as close as possible to the full scale specification, in order to have readings with good accuracy. On the other hand, since the dynamic pressure of the flow is proportional to the square value of its velocity, a small fluctuation in the inflow velocity means a much larger fluctuation in dynamic pressure, Therefore the expected pressure to be measured must not be too close to the full range in order to collect valid readings and not to damage the transducer itself. The HSCDRRN005NDAA5 pressure transducer presented the most compatible pressure range among all the other options considered.

The HSCDRRN005NDAA5 pressure transducer has an 0 to 5 V amplified output and is fed with 5 V DC input.

To simplify the pressure transducer's housing into the blade a simple circuit board has been printed in house and the pressure transducers have been soldered to it.
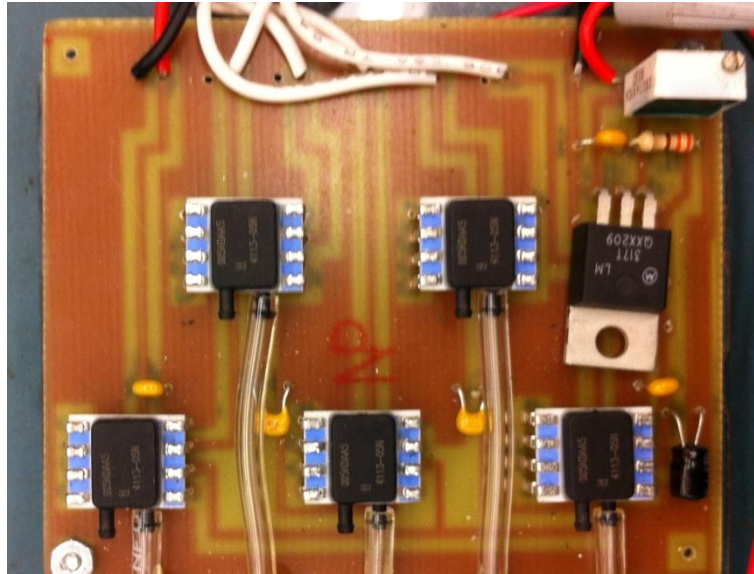
Figure 2.7 Five HSCDRRN005NDAA5 pressure transducers layout on the printed circuit board.

On the circuit board have also been housed a voltage regulator and potentiometer to convert the 9 V DC from a battery to the 5V DC required by the pressure transducers.

Before the five hole pressure probe calibration, a short extrapolation of the characteristics of the pressure transducers calibration curve was performed. The voltage value at zero differential pressure condition was measured, and, based on the manufacturer specification, a linear calibration curve was extrapolated. Due to time limitation a more in-depth calibration of the pressure transducers could not be performed, and the manufacturer's specifications were considerate accurate enough. However it is advisable that a full range calibration it's performed in the future to increase the accuracy of the measurements.

The signal from the pressure transducer is then transmitted from the circuit board to a differential analog to digital converter.

2.3.3 Analog to digital converter

The analog signal (voltage) from the pressure transducers is then converted to a digital signal by an analog to digital converter (ADC) chip, the AD7606 (19) produced by analog devices. The chip has a 16bit resolution, and can read 8 bipolar channels, it uses SPI (serial periphal interface) to communicate the voltage readings.

The AD 7606 was chosen mainly because of its unique feature, it is capable to sample simultaneously its 8 channels. This is crucial for multi hole pressure probe

application as the five pressure need to be measured exactly at the same time to get a correct reading from the probe.

Another important factor that influenced the choice, is that, this is the chip used by Rascal Micro to produce the voltage Arduino shield seen in Figure 2.8, more details about Arduino will be given later. This permitted to avoid the time consuming task of designing and manually building the connection between the small pins of the ADC and the Arduino microcontroller.
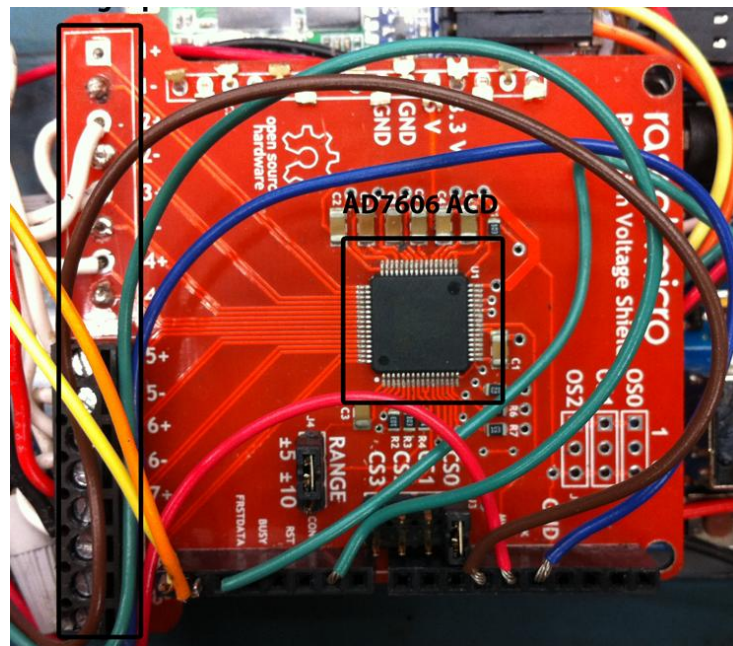
Figure 2.8 RascalMicro voltage shield with AD7606.
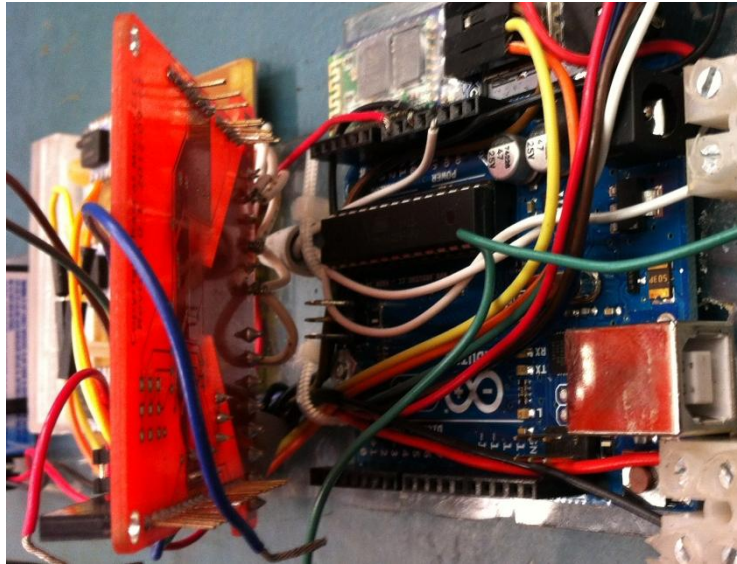
2.3.4 Arduino Microcontroller

The core of the whole data collection system is the Arduino Uno microcontroller.

Arduino Uno is a compact electronic board that includes a microcontroller and lots of connectors to interface it with different devices. Arduino is an open source hardware project established in Ivrea (TO), Italy. It comes with its own simple Integrated Development Environment (IDE), that installed on a regular PC it allows to program the microcontroller using C or C++.

Arduino Uno module features USB for computer connection, 6 analog input pins and 14 digital I/O pins that simplify the task to connect it to its add-on modules, the shields, like the above mentioned Voltage shield.

Arduino Uno was chosen for this project because of its many unique features. The price, it is commercially available for less than 30$, this makes it the perfect solution for the prototyping phase. It is very compact, 68 mm long, 53 mm wide

and a thickness of less than 1 cm. Very easy to connect to other devices, can be connected to shield using its unique and standardized pin configuration, or also to other devices through Serial, Parallel, SPI and I2C protocols. Because it is and open source hardware and works with open source software, Arduino became the most popular microcontroller board, it is very easy to find hundreds of examples online and the Arduino website's forum is very helpful for solving problems, this makes it the perfect tool for who does not have experience in electronics.

Figure 2.9 Arduino microcontroller and RascalMicro voltage shield

2.3.5 Data storage and communication

As anticipated one of the biggest challenges for the application of the multi hole pressure probe, and any instrument in general, to the rotating blade of a wind turbine is the impossibility of performing wired communication between the equipment on the blade and the computer used to collect the data. To overcome this problem, the device was designed to have the capability to internally store the voltage data and to communicate them wirelessly to the computer.

For the wireless transmission two possibility were taken into account: Bluetooth and Wireless communication. After an in-depth evaluation Bluetooth serial communication was picked as the most suitable technology both because of its major ease of use and its highest data transfer rate.

For data storage purpose the data acquisition system was also equipped with a microSD.

Being able to integrate into the project SD internal storage and Bluetooth serial communication, without any previous experience using these technologies, proved the potential that the Arduino board has for this kind of projects.

2.3.6 Power Supply

Another big challenge generated by the impossibility of wiring the instrumentation to the stationary world is providing the correct power supply level to each piece of equipment.

The choice was to power the whole system through a 9V battery, this voltage level was adjusted in different ways to provide the correct voltage to each part of the instrumentation.

A power supply of 9 V DC was provided to the pressure transducers printed circuit board, on board circuitry (potentiometer and voltage regulator) is used to change the power level to the 5 V DC required by the transducers.

The Arduino Uno Board was powered directly with the 9 V DC from the battery. The SD card reader and the voltage shield required 5 V DC that was provided by the voltage regulator on the Arduino Uno, like the 3.3 V DC required by the Bluetooth.

For optimizing the energy efficiency of the instrumentation a three position toggle switch allows to select between two working modes and an off position. In the first mode everything is turned off, in the second mode everything is turned on but the Bluetooth. This choice was made because the Bluetooth transreceiver was found to be, by far, the most energy demanding component in the whole setup.

Chapter 3   Analysis of calibration results

As said, data regarding the calibration of the five hole pressure probe was stored on internal microSD card and on the computer during the calibration process. In this chapter the post-processing procedure will be explained, then the results from the calibration will be analyzed in order to determine what is the best practice for the application of this instrument to characterize the local inflow on a horizontal axis wind turbine blade.

3.1 Calibration Setup

3.1.1 General Calibration Decisions

As said   the calibration of a five hole pressure probe consists in placing the instrument into a known flow field, while moving it through a matrix of known combinations of pitch and yaw angles.

The calibration matrix's size must exceed the expected maximum flow angle that will be encountered during the experiment. A total range of ±50° for both pitch and yaw angle was chosen for this calibration in order to considerably exceed the expected flow angle and give room to possible errors in the calibration.

Steps of 5° were chosen as the resolution for varying the pitch and yaw angle. This is a common value that was encountered a few times in multi hole pressure probe calibration literature (10) (14). Figure 3.1 Represents a matrix with all the points at which calibration data has been collected, 441 total points.
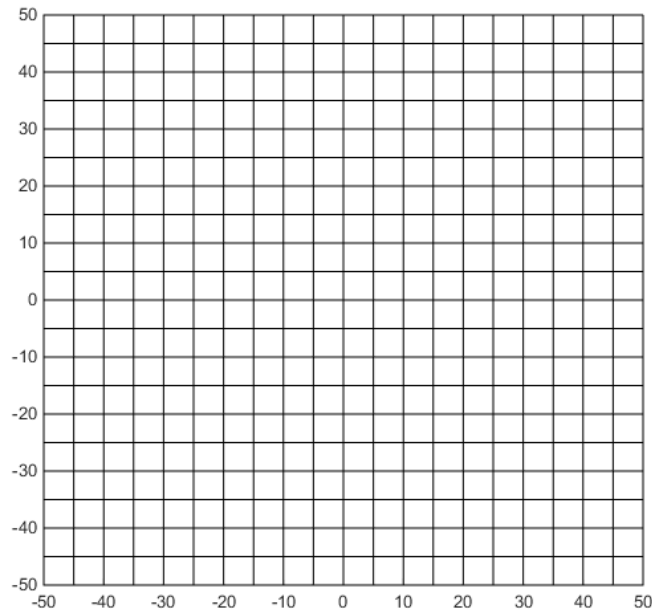
Figure 3.1 Matrix representing the points at which the calibration data has been collected.

As previously mentioned, carefully choosing the speed at which the calibration is performed enables us to avoid the small effects due to the influence of the Reynolds number. At the time at which the calibration was performed the actual experimental conditions had yet to be defined, the expected range of velocity was between 25 m/s and 33 m/s based on the location of the probe on the wind turbine blade, therefore a velocity of 29 m/s was chosen for the calibration.

Another issue that had to be defined was the number of measurements that had to be taken at every point of the calibration grid and then averaged to create truthful calibration data. This was very important in order to mitigate the effect of turbulence in the temporary setup of the calibration wind tunnel and the uncertainty of the measurement from the pressure transducers.

In order to determine the number of readings to be taken at each position of the grid a preliminary calibration was performed. A thousand data points have been taken with the probe in two different positions; low inflow angles (yaw 0°, pitch 0°; Figure 3.2, above) and high inflow angle (yaw 0°, pitch 30°; Figure 3.2, below). The figures representing the cumulative standard deviations of the data, show that after 400 measurements the standard deviation tends to stabilize, therefore this is the number of measurements that will be taken at each point.
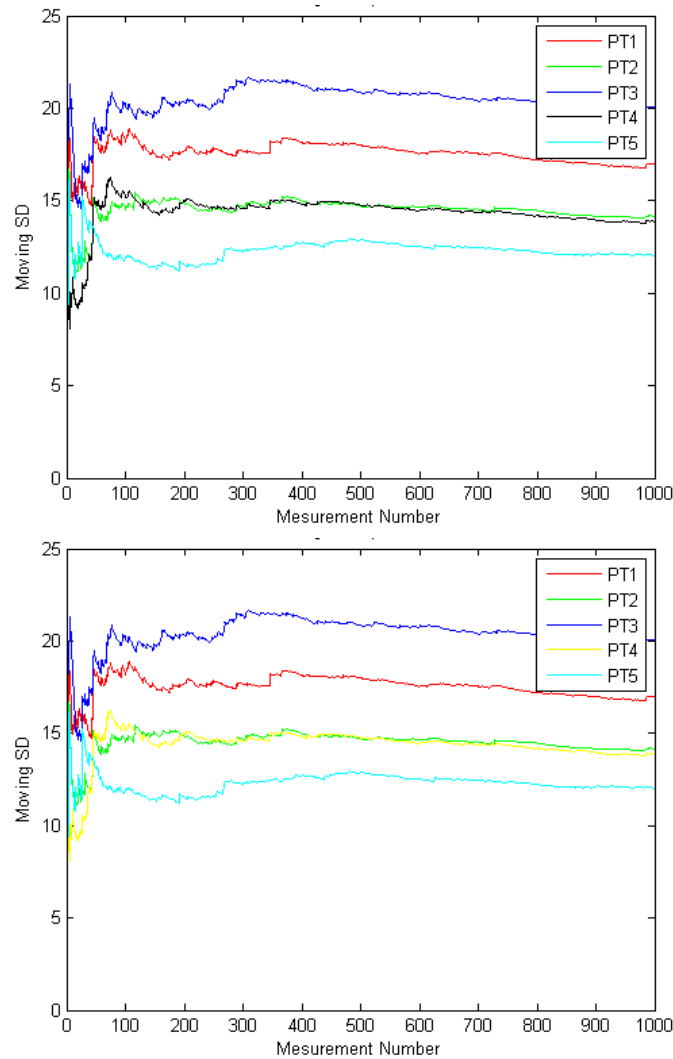
Figure 3.2 Cumulative standard deviation of 1000 measurements at two different combinations of pitch and yaw angle; 0° pitch and 0° yaw (above), 0° pitch and 30° yaw (below).

In order to create the pressure coefficients total and static pressure of the flow had to be acquired. For this purpose a Pitot Static Probe was used and the pressure reading was taken using a sixth HSCDRRN005NDAA5 pressure transducer.

3.1.2 Traversing device

In order to accurately calibrate the multi hole pressure probe a traversing device had to be designed and built.

The probe traversing device had to have the following characteristics. First, being able to cover the full range of calibration of ±50° and to accurately perform the 5° steps. It is also important for the tip of the multi hole pressure probe to be kept in the same position during the whole process to calibrate it in constant flow

conditions. Some kind of automation in the movement of the probe is required for reasons of precision and to reduce the time spent manually traversing the device. Lastly the structure of the device must be strong enough not to vibrate when inserted into the flow of air.

The device was entirely deigned machined and assembled in the machine shop using University of Waterloo facilities. To minimize the construction time and difficulty some of parts of the used to build the device were recovered from old instruments already present in the lab, owned by the Wind Energy Group, part of past researches, that were not in use anymore. A heavy rotary table was used as the base for the whole setup and as a support for the yawing device. A rotary platform, that had been part of a device used for a fluid dynamic investigation of centrifugal pumps using PIV laser technique was used as the pitching device.

From the Figure 3.3 the three fundamental parts of the device can be identified: in green the position of the five hole pressure probe, in blue the pitching device and in red the platform used as the yawing mechanism.

As it can be observed in Figure 3.3, in order to keep the tip of the probe in the same position, while pitching and yawing it, the device was designed in a way so that the tip of the probe is positioned exactly in the intersection between the axis of the yaw and pitch rotational movement.

The probe was traversed through the pitch plane with a rotary platform positioned vertically on a stainless steel post. The platform is moved using a Superior electric stepper motor with a resolution of 200 steps per revolution, this is connected to an endless screw that moves a gear that is attached to the platform about its axis. The motor was controlled by the Arduino microcontroller through the GeckoDrive G201X microstep drive, the motor driver increased the resolution of the motorized system to well below 0,1 degree that was the sensitivity of the digital level used to measure the pitch angle of the probe.
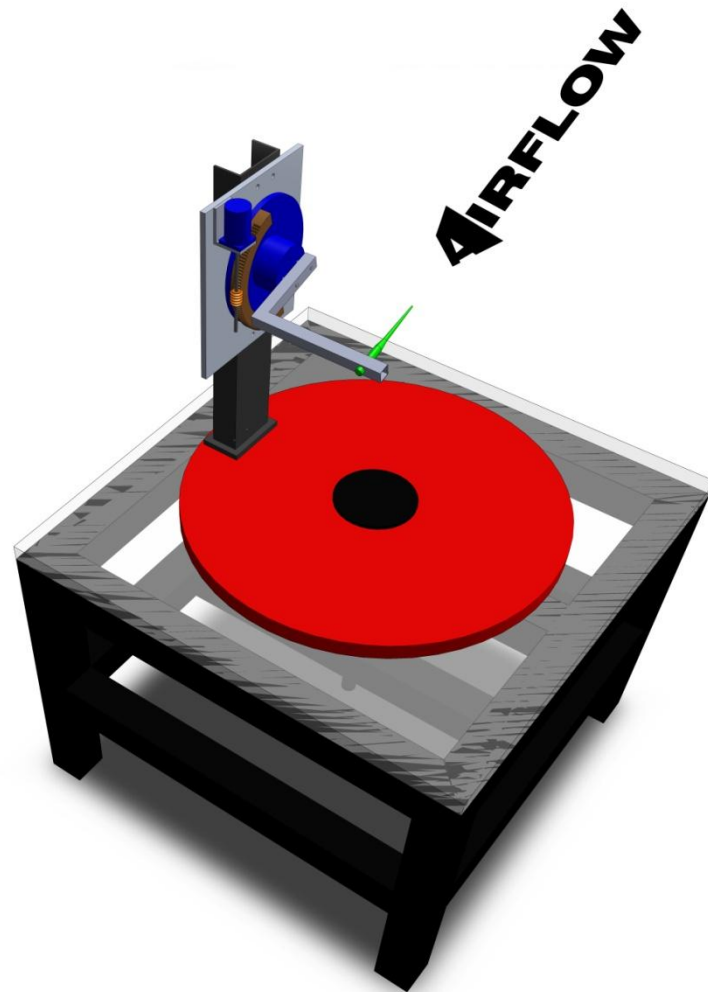
Figure 3.3 SolidWorks™ design of the probe traversing system.

The Figure 3.4 shows a detail of the rotating platform, the stepper motor (in blue), the endless screw, the main gear and the digital level.

The pitching device was connected through a vertical stainless steel post to a rotating wooden platform that, connecting to a rotary table, formed the yawing device. To minimize the time spent designing and building the traversing device, unlike the pitch, the yawing was done manually. A protractor on the rotary platform allowed for a resolution of 1°, the yaw was aligned with the aid of a manual laser level.
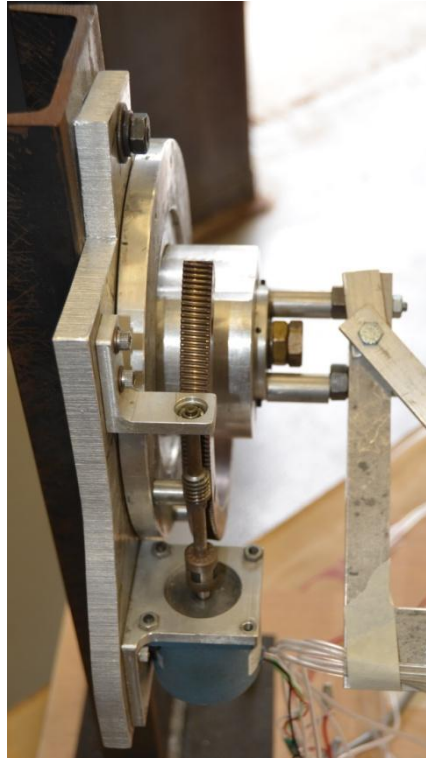
Figure 3.4 Detail of the automated pitching device.

3.1.3 Wind tunnel setup

As said the calibration is performed inserting the probe into a flow whose characteristics are known. The best way to do so is to use a small scale open jet wind tunnel. The wind tunnel used for the calibration of the five hole pressure probe is owed by the University of Waterloo and it is activated by a centrifugal compressor. The last section of the wind tunnel consists in a Plexiglas contraction, with the contraction installed a maximum wind speed of 50m/s can be achieved. The outlet of the contraction was one foot high and two feet wide (around 0.3m by 0.6 m)

The use of the open jet wind tunnel was the cause one of the major delays in the project. Before the calibration could be performed the Lab where the wind tunnel was initially installed was closed for renovations, therefore it had to be moved to another smaller lab. Due to the space limitation in the new laboratory the wind tunnel was modified from its initial straight configuration, to a new setup that presented a 90° corner 8 feet (2,84m) upwind of the outlet as it can be seen in figure.

Moving the wind tunnel affected the experiment not only because of the delay it generated, but mainly because specifications about turbulence, axiality and uniformity of the flow from the old configuration could not be applied to the new

one due to the presence of the elbow. A brief characterization of the flow at the outlet was necessarily performed before the calibration started.

The flow was found not uniform across the outlet section of the outlet, a remedy to this problem came from the design of the traversing system, as mentioned above it was designed so that the tip of the multi hole probe remained in the same position of the wind tunnel outlet throughout the whole calibration.
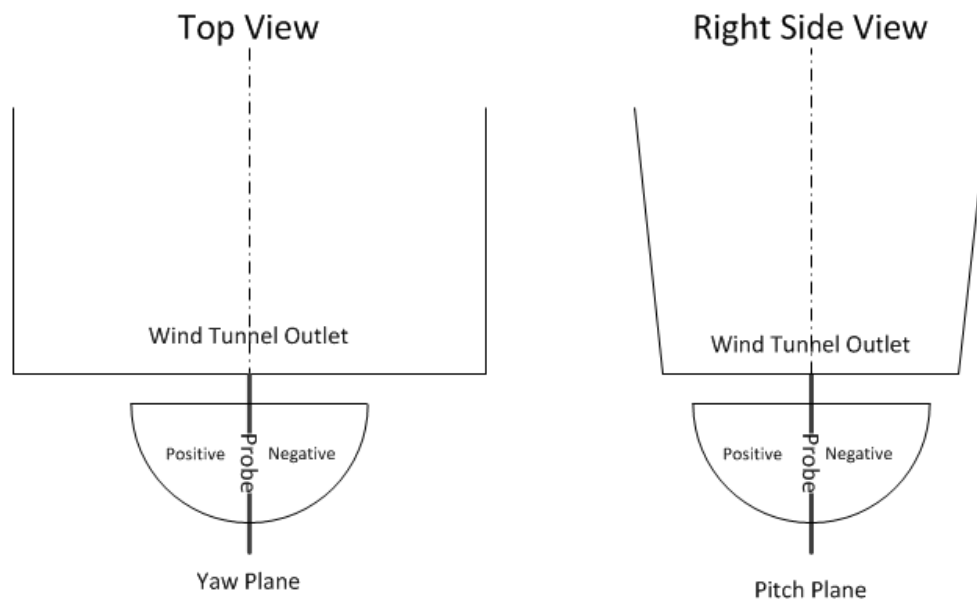
Figure 3.5 Detail of the wind tunnel outlet and angle convention.

The flow was found not to be completely axial either due to the corner introduced in the wind tunnel after it was moved. At the probe's tip location it presented a 4° negative deviation from the axial direction on the yaw plane. This deviation of the flow was kept into account during data analysis and in the process of creating the calibration curves.

It was not possible to perform a full characterization of the turbulence of the flow in such a limited time. It is logic to expect the flow to present a considerable turbulence, due to the presence of the 90° corner. This finds a confirmation in Figure 3.2, it can be observed that the standard deviation of the measurements becomes stable after more than 400 readings, and it stabilizes at quite consistent value, 10 to 20 mV, depending on the pressure transducer, compared to measurement value of around 300 to 500mV over the 0 pressure value of 2500mV.
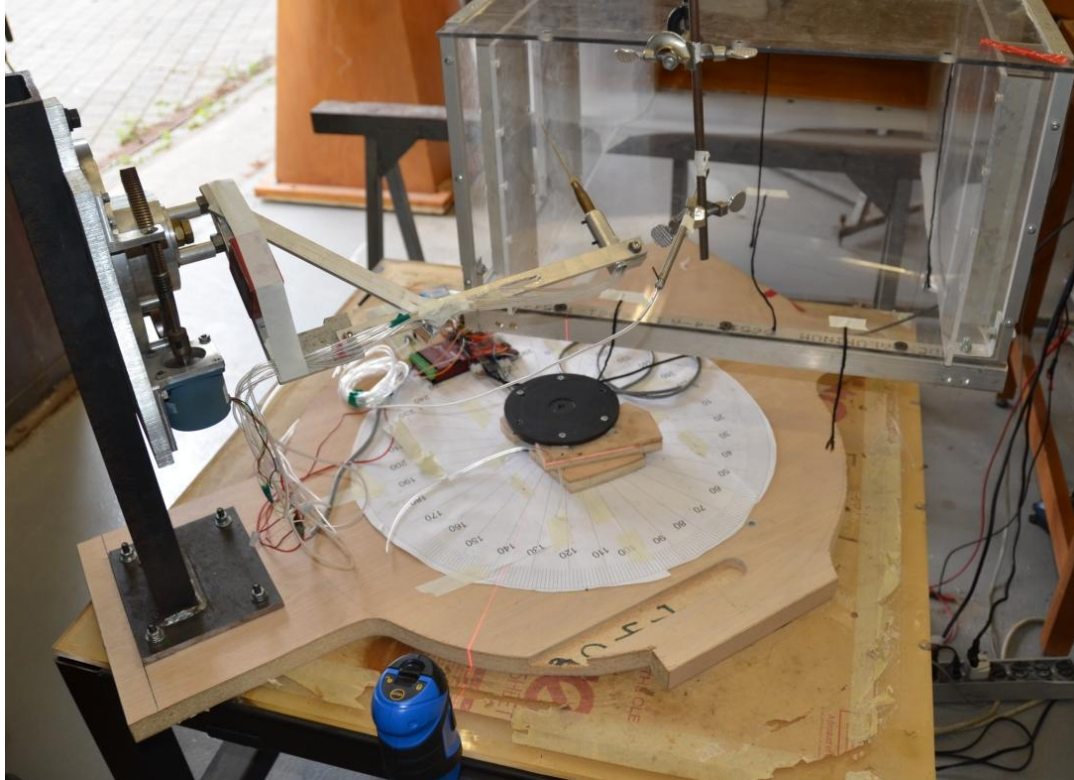
Figure 3.6 Prove traversing device positioned in front of the calibration wind tunnel outlet.

3.1.4 Collection of calibration data

HP Pavilion dv6000 computer with Intel Core 2 Duo processors, running at 1.86 GHz with 4 GB of RAM were used for data acquisition during calibration. The Data Acquisition System described above was connected to the computer with serial USB connection, Bluetooth transreceiver was not used at this stage.

Data was both transmitted to the Computer, to be displayed on serial monitor built-in to the Arduino IDE, and stored on the microSD present in the DAQ. Voltage data from the pressure transducers was stored to be then converted to pressures at a later stage during post processing.

Data was stored as a .CSV file with comma (,) as field separator and dot (.) as decimal separator. Following, a few lines to represent the typical form of the stored calibration data:

```
timeStamp,yaw,pitch,PT6(totalP),voltageSupplyToPTBoard,PT5(
hole5P),PT4,PT3,PT2,PT1,
2447661,20,30,3266.30,4990.08,2906.19,2314.45,2206.57,2912.
14,3093.87,
2447691,20,30,3273.16,4990.08,2900.24,2332.61,2202.00,2897.
95,3103.49,
```

3.2 Acquired calibration data

In Figure 3.7 it is possible to see a typical example calibration data. The two lines are represent a plot of a 100 data points each from hole number 5(center hole), at two different combinations of angles, taken from the calibration data. The green line represent a sample of data taken with the probe parallel to the flow (0°pitch and 0° yaw angle, position 1), the blue one when the probe is positioned at an angle with the flow (30° of pitch and 35° of yaw angle, position 2). The red horizontal line represents the voltage reading in a zero pressure condition.
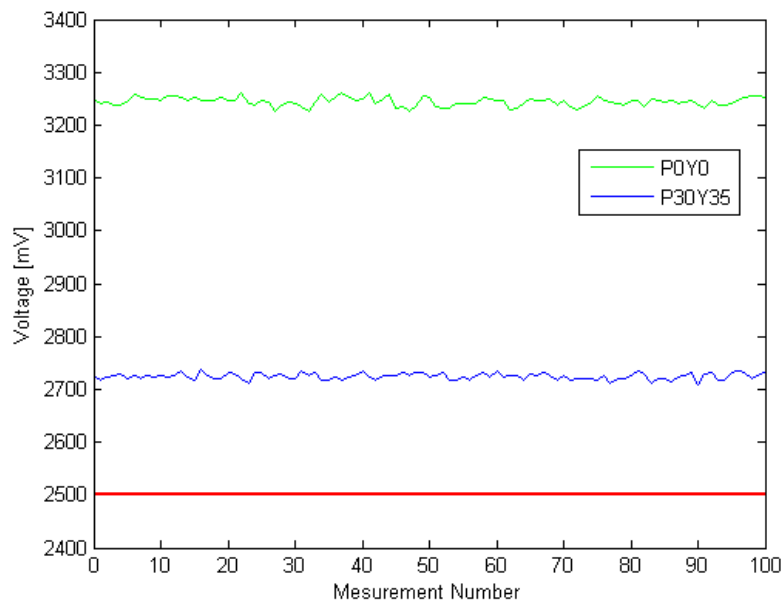
Figure 3.7 Sample of voltage measurement at two different combinations of angles.

As it is logical to expect, when the probe is parallel to the flow the voltage measured by the centre hole, and therefore the corresponding pressure, is higher compared to the case when the probe is at a higher angle with respect to the flow direction.

3.2.1 Standard deviation analysis of the data

This sample data presents a considerable standard deviation, as it can be seen in the figure. The whole population of data from the centre hole of the five hale probe has an average standard deviation of 10.57 mV. This high standard deviation in the measurements can be attributed to two different factors: uncertainty in the pressure transducer reading and high levels of turbulence in the calibration wind tunnel.

Another observation that can be made on the standard deviation of the calibration data is that, if the calibration grid is divided into two portions, a high angle zone, one or both among pitch and yaw angle above 35°, and low angle zone, both angles below or equal to 25°, the high angles zone presents a standard deviation of 11.89 mV while, for the low angles zone, this is 7.53 mV. This different level of uncertainty in the measurements confirms what has been stated in section 2.1, that, at high angle of incidence, the flow on the probe begins to separate and flow separation results in more uncertainty in the pressure readings.

Taking a high number of measurements (400) at each location of the calibration grid is expected to mitigate the effects of such a high standard deviation on the quality of the calibration data.

3.2.2 Visual analysis of the data

The calibration data was also analyzed visually, this has been done by creating a 3D surface representing the voltage readings versus pitch and yaw angle at which the readings had been taken.

Figure 3.8 **Voltage measured at hole 5, surface seen from the pitch vs voltage plane (above) and from the yaw vs voltage plane (below).**Figure 3.8, below, and Figure 3.8, above, respectively represent the voltage from pressure transducer connected to hole 5 seen on the voltage vs. yaw plane and on the voltage vs. pitch plane. The same kind of graphic representations were created for the measurement at each one of the five holes of the pressure probe.

The plots present a smooth surface and no particular spikes, indicating anomalies, have been spotted in the data.
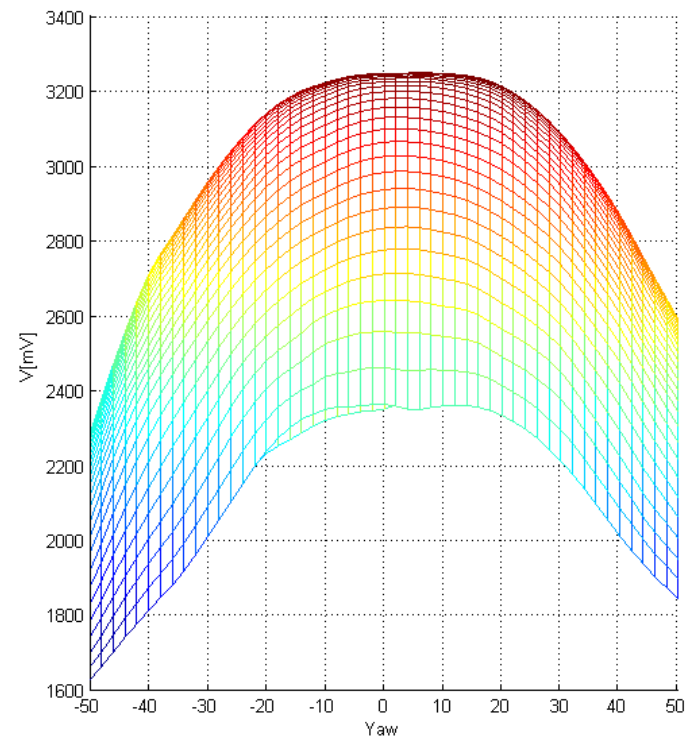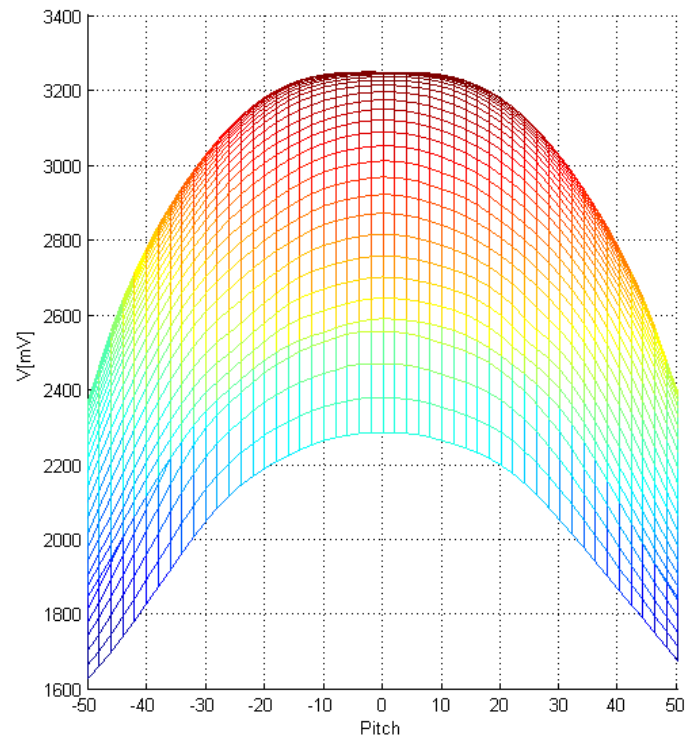
Figure 3.8 Voltage measured at hole 5, surface seen from the pitch vs voltage plane (above) and from the yaw vs voltage plane (below).

However it can be seen in Figure 3.8, below, that the voltage surface is not symmetric with respect to the 0° yaw angle line, on the contrary of figure, representing voltage vs. pitch surface. Since the probe has been machined and adjusted to be perfectly straight and the yaw was carefully aligned during calibration the only possible reason for this anomaly is that the flow was not completely straight and parallel to the axis of the wind tunnel. This was possible also considering that the calibration wind tunnel, in its temporary setup, presented a 90° corner 8 feet (2.44 m) upwind of its outlet.

The misalignment in the flow at the location where the calibration was performed was measured and quantified to be negative 4° in the yaw angle plane. Figure 3.9, above, shows a zoom of the surface representing the voltage from hole 5 in a range of ±25° in the yaw plane, the misalignment is easily visible, as the surface reaches its maximum around positive 5° yaw. Figure 3.9, below, shows the same kind of plot after the 4° correction has been applied, the surface obtained is more symmetrical to the yaw axis then the previous.
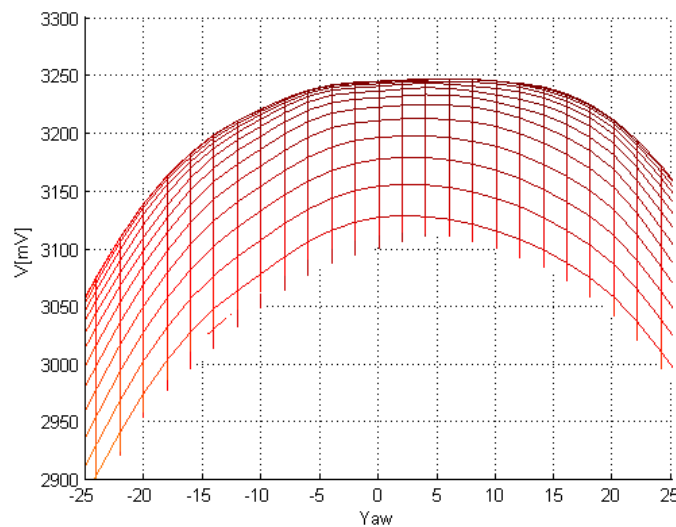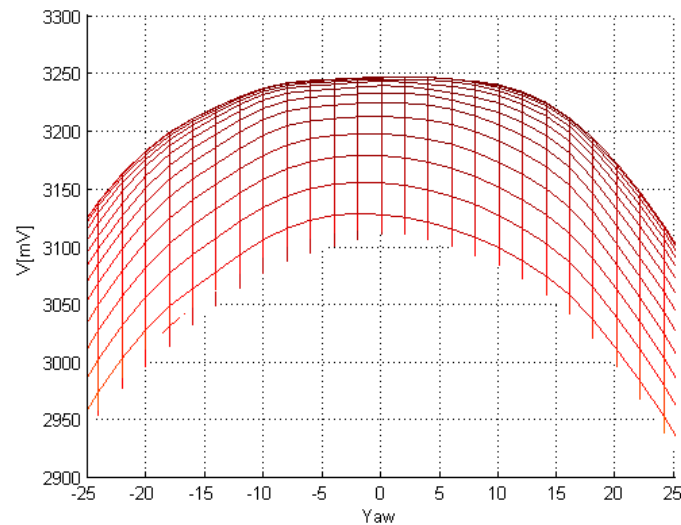
Figure 3.9 Surface representing the voltage reading from hole 5 seen from the yaw vs voltage plane, before yaw correction (above), after yaw correction (below).

Due to the restricted time available for the calibration it was not possible to adjust the flow in the wind tunnel, therefore the correction was applied directly to the data during post processing. The application of this correction restricted the total calibration angle range from ±50° to ±45°, in practice this does not constitute a problem because the new calibration range still exceeds the expected maximum flow angle expected to be encountered during the experiment.

3.3 Data Processing with MATLAB™

Data post-processing is a crucial phase of the calibration procedure. not only because this is the phase where the voltage readings, obtained from the pressure transducers during calibration, are converted to pressures and the pressure coefficients are created, but also because the raw data is analyzed and, if necessary, corrections can be made to the data itself or to the calibration setup.

3.3.1 Pressure coefficient creation
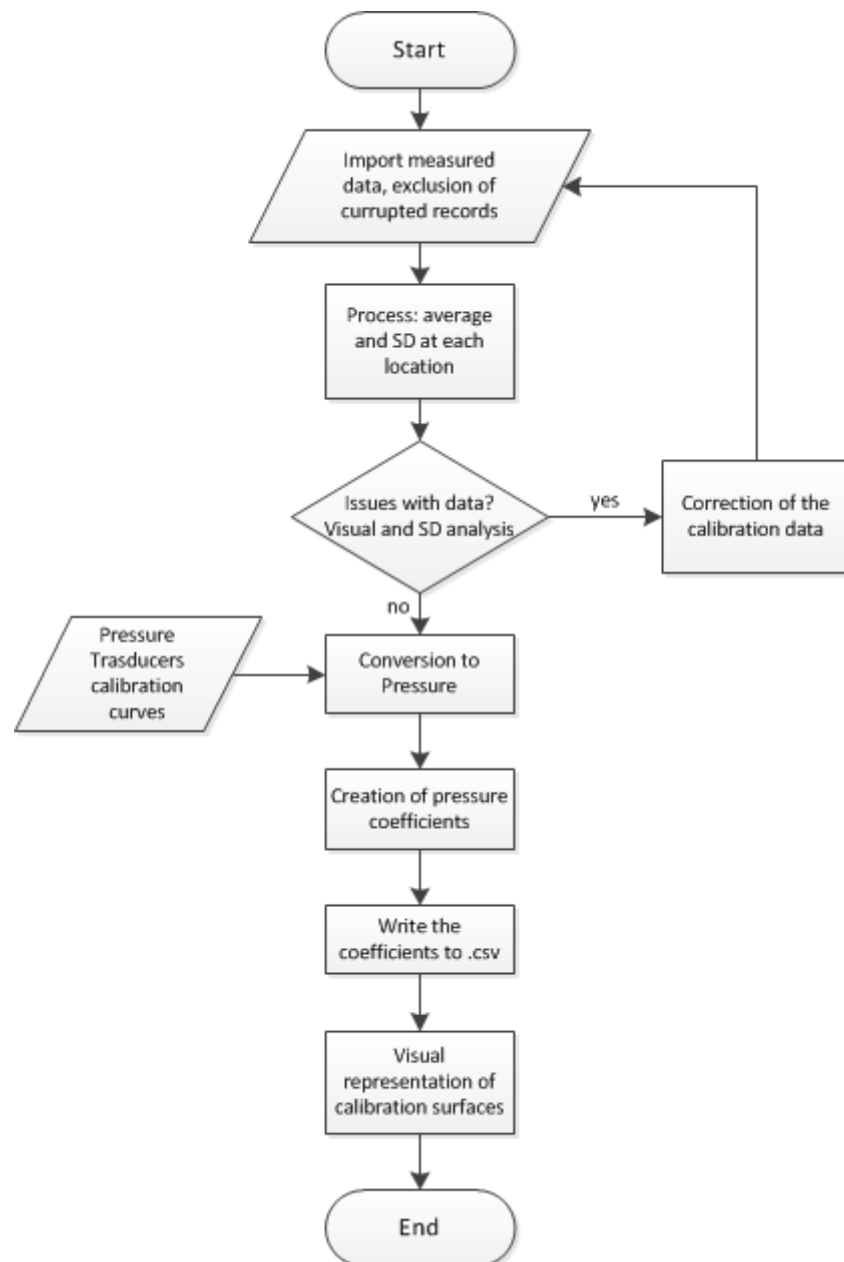
Figure 3.10 Flowchart representing the MatLab™ code used to create the calibration surfaces.

Figure 3.10 shows a flow diagram that synthesizes the post processing procedure of the calibration data, this is performed using MATLAB™ R2014a, license is provided by Politecnico di Milano.

Raw calibration data is imported from the .csv file retrieved from the microSD installed in the DAQ during calibration, here data undergoes a first check where incomplete lines are erased from it. The complete set of data is then processed, the 400 data points for each location are averaged and the standard deviation is calculated. At this point some partial results are examined. Using a visual representation of the voltage measurements as an aid, like the one shown in Figure

3.8, anomalies in the data can be spotted, as explained in the previous section. Standard deviation of the population of data points at each calibration location is also checked for values that exceed 2% of the measurement average itself.

If the calibration data is good enough to pass this validation the voltage values are converted to pressures, using the calibration curve obtained for the pressure transducers. Pressures are then used to create the three different sets of pressure coefficients, that are then written on separate .csv files to be used during the experiment. The pressure coefficients are then visualized on surface plots in order to visually look for anomalies.

3.3.2 Converting pressure readings to inflow conditions

Just as important as creating the pressure coefficients, it is to be able to understand the flow-field measured by the five hole pressure probe starting from the measured pressures.

Figure 3.11 shows a schematics that synthesizes the post processing procedure of the experimental measurement data, this is performed using MATLAB™ R2014a, license provided by Politecnico di Milano.

First some options have to be set: whether or not the dataset was averaged or not, if the characteristics of the flow are known in advance, and if the azimuthally position of the blade is included in the dataset, as it is with the measurements from the actual experiment. Then The dataset is imported into the MatLab™ script to be elaborated. Using the calibration curves of the pressure transducers the voltage is transformed into pressure.

At this point , depending on which of the three sets of pressure transducers have to be used a different subroutine is used to estimate the characteristics of the flow.
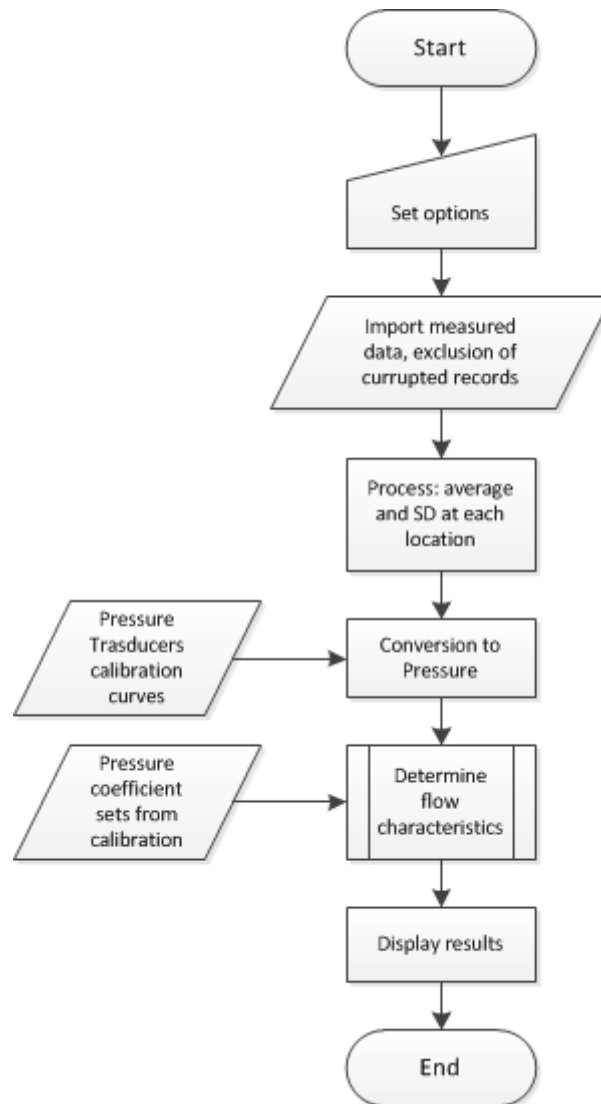
Figure 3.11 Flowchart representing the MatLab™ code used to determine the flow characteristics from the pressure readings.

3.3.3 NREL pressure coefficient

The iteration sequence schematized in Figure 3.12, is the same described by Fingers et al. (13) for the application of a five hole pressure probe on the turbine used for the NREL experiment, with the only change that the initial assumption for dynamic pressure is equal to the highest pressure measured at the five holes and not the reading from pressure 5. This expedient enhanced the capacity of this methodology to determine high flow angles.
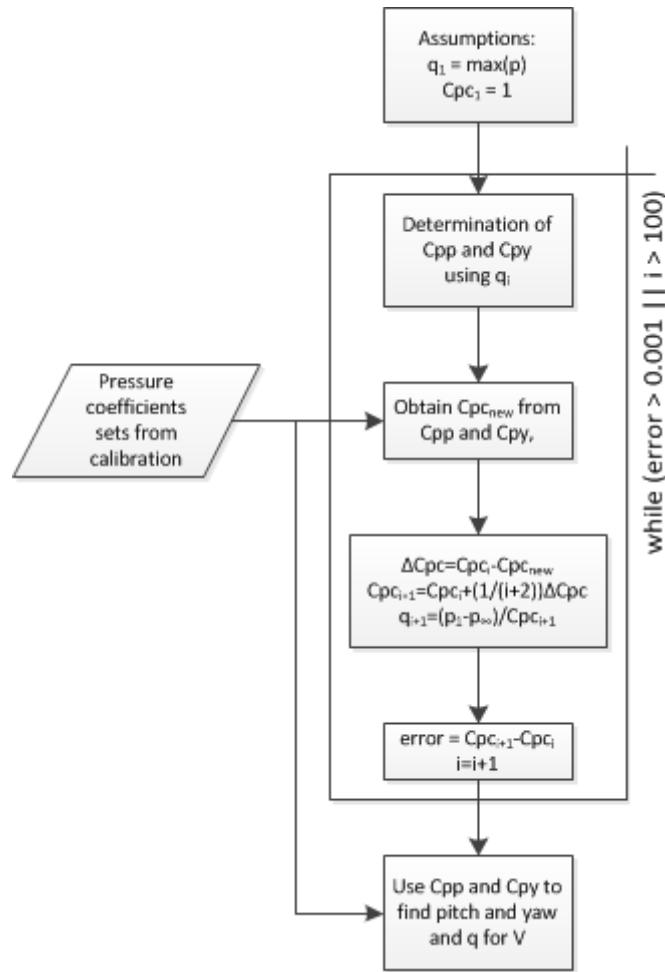
Figure 3.12 Flowchart representing the iterative procedure to determine the flow characteristics using the NREL set of PCs

The iterative process ends after 100 iterations or when the new Cpc differs from the old one by less the 0.001.

Convergence of the result with this method on average is obtained after less than ten iterations.

MatLab™ code used for this approach can be found in Appendix A.

3.3.4 Mono zone pressure coefficient

This is the approach to determine velocity and angles of the flow using the mono-zone pressure coefficients. Schematics of this approach is shown in Figure 3.13.
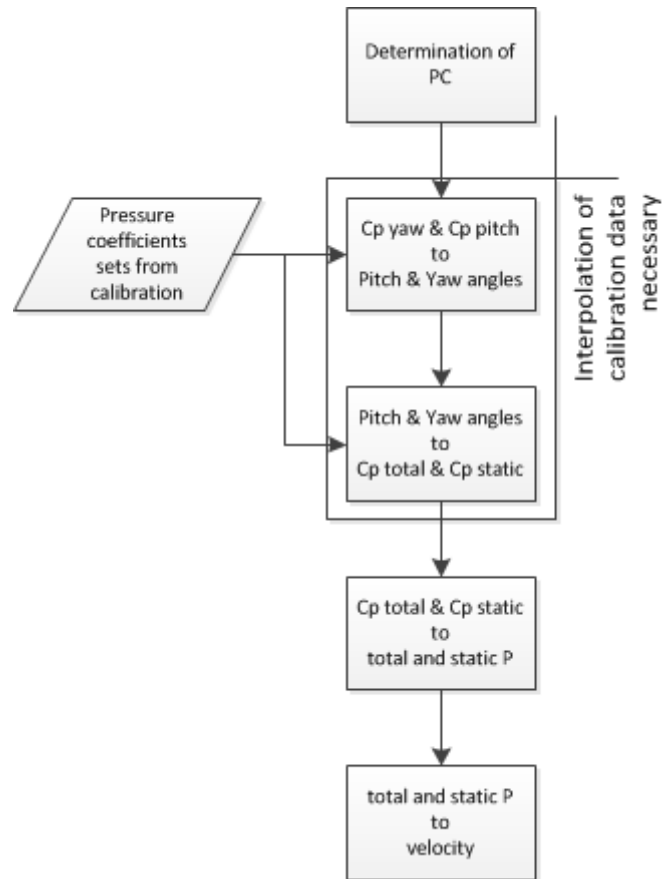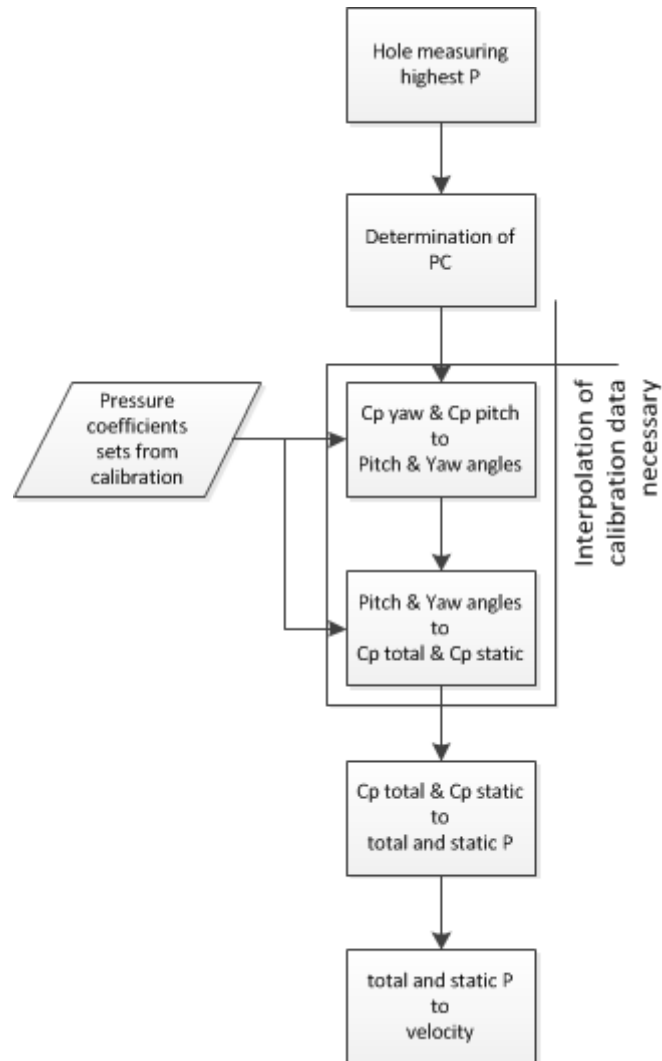
Figure 3.13 Flowchart representing the procedure to determine the flow characteristics using the mono-zone PCs.

MatLab™ code used for this approach can be found in Appendix A.

3.3.5 Multi zone pressure coefficients

Figure 3.14 represents a schematics of the approach used to determine velocity and angles of the flow when the multi-zone pressure coefficients are employed. It differs from the previous approach only in the fact that, based on the hole that it's measuring the highest pressure a different combination of pressures is used to obtain the coefficients and consequently the characteristics of the flow.

Figure 3.14 Flowchart representing the procedure to determine the flow characteristics using the multi-zone PCs.

MatLab™ code used for this approach can be found in Appendix A.

3.3.6 Surface interpolation method

For a precise determination of the characteristics of an unknown flow using a five hole pressure probe, it is fundamental to find the best way to interpolate the calibration data. As explained calibration was performed over a grid of angles equally spaced by 5° steps increment, as the flow, during experimental measurement, will not necessarily come from one of the angles on the calibration grid, the necessity for a valid interpolation method becomes clear.

Three different interpolation methods have been taken into analysis, the most conventional one, that is based on the interpolation of calibration data with fourth

order polynomial, and two direct interpolation methods, linear and cubic interpolation.

Silva et al. (20) give a clear view on the different result that the application of fourth order polynomial or linear interpolation have on the validity of the measurement, they found that the inaccuracy errors for both angles and velocity, decrease from 1.5% with 4th order polynomial to 0.8% with linear interpolation. This same result was also confirmed by Zillac (14).

Since the analyzed five hole pressure probe literature, is strongly in favor of direct interpolation methods instead of polynomial interpolation, the choice was between linear interpolation and cubic interpolation.

In order to allow to assess the error resulting from the use of one interpolation method or the other, data at different probe position other than the one the calibration grid one was acquired during the calibration procedure. For those points the characteristics were calculated based on the data obtained from the calibration and using the pressure readings from the five hole pressure probe. Since the flow characteristics were actually known from the beginning, it was possible to estimate the errors caused by different interpolation methods by subtracting the calculated value to the known ones.
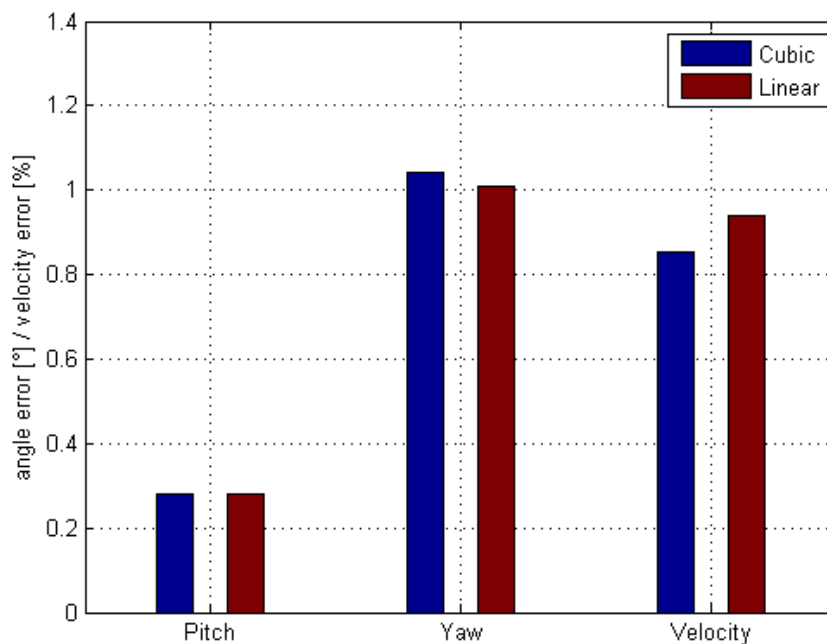
Figure 3.15 Computed five hole pressure probe errors due to cubic and linear direct interpolation method.

Figure 3.15 represents the computed errors. In a general way it is possible to see that the two direct interpolation methods give almost equivalent results. Normally

one would expect cubic interpolation to be more precise, the reason for this substantial equivalence can be identified in the fact that the calibration grid has a quite high resolution.

Another fact that can be noticed is that errors on the yaw plane tend to be much higher than errors on the pitch plane 0.28° pitch compared to around 1° yaw. The reason for this trend can be identified with the higher uncertainty generated by the manual yawing mechanism compared to the automated pitching mechanism.

After an accurate evaluation of the difference in the two interpolation methodologies cubic interpolation was chosen mainly for two reasons. First, it is the one that seems to give a slightly better results when it comes to the determination of the velocity of the flow. Also, cubic interpolation had been previously employed by the research group for different purposes, always with a reliable outcome.

3.4 Interpolated calibration surfaces

As said, three different sets of pressure coefficients have been comparatively evaluated during data post processing. This process has the scope to lead to the identification of the set of pressure coefficients that is more suitable for the application of a five hole pressure probe for local inflow studies on an horizontal axis wind turbine.

3.4.1 NREL PCs

In order to understand the goodness of the data collected during calibration, 3D surfaces obtained with pressure coefficient cubic interpolation have been compared to some examples that were found in literature.

The plots in Figure 3.16 represent the surfaces obtained interpolating the pressure coefficients obtained using the same approach that was used during the NREL unsteady aerodynamics experiment. When confronted with Figure 3.17 it is clearly visible that the surfaces shape match with a good degree of accuracy. The surface representing the yaw angle was omitted for brevity.

This is very important because until this stage of the experiment it hadn't been possible to be sure in any way that the approach and the choices made for the calibration and data collection were correct, or even that the five hole pressure probe and the instrumentation itself were working properly.
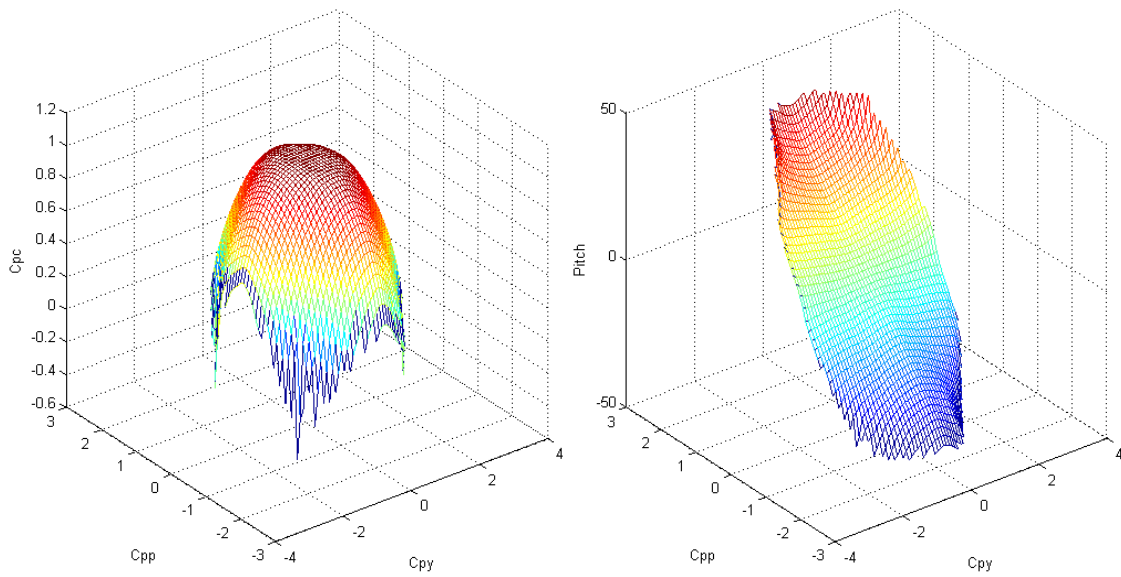
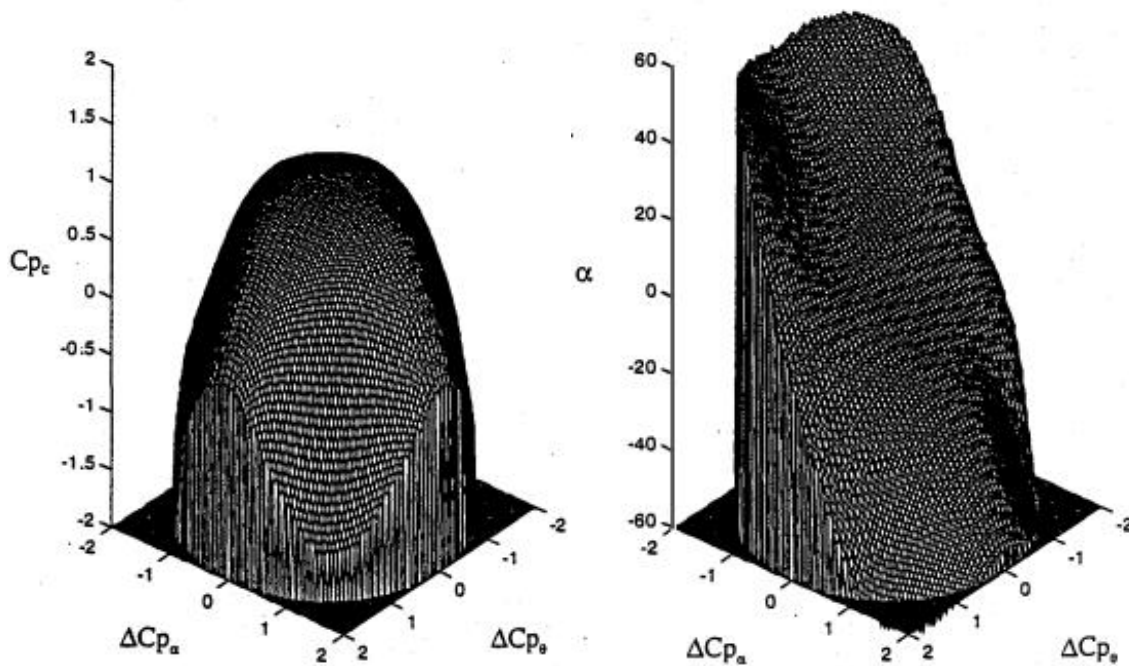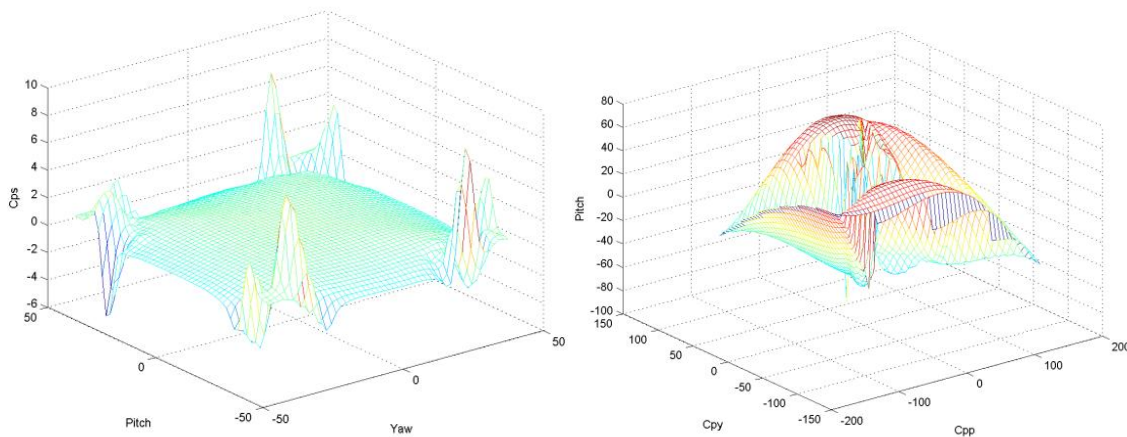**Figure 3.16** Calibration surfaces obtained with the NREL set of PCs, Center hole PC (left), Pitch PC (right).

Figure 3.17 Calibration surfaces taken as reference for the NREL set of PCs, Center hole PC (left), Pitch PC (right) **(13)**.

3.4.2 Mono-zone PCs

The second set of pressure coefficients analyzed is the one that was firstly introduced by Krause an Dudzinsky (12) in 1969, considered the more normal way to normalize pressures.

Figure 3.18 shows the calibration surfaces referred to the static pressure coefficients and the pitch pressure coefficient obtained using this approach. It is clearly visible that the figures present a surface that is not smooth as the one obtained with the NREL pressure coefficients, it is therefore possible to assume that some kind of errors are present using this approach.

Figure 3.18 Calibration surfaces obtained for ±50° yaw and pitch angle range using the mono-zone PCs, Static PC (left), Pitch PC (right).

The reason for this "pointy" calibration surfaces has been identified in the fact that the flow on the lee side of the pressure probe begins to separate at high flow angles. As anticipated in section 2.1 Zillac (14) reports that at flow incidence angles exceeding approximately 30° this separation phenomena begins to take place, therefore calibration coefficients based on the pressure variations sensed by holes located beneath the separated region will no longer uniquely determine the flow angle of the probe.

This hypothesis finds an additional confirmation in Figure 3.19, this represents the same interpolated surface, with the difference that the calibration range has been cut down to 30° pitch and yaw angle. This restricted calibration range is not affected by flow separation on the lee side of the probe and therefore the obtained calibration surface is smooth, and accurate results can be obtained using it as long as the flow angle remain in this limit.
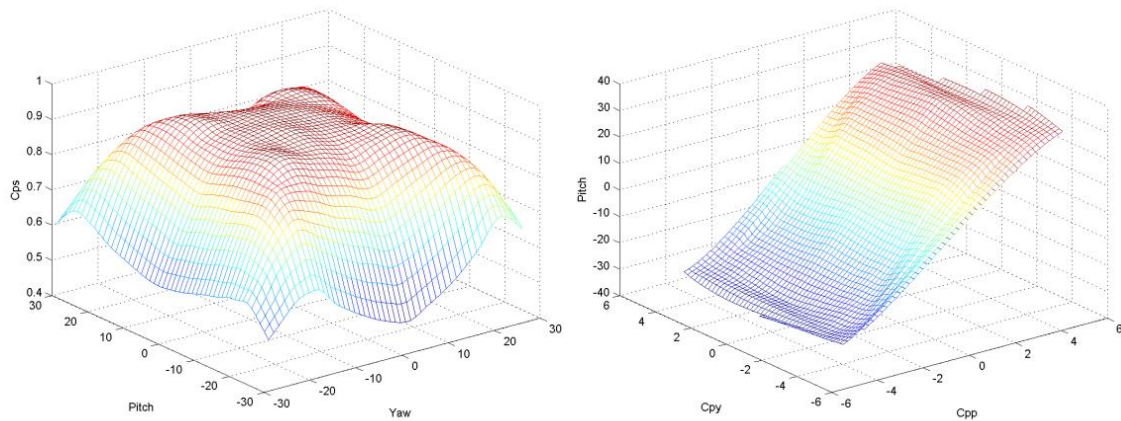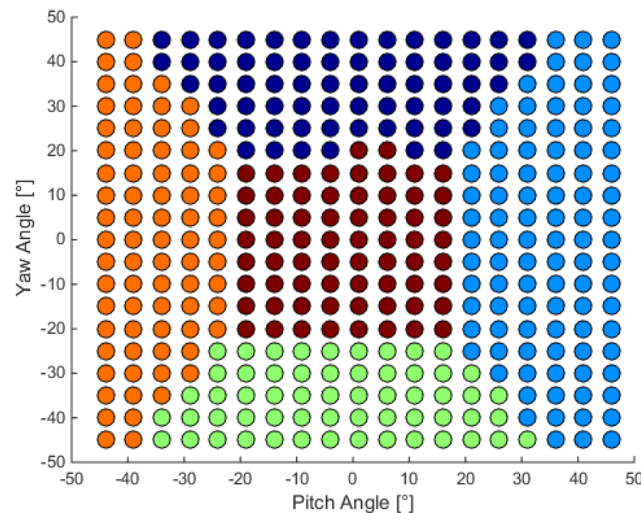
Figure 3.19 Calibration surfaces obtained for ±30° yaw and pitch angle range suing the mono-zone PCs, Static PC (left), Pitch PC (right).

The particular shape of the static pressure coefficient surface is the same found in Treaser et al (11), this is a further confirmation of the validity of the calibration data collected.
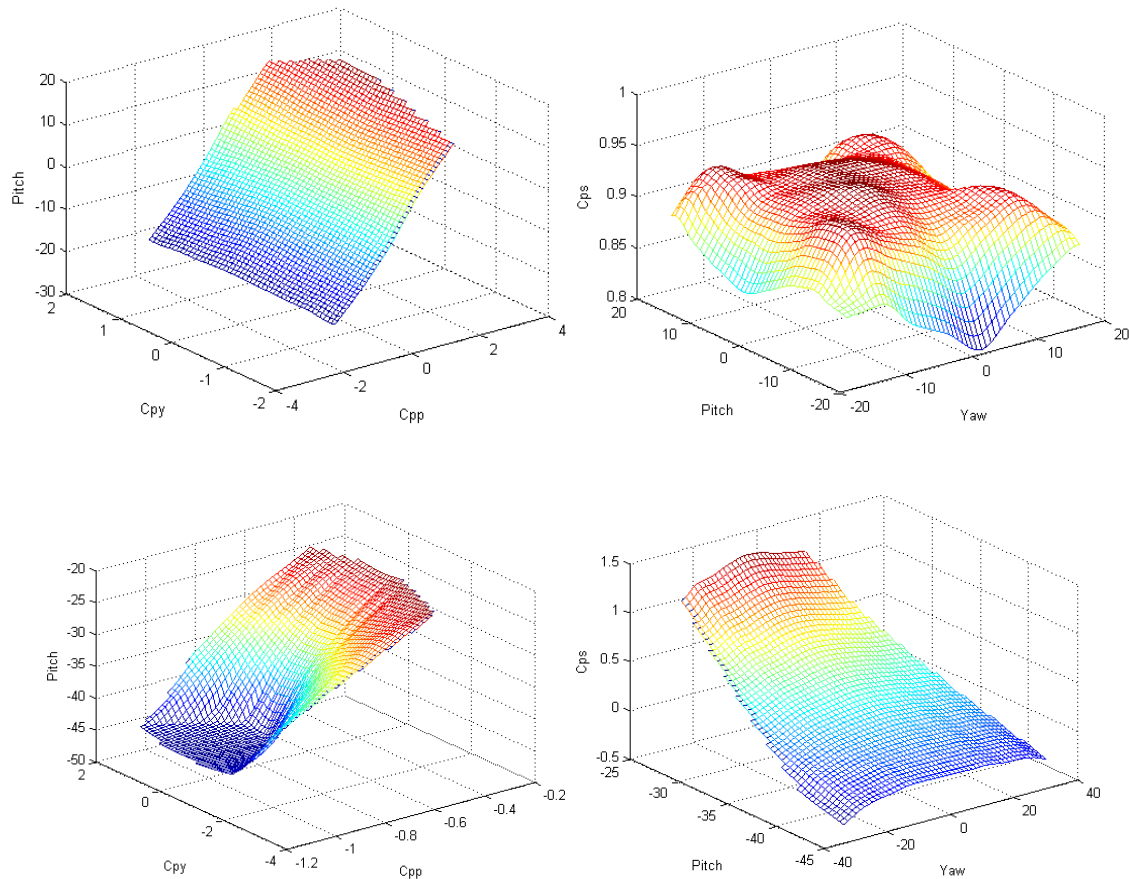
3.4.3 Multi-zone PCs

The last set of pressure coefficients analyzed is based on a particular approach, the sectoring scheme, introduced in section 2.1 Figure 3.20 shows the subdivision in zones of the calibration grid, this is based on the hole that is as sensing the highest pressure at each location during calibration.

Figure 3.20 Plot representing the division in zones based on the hole that is measuring the highest pressure; blue zone1, azure zone2, green zone3, orange zone4, red zone5.

Below is an example of the typical calibration surfaces obtained with the sectoring scheme approach, figure shows the centre zone, when hole 5 is measuring the highest pressure, while figure shows calibration surfaces for zone 3. For brevity zones 1,2, 4 and total and yaw pressure coefficients have been omitted.

Figure 3.21 Calibration surfaces obtained using the multi-zone PCs, Pitch PC zone 5(top left), Static PC zone 5(top right), Pitch PC zone 3(bottom left), Static PC zone 3(bottom right).

Compared to the previous set of pressure coefficients, the sectoring scheme allows to omit the pressure reading that are subject to flow separation. Figure 3.21 shows how, even for angles of incidence up to 45°, the surface remains smooth and no singularity points are shown. Zillac (14) claims that this calibration technique gives valid result up to 70° of incidence, after this limit extensive flow separation happens on the probe's tip causing this type of calibration to fail to give accurate results.

3.5 Experimental error analysis

Figure 3.22 shows the experimentally obtained errors for each one of the three sets of pressure coefficients.

These errors have been determined by placing the probe into a known flow field. For this purpose the same setup used for the calibration was employed, the five hole pressure probe was moved to a number of known angles using the traversing system and, the calibration wind tunnel was set to various wind speeds, this allows to virtually reproduce any flow condition that could be encountered during the use of the probe on the wind turbine.

Accuracy of the yaw angle measurement is greatly influenced by the low resolution of the manual yawing device (one degree), this is by far the dominant source of error when it comes to yaw angle determination, in fact the only difference between the pitch and yaw angle determination procedure is the mechanism employed to traverse the five hole pressure probe. Using an automatic yawing device in the future is expected to highly improve the overall performance of the five hole pressure probe.

Figure 3.22 reveals that the set of pressure coefficients that was used for the NREL study gives worst results then the other two sets employed, both for flow angle determination and velocity determination.

The other two methodologies, mono-zone and multi-zone pressure coefficient set, present almost the same degree of accuracy, with the results of the error analysis slightly in favor of the multi zone pressure coefficient approach.
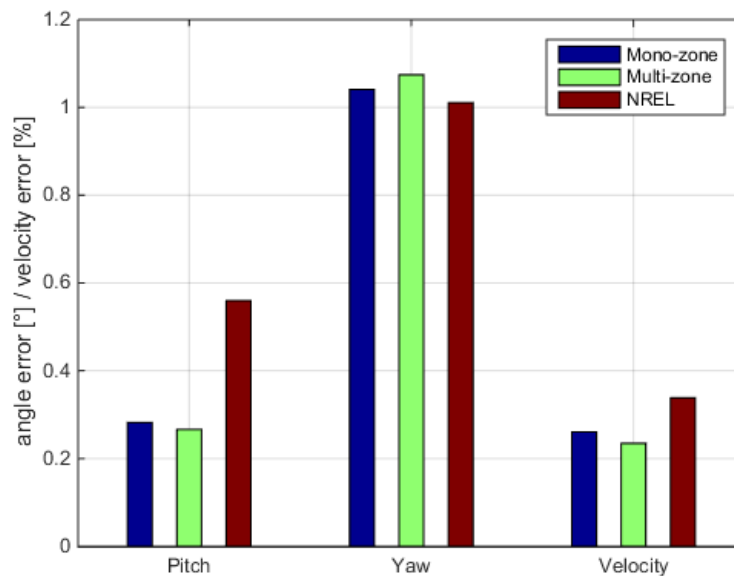
Figure 3.22 Experimental errors for the three sets of pressure coefficients.

Another factor that favors the choice of the multi-zone set over the mono-zone one, is, that the latest allows to extend the range of incident angles where this measurement method is applicable, as explained in section 3.4.2, by ignoring the pressure measurement from the hole where the flow is detached.

This factor is not shown in the result of the error analysis because the angles that have been measured for this analysis are all below ±30°, that, according to Zillac (14), is the maximum angle that the mono-zone pressure coefficient set is accurate at.

The present analysis has been performed on a low number of measurement points, increasing the number of this points to a few hundred at least would allow to have more accurate results. As suggested by Zillac (14), it is also advisable to subdivide the onset flow angle studied in two zones for error determination, one for higher angles and one for angles that are below 30°, this is because of the different probe response in those two different flow conditions.

3.6 Preferred method

Subsequently to the error analysis it has been decided to employ the multi-zone pressure coefficient set for the application of five hole pressure probe to study the local inflow characteristics on a horizontal axis wind turbine.

This approach presented a some considerable advantages over the two others analyzed:

- The experimental error analysis showed that this methodology is consistently more precise than the NREL approach and slightly more than the mono-zone.
- The multi-zone pressure coefficient set allows to extend the range of the acceptable inflow angles up to ±70°, compared to the ±30° of the mono-zone set.
- Compared to the NREL pressure coefficient set the multi-zone set doesn't need actual flow static pressure as a reference, and this is a considerable advantage compared for the application of the five hole pressure probe on a rotating support, like the blade of a wind turbine, subjected to highly unstable flow conditions. This aspect will be examined in more detail in section 4.4.2.

3.7 Possible improvements to the calibration procedure

The calibration of the five hole pressure probe was not in the initial experimental plan. The plan was to retrieve a probe that had already been calibrated, to be used for the experiment. Due to logistical problems it was not possible to retrieve the calibration data regarding the pressure probe that was found in the laboratory, therefore, the calibration had to be obtained on a really tight time schedule.

The scarcity of time available for the calibration of the pressure probe, made it necessary to take rushed decision that certainly influenced in different ways the accuracy of the calibration data.

In this paragraph I'll identify those choices and explain how, after data post processing and its evaluation, they could be modified or corrected in order to obtain a more accurate calibration of the pressure probe.

- **Changing the manual yawing device (1° of resolution) with a more precise automated one**.
  The choice was to use a manual yawing device to save time in the design and construction stage of the traversing system. The manual yawing device was identified as the only source of the error difference between the accuracies on the yaw plane compared to the pitch plane (0.25° error on the pitch plane compared to more than 1° on the yaw plane).
- **The temporary setup of the calibration wind tunnel also contributed to increase experimental uncertainty of the calibration**.
  The elbow that was present 8 feet (2.44m) upwind of the tunnel's outlet influenced the turbulence conditions and the axiality of the flow. this two effects have been accounted for and partially corrected during data post processing, but it is a sure fact that employing a better wind tunnel would give more accurate calibration results.
- **A more accurate error characterization can be performed if more points were available to read the flow characteristics after the calibration.**
- **It is also advisable to perform a calibration of the pressure transducers**.
  For this experiment the zero-pressure point of each pressure transducer has been measured and then linear characteristic has been assumed based on the specification given by the producer. Pressure transducer calibration must be performed with great care and employing an instrument with a very high resolution, because, error in this procedure could lead to higher inaccuracies that simply relying on the producer's specification.

Chapter 4   Experimental setup

The calibrated five hole pressure probe had then to be installed on the wind turbine for the actual experiment to take place. The wind turbine is a newly custom built wind turbine installed inside a large scale wind tunnel at the University of Waterloo, in this chapter more details will be given about the wind tunnel, the wind turbine and the installation of the probe.

## 4.1 Large scale wind tunnel facility (FireLab)

The University of Waterloo Fire Testing facility, the FireLab, is to be used for the experiment, this is an open circuit wind tunnel. The air flow is created by a set fans. Compared to other wind tunnel this facility has the advantage of presenting a relatively high turbulence and, due to the relatively large plenum (12.96m high by 15.4m wide at its largest dimension), a low flow blockage ratio, this is a good resemblance of realistic flow conditions for wind turbine during actual operations. The facility has a turbulence intensity in the range of 5.9% to 6.2%, as reported by Gertz and Ahmed (21), and nominal wind speeds between 0 and 11.5 m/s. In detail wind velocity measurement at the location where the wind turbine is installed can be found in Gaunt and Johnson (22).
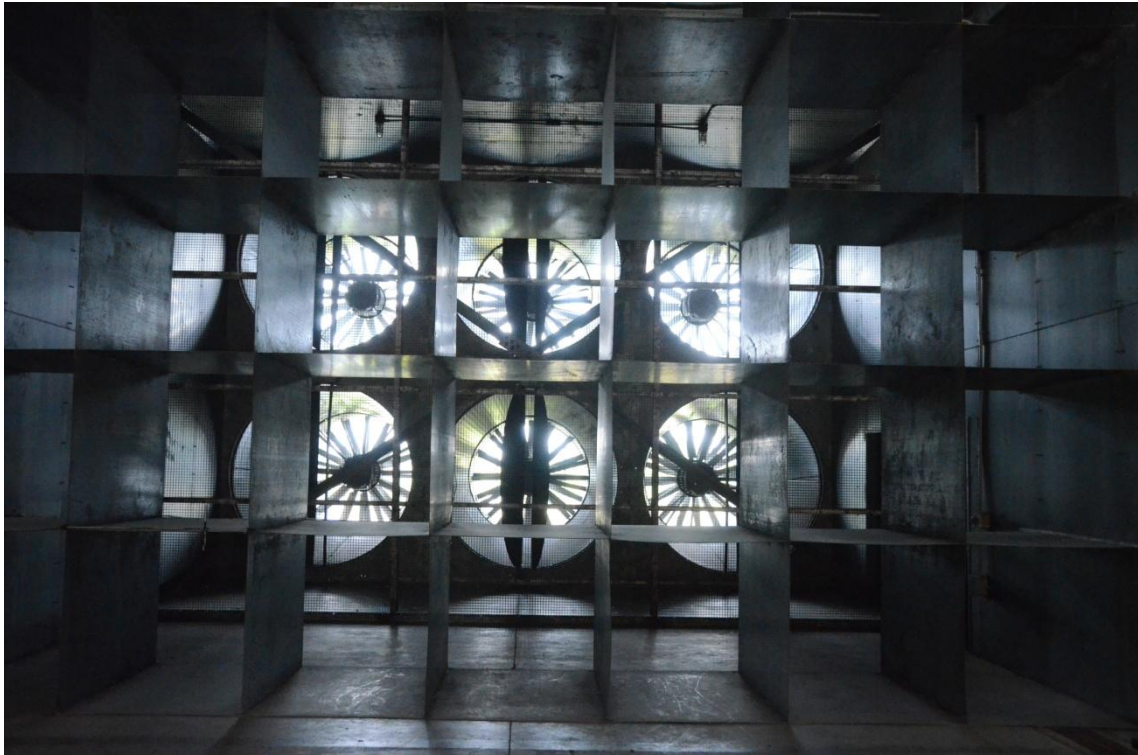
Figure 4.1 Array of 6 fans to drive the flow in the wind tunnel and flow strengtheners.

The fans used in the wind tunnel are six Howden-Buffalo Model 78-26 Series 1000 with a diameter of 1.98 m each. The six fans are arranges in a 3x2 (horizontal x vertical) array. The fans and flow strengtheners layout can be seen in Figure 4.1. Wind speed is controlled by changing the fans rotational speed, this is done by controlling the frequency of six the driver motors. The motors can be remotely controlled from a separate control room. Fans can individually be set at different rotational speeds, this is important in order to simulate horizontal and vertical wind shear if necessary.

Figure 4.2 reports the layout of the wind tunnel facility, with the pink surface being the inflow area and the blue surface the outflow to the wind tunnel.
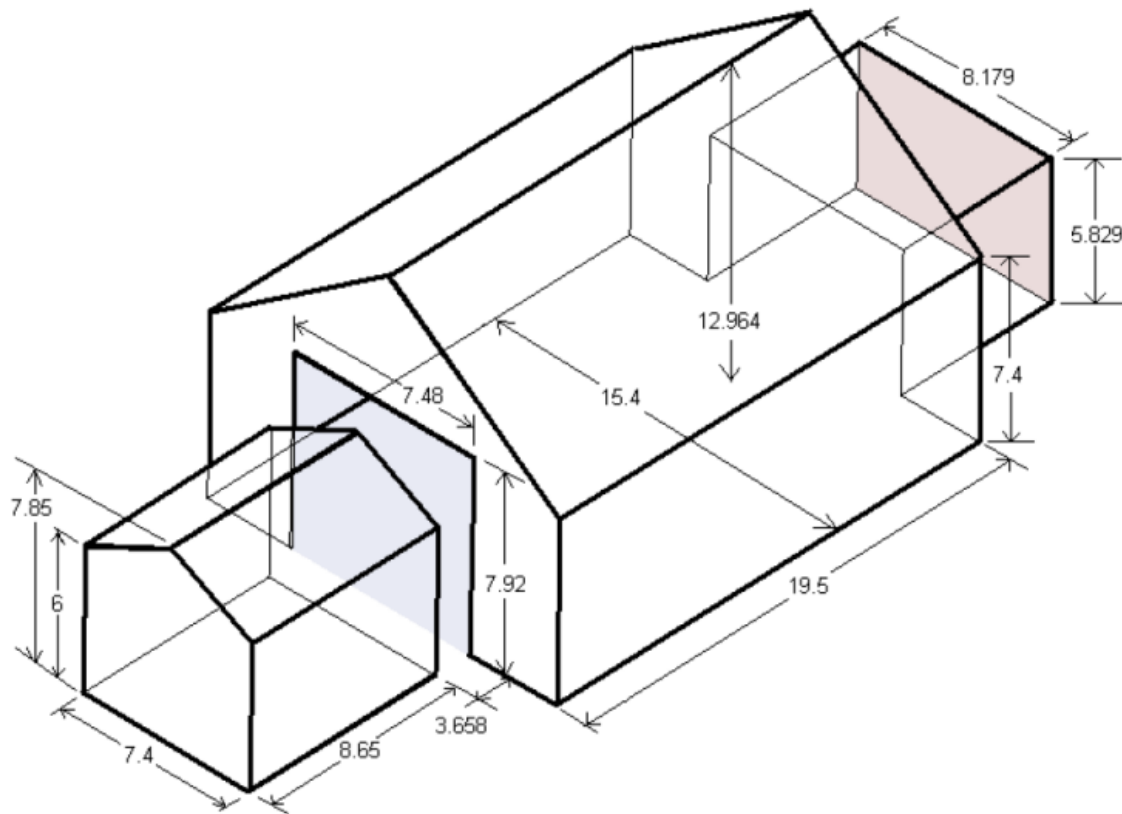
Figure 4.2 Model of the FireLab wind tunnel, position of the 6 fan array (inlet) in red, wind tunnel outlet in blue, dimensions in meters **(23)**.

4.2 Horizontal axis wind turbine test rig

The horizontal axis wind turbine on which the five hole pressure probe had to be installed for the experiments is a custom built new machine, whose main characteristic is its versatility, it had been designed in order to be employed in a number of different experiment.

4.2.1 Test rig characteristics

The test rig's most important characteristics are shown in Table 4.1. An in depth description of the wind turbine, its components, of the design and construction process can be found in Ahmed (23).

Chapter 4

Table 4.1 Test rig main specifications.

Specification	Value/Range	Details
rotor diameter	3.4	m
max dimensions (W/H/L)	3.4 / 1.5 / 0.3	m
hub height	3.05	m
total weight	350	kg
natural frequency	108	Hz
nacelle dimensions (W/H/L)	0.3 / 0.36 / 1.45	m
rotation speed	0-230	rpm
yaw angle	±30	degrees
max rotor weight	80	kg
power capacity	3.7	kW

What can be considered the test rig main characteristic, it's its versatility, the wind turbine has been designed to be subject to continuous improvements. The "Wind Energy Group" aims to keep adding different pieces of instrumentations to this small scale wind turbine, the installation of five hole pressure probe is part of this program to have a test rig that is completely instrumented and capable of measuring a wide range of different parameters.

The hub that assembles the rotor at the end of the drive shaft has been designed considering that the test rig must be capable of supporting very different rotors. As it can be observed in Figure 4.3, the main components of the hub are two steel plate separated by a PVC spacer, different kinds of blades can be installed on the turbine by simply machining new steel plates and a new PVC spacer.

Yaw of the wind turbine can also be adjusted in a range of ±30°, with a resolution of 5°, in order to simulate cross wind situations.
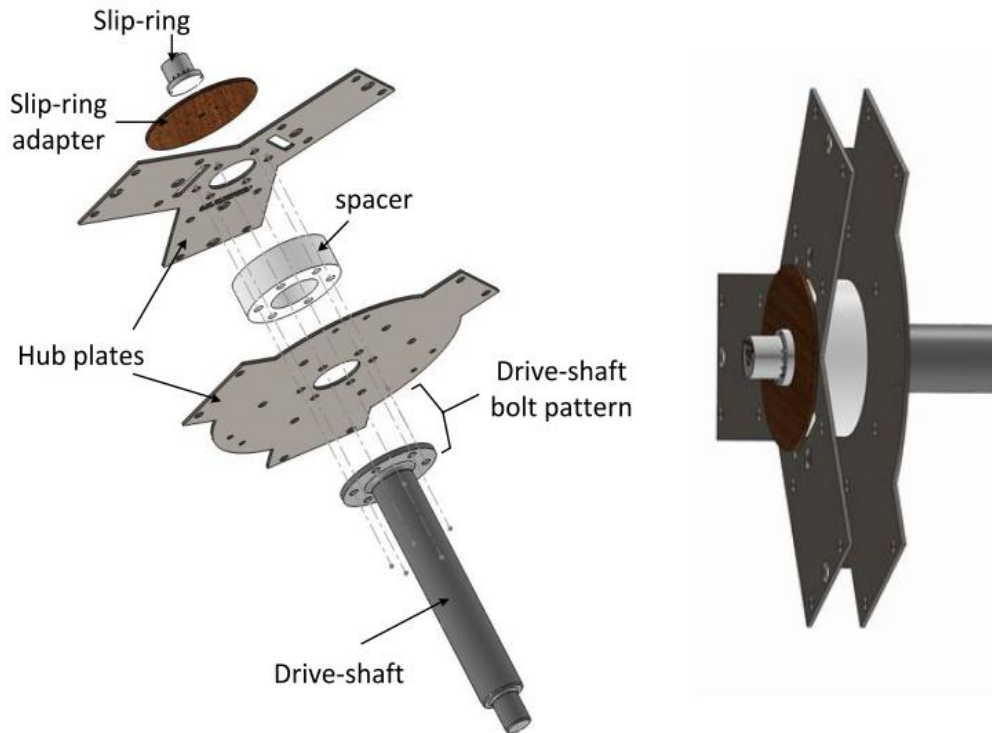
Figure 4.3 SolidWorks™ hub and drive-shaft design **(23)**.

4.2.2 Test rig's main components

Figure 4.4 shows a 3D model of the test rig and its main components.

The motor/generator used is a Marathon Electric Y287 184TC frame vector motor (24). It has a maximum power of 5 Hp and a maximum rated rotational speed of 1800 rpm. It is equipped with a encoder and accurate speed control can be achieved through the main wind turbine controller. The motor's rotational speed is varied through a variable frequency drive (VFD), this is mounted on a panel that is connected to the main controller through and underground duct and it's controlled by it. The motor is coupled with a brake for parking the rotor when it is not in use and for emergency braking, this can as well be electronically triggered through the main control.

The gearbox used is the Nord Helical in-line Gearbox SK572.1, this is used to reduce the motor speed to the required operational range of the wind turbine and it has a 7.49:1 reduction ratio

The Futek TRS 605 torque sensor was selected to be installed on the test rig, as seen in Figure 4.5. This is a non contact shaft to shaft rotary sensor with 200 Nm torque capacity and is equipped with rotary encoder. Since this component is very delicate piece of equipment and very sensitive to misalignments it is placed in between two couplings used to connect it to the shaft.
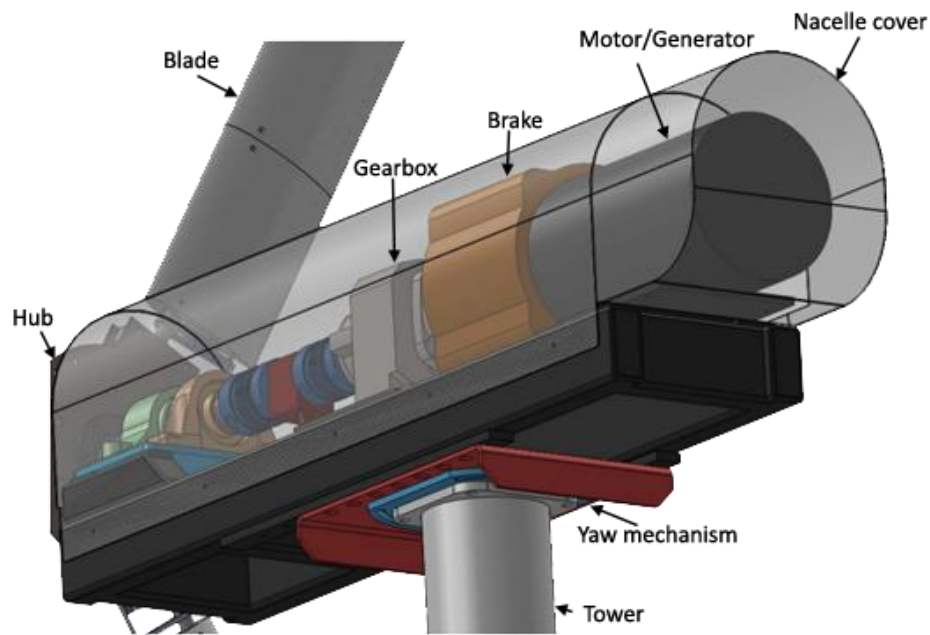
Figure 4.4 SolidWorks™ model of the wind turbine nacelle and its internal components **(23)**.
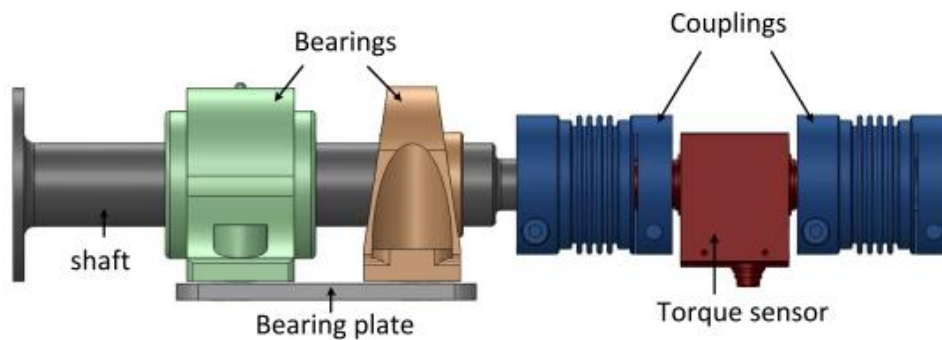

Figure 4.5 SolidWorks™ model of the drive shaft and torque sensor position **(23)**.

4.2.3 Control system

As said the test rig is remotely controlled from the wind tunnel's control room through a control sub-panel and a computer. Figure 4.6 shows a schematics of the connections between the test rig and the control equipment, located in the wind turbine control room, through the underground access duct.

The sub panel in the control room is the main control tool used for the test rig. Through this device's touch screen it is possible to control and monitor rotational speed, acceleration of the blades and power production/consumption. The sub panel also includes start, stop diagnostic and emergency stop buttons. The sub

panel is also accessible from a personal computer through Ethernet connection, the code to fully control the turbine from a personal computer is currently work in progress.

The sub panel is connected through Ethernet connection to the main control panel of the wind turbine, this, with a variable frequency drive, controls the rotational speed of the blade. The main panel also has the function of controlling the brake and providing power to the motor. This is placed 4 meters downwind of the wind turbine inside the wind tunnel, this choice was made in order to allow it to eventually dissipate in the air flow the energy generated by the turbine in the form of heat.
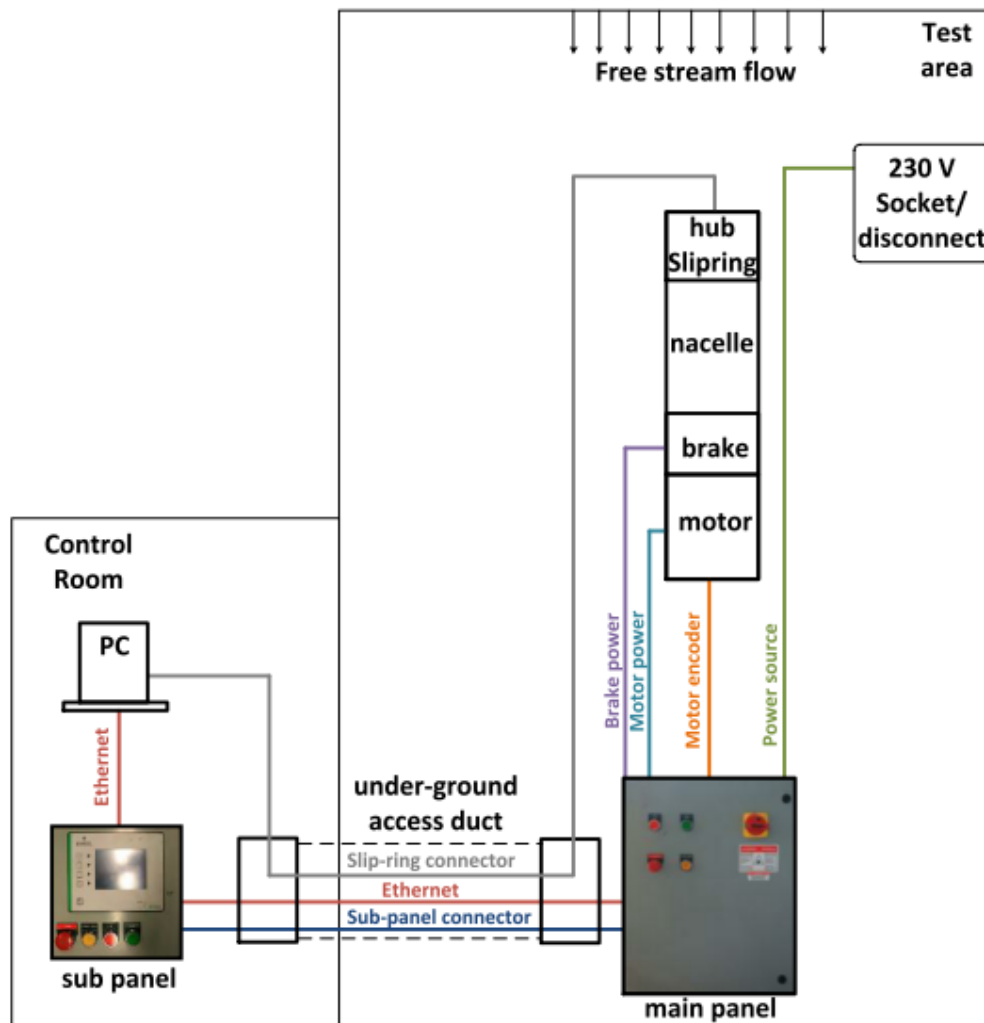

Figure 4.6 Connections between the turbine and the wind tunnel control room **(23)**.

4.2.4 Instrumentation installed on the wind turbine

As mentioned above the test rig is instrumented with various pieces of equipments that allow to monitor a number of operational parameter of the wind turbine. Table 4.2 reports details about this measurable parameters and the instruments used to measure them previous to this experiment.

Table 4.2 Instrumentation installed on the wind turbine

parameter	instrument	unit
rotor's speed	motor's encoder	rpm
wind speed	sonic anemometer	m/s
turbine's yaw	compass	degrees
power production/consumption	variable frequency drive	W
blade's strain measurements	3x SGD-7/1000-DY11 strain gauges	mV/V (converted to Nm)
temperature	sonic anemometer	°C

The present experiment aims to add a number of measurable functioning parameters, like the instantaneous position of the rotor's blade, instantaneous local inflow characteristics and generated torque.

4.2.5 Torque sensor installation

As said Futek TRS 605 (25) was chosen to be installed on the test rig, also because of the built-in rotary encoder. The rotary encoder is a fundamental equipment for the present experiment, this is because inflow measurements from the five hole pressure probe, are almost meaningless if not precisely associated with the blade's azimuthal position at which they have been taken.

Due to delays in its shipping the torque sensor had not been installed on the test rig previous to the beginning of this experiment.

The torque sensor was tested and installed and the code for reading the rotational encoder had to be written in order to retrieve the azimuthal position of the blade during its rotation. The torque sensor's rotary encoder outputs 360 pulses per revolution and therefore has a resolution of 1°.

Some noise issues have been encountered to read the signal sent by the rotary encoder to the computer used for data acquisition purposes. Initially a cable with low noise shielding was employed to send the signal from the sensor in the turbine's nacelle through the underground duct to the computer used for data acquisition. Since the digital pulses from the sensor's encodes must be very clean to be correctly interpreted by the computer, the electromagnetic noise generated by the motor/generator in the nacelle and by the other cables in the underground duct, was corrupting the signal. To solve this problem a new 30 feet cable with a high noise resistance had to be purchased, the time required for the purchase of the cable made it impossible to retrieve the encoder's signal and therefore to use the encoder to trigger the pressure measurement for the present experiment.

Installation of the newly purchased cable and retrieving data from the encoder is currently work in progress.

4.3 Multi hole pressure probe on the turbine's blade

This section outlines the aerodynamics and structural characteristics of the rotor that was used in this study, and the installation of the calibrated multi hole probe on one of its blades.

4.3.1 Present rotor's characteristics

The rotor that was used in the present study, on which the multi hole probe had to be installed, is a custom built 3D printed modular rotor, designed by Ahmed (23) and previously used to perform a study on the possible use of TEFs (trailing edge flaps) for active flow control applications.

The rotor was assembled to the test rig and operated in the UW Firelab facility, therefore it had been design and optimized based on the ranges of operating conditions of the above cited facility and wind turbine.

The rotation speed chosen for the blade design was 200 rpm. It was also concluded from studies done on the flow characteristics of the facility mentioned in section 4.1 that the rotor diameter should not exceed 3.3 m for blockage reasons, therefore the design blade length was set to be between 1.6 and 1.7 m. Even if the maximum wind speed produced by the UW wind facility is 11 m/s, in order to avoid stall, which would have distorted the load distribution on the blade, the design conditions for inflow wind speed were set to be between 6.5 and 8.5 m/s.

Although the standard for HAWTs is to have a three bladed rotor, a single bladed balanced rotor was installed on the test rig. This choice had been made for several

reasons. Firstly there were not enough communication channels (provided by a slip ring) to instrument more than one blade. Secondly the load patterns are symmetric and since the goal of the experiment is not to maximize or measure efficiency, but to study the aerodynamic behavior of the blade and correlate it to the loads on it, one blade was thought to be enough. Lastly consideration is made for prototyping time and cost for the test rotor. The rotor was set to have one aerodynamic blade and two counter-weights attached to the three-bladed hub, those were installed for the sole purpose of balancing the rotor in order to reduce excessive vibrations and loads on the hub, bearings and on the tower.

Table shows the rotor's main characteristics.

Table 4.3 Designed rotor main characteristics, rotor design **(23)**.

Parameter	Range/value	Unit
Aerodynamic blades	1	unit
Rotor radius	1.7	m
Design rotational speed	200	rpm
Design wind speed	6.5 – 8.5	m/s
Number of flaps	2	unit

The only aerodynamic blade presented constant airfoil, chord and twist angle. This choice had been made by Ahmed (23) in order to be able to easily accommodate the flaps, change their location on the blade and to dynamically control their angle with a stepper motor.

The airfoil that had been chosen for the blade is the NREL S833 airfoil, it comes from a set of airfoils that was specifically designed for wind turbines with blade lengths from 1 to 3m.
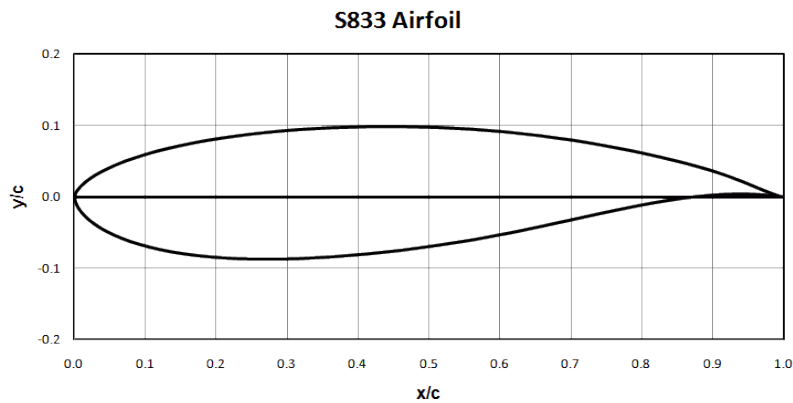
S833 Airfoil

Figure 4.7 NREL S833 airfoil shape **(26)**.

The detailed geometry had been determined using the BEM design code and the constrains above, to optimize the efficiency of the blade. The simulation results suggested a 178mm chord and 6° pitch angle for the blade.

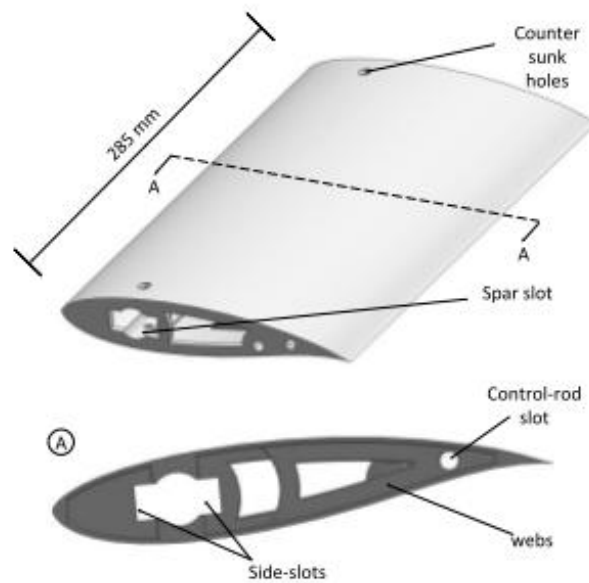Figure 4.8 shows a SoliWorks™ model of the one of the 5 section in which the blade was subdivided.

Figure 4.8 SolidWorks™ model one of the five 3D printed section composing the aerodynamic blade **(23)**.

The 3D printed blade's section are not structurally strong enough to support the aerodynamics loads, therefore a main tubular spar was inserted in the aerodynamic center of the blade. The spar has multiple purposes, support the loads on the blade, connecting the different section in which the blade was built

and connecting the blade to the hub. The spar is also the support on which the strain gauges had been installed.

Figure 4.9 Frontal view of the assembled test rig with rotor installed

Figure 4.9 shows the assembled rotor installed on the test rig.

4.3.2 New blade section design requirements

The main goal of this project was to build, install and test an instrument capable of instantaneously measuring the characteristics of the incident flow to a wind turbine blade. One of the most crucial step of was the installation of the multi hole pressure probe on the wind turbine itself. The general design requirements for this task are listed below:

- **Adapting to the existing blade design.**
  To minimize time and resources necessary for the project it was important that the instrument could be installed without modifying the existing rotor.
- **Minimize interference with the flow**.
  The instrument muss be installed in a way to minimize its interference with the flow on the blade.
- **Accommodate the instrumentation.**
  Enough space must be found to fit the multi hole pressure probe and all the related instrumentation (Pressure transducers, analog to digital converter, Arduino, batteries, etc...).
- **Allow precise strain measurements.**
  The strain gauges that must be used to measure the forces acting on the blades are placed on the blade's rod, the instrument must be installed without interfering with the strain gauges.

- **Easy to mount and accessible.**
  It is important that the multi hole pressure probe and the DAQ is easy to install and remove from the blade and that it can be easily accessed for minor adjustments.
- **Robust setup.**
  The instruments installed on the blade will be subject to an harsh environment characterized by high centrifugal forces and vibrations, structural integrity and safety must be primary concerns.


Figure 4.10 SolidWorks™ model showing the internal present design of the blade sections.

4.3.3 Design

The modular design of the wind turbine blade made it easier to fit the instruments on the test rig. To minimize time and price of the new design the choice was made to install everything onto one of the 5 modules of which the blade is composed, this also permits to move the instrument to five different positions on the blade by simply switching the module's order.

To minimize flow interference all the instruments used for data acquisition must find a place inside the blade's section, for obvious reasons only the five hole pressure probe can be outside of the airfoil. The tip of the pressure probe, where the five pressures are measured, must be far enough of the airfoil's trailing edge so that the measured characteristics of the flow are not influenced by the presence of the airfoil itself. The probe's tip was placed 80% chord upwind of the trailing edge, this is the same value used in the NREL experiment (8).

Finding a place for the DAQ inside the turbine blade has been one of the main challenges of whole project, size was an important parameter in the choice of every single piece of equipment that composes the DAQ. The existing blade section design was modified in order to gain as much space as possible inside the airfoil's boundaries.
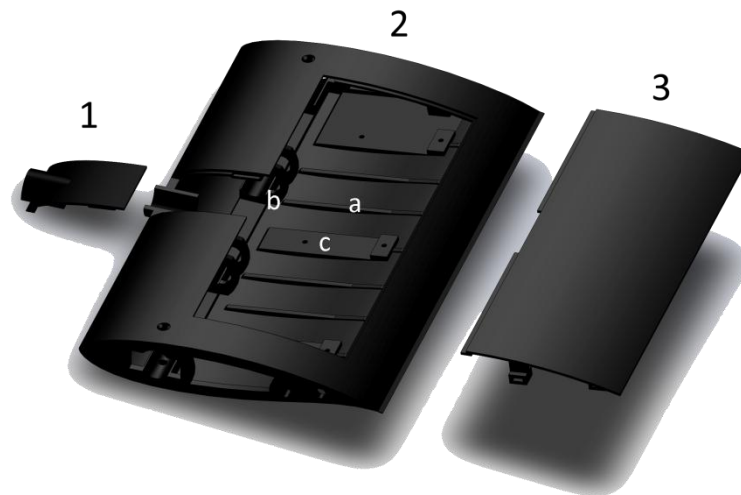
Figure 4.11 SolidWorks™ model of the new design of the instrumented blade section.

Figure 4.11 shows the new blade design, it is composed of three main parts, this modular design allows to access the instrumentation inside the blade and easily install the module on the rotor. The section's main body (Figure 4.11, 2) is based on the basilar blade design, all the data acquisition instrumentation is fitted in it, the probe will be protruding out of its leading edge and protected and kept into place by the probe's access lid (Figure 4.11, 1). The instrumentation access lid (Figure 4.11, 3) slides under the main body and it's kept into place with 6 screws accessible from the blade's pressure side.

Structural solidity, in a harsh environment characterized by high centrifugal forces and vibrations, was a key factor that influenced design decisions. As it can be seen in Figure 4.11, compared to Figure 4.10, showing the existing blade design, the interior webs, that acted as a support between the suction and pressure side of the blade, had to be eliminated in order to gain precious room for the instrumentation. In their place a transversal grid of thin reinforcement elements has been placed inside the pressure side (Figure 4.11, a) along with four small support (Figure 4.11, b), to join the two surfaces, that have been placed around the location where the blade's main spar will be. This elements give enough structural strength to the blade's main body.
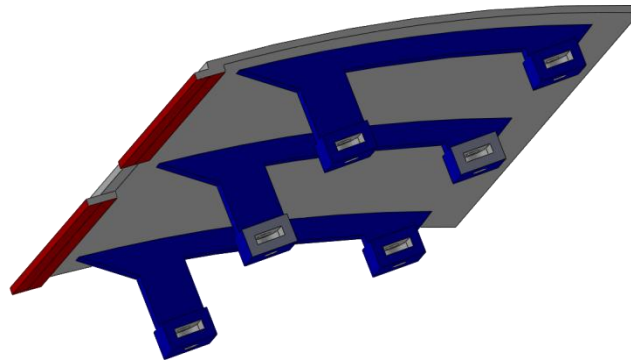
Figure 4.12 SolidWorks™ model of the instrumentation access lid.

In addition, three supports (Figure 4.12, blue) have been placed on the instrumentation access lid. Those have the triple functionality of tightly joining the lid to the main body through six screws accessible from the pressure side of the blade, keeping the equipment in place and give additional structural solidity to the blade itself. The flap (Figure 4.12, red) slides under the main body and helps keeping the lid in place and creating a smooth aerodynamic surface.

Another characteristic of the design is that it must not interfere with the strain measurements. As it can be seen in Figure 4.13 space has been left on two sides of the collar that will slide on the main blade spar. This allows to slide the blade's section onto the spar without damaging the strain gauges and later rotate them 90° into place.

Figure 4.13 Detail of the design that allows not to damage the strain gauges while sliding the blade section onto the main spar.

4.3.4 3D printing

The search for a fabrication method for a piece of such a high complexity led to 3D printing instead of more traditional methods like creating a mold and using fiber glass. 3D printing is a rapid prototyping method, where successive layers of material are placed in different shapes using robotic jets guided by lasers, the layer thickness is the main determinant of the precision of the product (27). The

availability of a high quality 3D printer on-campus at the University of Waterloo was a further motivation to examine such method.

Two machines are available on campus for 3D printing, one of them is the Fortus 360mc is a 3D rapid prototyping machine made by Stratasys (28). This is a high accuracy direct digital manufacturing system, which means that it only requires a 3D model, converted to .STL format file, that is then directly printed out using the specified material. Table shows the specification of this 3D printer.

Table 4.4 Stratasys 360mc 3D printer specifications.

Specification	Value/range
Max product dimensions [mm]	406/335/460
Layer thickness [mm]	0.127 – 0.33
Maximum resolution [mm]	0.127
Materials	PC, ABS, PC-ABS

Due to its higher strenght PC-ABS was chosen as the best material for this application.

There are several advantages of 3D printing comapred to traditional prototiping methods:

- **Virtually any level of complexity.**
  3D printing enables the full freedom to design a blade with any required internal structure complexity.
- **High precision and accuracy.**
  3D printing produces models of consistent high accuracy, any detail whose dimension is higher than the minimum resolution can virtually be 3D printed.
- **High speed.**
  Compared to the time required for machining, creating molds, and the application of fiber glass or similar composites, 3D printing clearly has the advantage.

4.3.5 Clamp design

Although it allows to achieve virtually any level of complexity the 3D printing was not considered tough enough to support the five hole pressure probe and the centrifugal force applied to it during wind turbine operation. It was therefore agreed that the safest way to attach the probe to the blade would be to clamp it directly to the blade's shaft.

The clamp, as well as the blade sections, had to be designed in a way to provide a firm support for the probe and also be able to easily slid onto the blade's shaft without damaging the strain gauges. Another major difficulty was that the clamp must be able to fit in the tight space between the rod and the two exterior surfaces of the blade's section (less than 2 mm).

The clamp design can be seen in Figure 4.14, the clamp is slid into place and then is tightened directly to the blade's shaft giving it major solidity.
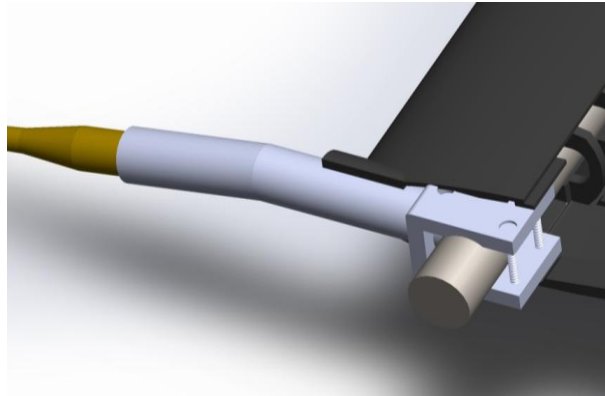
Figure 4.14 SolidWorks™ model of the clamp installed on the blade shaft along with the modified blade section.
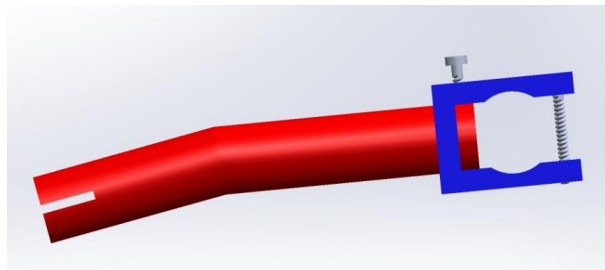
Figure 4.15 SolidWorks™ model side view of the probe clamp.

The clamp was autonomously machined at the University of Waterloo student machine shop, it was machined out of aluminum, that, on top of being the lightest material available at the shop is also the easiest one to work on for an inexperienced person.

The clamp is composed of two main components. The first one (Figure 4.15, red)extends the probe and enters into the blade's section through an hole on the trailing edge of the 3D printed object, it is made from a tube with the same inner diameter as the probe's outer diameter (12.7 mm), the slot on the tip of the extension permits to tighten the probe to it. The extension forms an angle of 15°, the part closest to the shaft is parallel to the airfoil's chord, while the further part brings the probe at an angle of 15°, the nominal angle of attack at the probe's location, see Figure 4.16. The other part of the clamp (Figure 4.15, blue) has the function of tightening the device directly to the blade's shaft with two screws seen on the right side of the figure. The two parts are connected to each other with a third screw that can be seen in Figure 4.15.
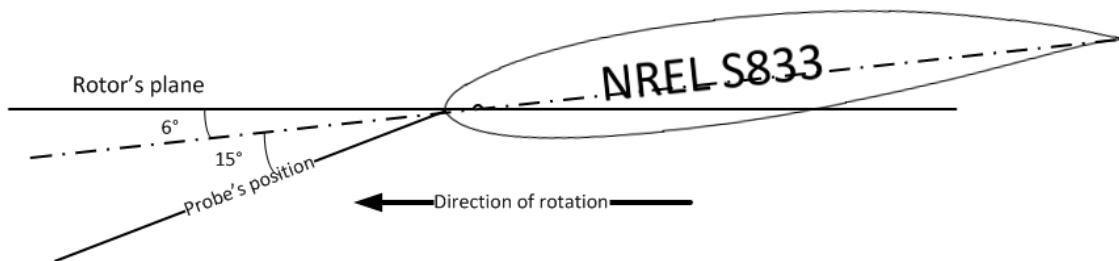
Figure 4.16 Schematics showing the probe's angular position with respect to the rotor's plan and the airfoil's chord.

Figure 4.17 shows the probe's extension and clamp assembled to the five hole pressure probe. A hole has been made at the far end of the extension to fit the small tubes going from the probe to the pressure transducers.

Figure 4.17 Probe extension assembled to the probe.

4.3.6 Component's assembly
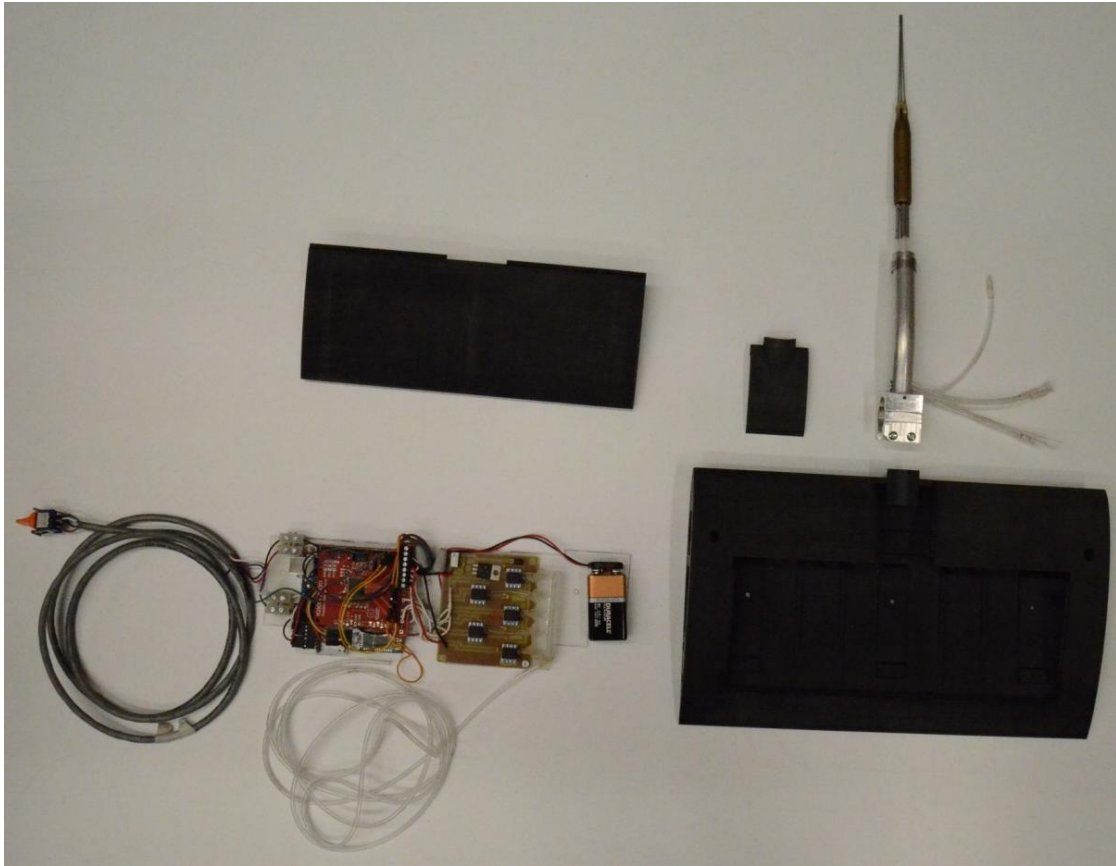
Figure 4.18 3D printed blade section, probe extension, five hole pressure probe and data acquisition system.

Figure 4.18 shows all the components before assembly and installation on the test rig. It is possible to see the data acquisition system designed for the application of a five hole pressure probe on a wind turbine, the 3D printed blade section, the probe extension and the five hole pressure probe itself.

Figure 4.19 shows all the above mentioned components assembled into the blade section after this has been installed on the test rig in the wind tunnel.
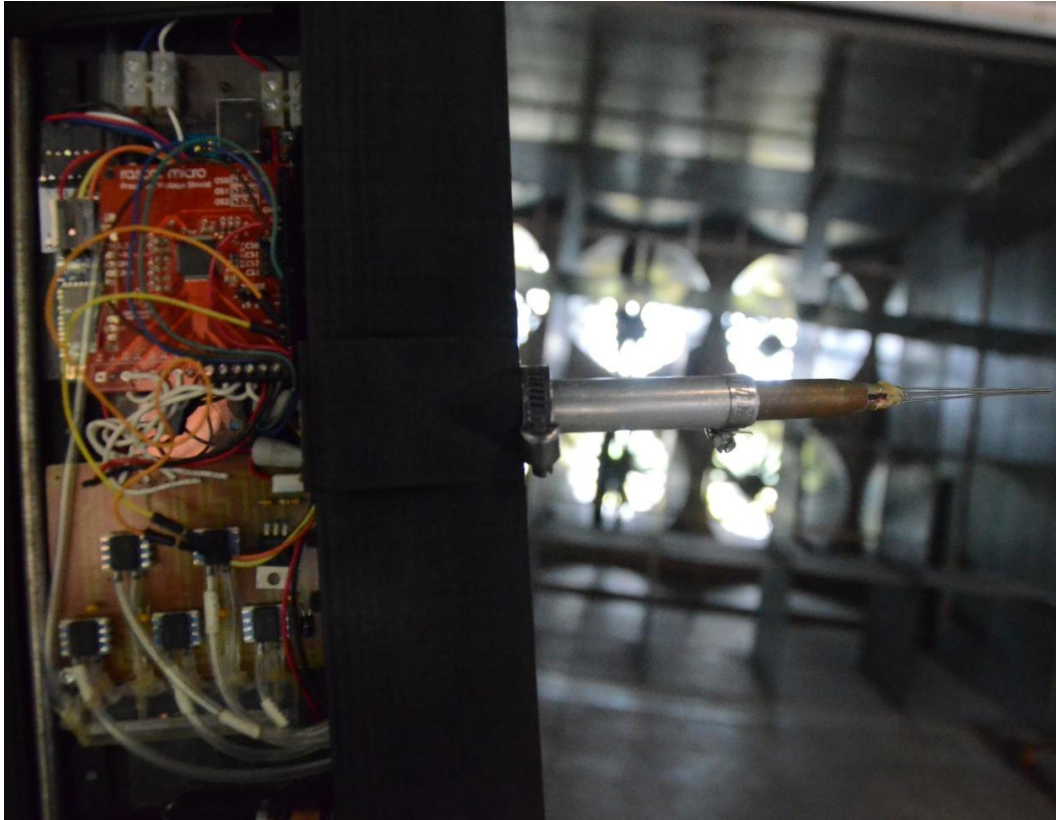
Figure 4.19 Components installed on the test rig in the wind tunnel

4.4 Pressure system

4.4.1 Reference pressure line

As said the pressure transducers used in the experiment measure differential pressure, meaning that the voltage output is proportional to the difference between the actual total pressure at the probe's tip and a reference pressure used as a baseline for the measurement.

In order to provide this reference pressure level to the pressure transducers a reference pressure line had to be developed, this was built in a way to provide the same pressure level to the five pressure transducers used.

It was also considered important that the reference pressure line could provide the steadiest pressure level as possible. This is to minimize acoustic distortion in amplitude and phase that is due to the compressibility of the medium and thus the presence of viscous flow inside the tubing. Distortion is a function of many factors, including tubing length and diameter. If the pressure varies at high frequencies massive attenuation is observed (9).

Installing the reference pressure inlet close to the rotational centre of the blade, was considered the best way to minimize fluctuation in the reference pressure level and therefore to minimize its distortion. This is also convenient to minimize the errors due to pressure transducers hysteresis.

The most suitable place to install the reference pressure line's inlet was identified to be the PVC spacer between the two steel pates used to assemble the blades to the test rig, this can be seen in Figure 4.3. The PVC spacer presents a hollow space inside, three holes of 3,17 mm diameter have been drilled in the PVC spacer, through one of them the reference pressure line was inserted, the other two holes were left for the air to enter into the spacer. Figure 4.20 shows the reference pressure line secured to the PVC spacer.

Figure 4.20 Reference pressure line into the hub spacer.

Since the PVC spacer presented a hollow cavity it was filled with foam to try to further minimize the reference pressure fluctuation.

4.4.2 Inflow determination independent from reference pressure

A peculiarity of the five hole pressure probe system used in the NREL experiment (8), is the need for a steady pressure level that must be used as a reference to measure pressure using the differential pressure transducers. The set of pressure coefficients used in the NREL experiments requires this pressure to be the tunnel's centerline static pressure.

Referencing the measurements to this pressure levels represents a notable challenge. Engineers from the NREL experiment used a complex pressure measurement path, shown in Eq. 4.1 to obtain the difference between the measurement and tunnel's static pressure ($P_{hole} - P_\infty$). The transducers measured the differential pressure between a one port of the five-hole probe (P_{hole}) and the instrumentation box (P_{PSC}) installed on the hub. Another pressure sensor measured the differential pressure between a Gill port atmospheric pressure (P_{atm}) and the box enclosure (P_{PSC}). The wind tunnel inlet was instrumented to measure the differential pressure between the tunnel centerline static pressure (P_∞) and the Gill port atmospheric pressure (P_{atm}).

$$P_{hole} - P_\infty = [P_{hole} - P_{PSC}] - [P_{atm} - P_{PSC}] - [P_\infty - P_{atm}] \qquad \text{Eq. 4.1}$$

The most challenging part in this measurement chain is measuring the pressure difference between the atmospheric pressure (P_{atm}) and the pressure in the instrumentation box (P_{PSC}). The instrumentation box, where P_{PSC} is measured, is rotating with the turbine's rotor, while P_{atm} is measured by a Gill port outside of the wind tunnel, this requires a very complex tubing system whose crucial component is a pneumatic coupling, an airtight joint, that brings the pressure level from a rotating support to a static support (typically used for brakes). On top of this, tunnel's static pressure must be measured as well.

Installing a pneumatic coupling on the current test rig proved to be impossible, since the test rig had not been designed to accommodate one in first place.

Another advantage of using the multi-zone pressure coefficients instead of the NREL pressure coefficients, is that use of a steady reference pressure is not necessary. This is only true if the ultimate goal is measuring velocity and not total and static pressure, and as long as all the measurements are referenced to the same pressure level, see following demonstration.

The pressures measured by the pressure transducers (P_{meas}) are in reality pressure differences between pressure at one of the holes(P_{hole}) and the reference pressure (P_r).

$$P_{meas:1,2,3,4,5} = \left[P_{hole:1,2,3,4,5} - P_r\right] \qquad \text{Eq. 4.2}$$

The pressure coefficients used for zone 3 (when hole 3 is measuring the highest pressure) will be analyzed to show how the reference pressure is not influential if the ultimate goal is to measure velocity.

$$Cp_p = \frac{(p_5 - p_r) - (p_3 - p_r)}{(p_3 - p_r) - \left(\frac{(p_2 + p_4 + p_5)}{3} - p_r\right)} = \frac{p_5 - p_3}{p_3 - \left(\frac{(p_2 + p_4 + p_5)}{3}\right)} \qquad \text{Eq. 4.3}$$

Same thing can be demonstrated for the Yaw pressure coefficient, the reference pressure gets erased and therefore using an absolute measurements or a measurement referred to a reference pressure is totally non influential in order to determine yaw and pitch angles.

Once those angles are known, static and total pressure coefficients can be determined using the surfaces obtained through calibration, form those, total and static pressure can be estimated. Total and static pressure are not independent from reference pressure, but their difference is, as shown below.

$$P_T = (p_3 - p_r) - Cp_p \left[(p_3 - p_r) - \left(\frac{(p_2 + p_4 + p_5)}{3} - p_r \right) \right]$$

$$= (p_3 - p_r) - Cp_p \left[p_3 - \frac{(p_2 + p_4 + p_5)}{3} \right]$$

<div align="right">**Eq. 4.4**</div>

$$P_S = \left(\frac{(p_2 + p_4 + p_5)}{3} - p_r \right) - Cp_p \left[(p_3 - p_r) - \left(\frac{(p_2 + p_4 + p_5)}{3} - p_r \right) \right]$$

$$= \left(\frac{(p_2 + p_4 + p_5)}{3} - p_r \right) - Cp_p \left[p_3 - \frac{(p_2 + p_4 + p_5)}{3} \right]$$

<div align="right">**Eq. 4.5**</div>

Since V is equal to:

$$V = \sqrt{2\rho(P_T - P_S)}$$

<div align="right">**Eq. 4.6**</div>

The two remaining reference pressures (p_r) in Eq. 4.4 and Eq. 4.5 erase with each other and therefore the velocity is not dependent from the reference pressure used.

Another confirmation of the fact that the reference pressure practically does not influence the measurements obtained with the probe, when using the multi zone pressure coefficients, can be obtained by comparing this results to the ones obtained with the NREL set of pressure coefficients.

Changing the reference pressure can be thought as adding an offset to the measurement. An offset of 10 Pa has been added to the first set of measurements obtained after the probe was installed on the turbine, subsequently velocity has been estimated using the multi-zone pressure coefficients and the NREL pressure coefficients and the results with and without the 10 Pa offset have been comparatively evaluated.

The results obtained with the NREL pressure coefficients present a slight variation due to the presence of this 10 Pa offset both for the velocity and angle, while the multi-zone pressure coefficients present exactly the same result.

Having no need for a steady reference pressure is a large improvement compared to the methodology used during the NREL experiment, this allow to avoid building a much complex airtight preference pressure line.

4.4.3 Influence of centrifugal force and vibrations on the pressure transducers

The influence of centrifugal force and vibrations on the performance of the pressure transducers has also been assessed.

A first precaution was taken in order to minimize the effect of the centrifugal force, the pressure transducers have been installed with their measuring surface parallel to the rotational plane of the rotor, this is the plane where the centrifugal force acts.

After the instrumentation was installed on the wind turbine blade a characterization of the effect of the centrifugal force and vibration has been made by comparatively evaluating the readings taken with the blade parked and with the blade rotating at different speeds (50,100,200 rpm). For this phase of the experiment the five hole pressure probe and the reference pressure lines have been blocked so that the readings are not influenced by dynamic pressure.

If the centrifugal force has an effect the difference, if there is any, between the readings with the parked blade and the ones when the blade is rotating should proportionally increase or decrease depending on how this force acts on the pressure transducers.

If the vibration generated by the rotation of the blade influences the pressure transducers in any way the SD of the set of readings is expected to increase with increasing RPM.
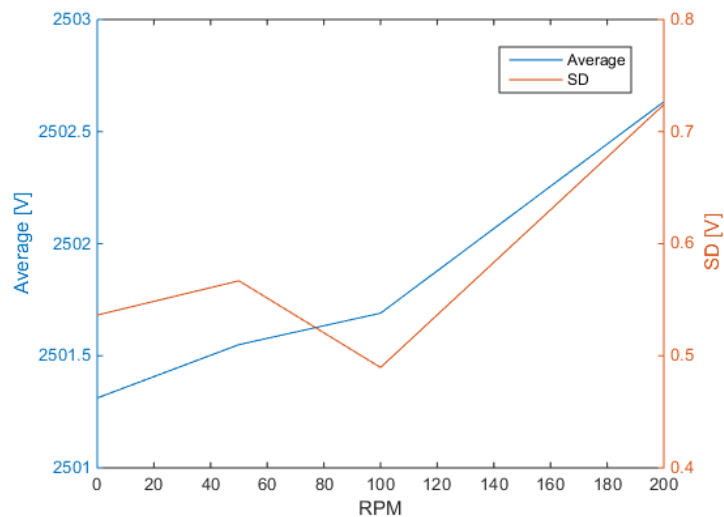
Figure 4.21 Effect of centrifugal force and vibrations on the pressure reading once the pressure probe is installed on the test rig.

Figure 4.21 Figure 4.21 **Effect of centrifugal force and vibrations on the pressure reading once the pressure probe is installed on the test rig.**is an average made from the readings obtained by the 5 pressure transducers.

The average value is influenced by the rotation of the blade and the centrifugal force that it generates, this influence can be quantified in the order of 1 mV. This offset generated by the centrifugal force, is kept into account during data post-processing.

The dependency of SD on the rotational speed cannot be clearly identified from the available data.

4.4.4 Effect of centrifugal force on the reference pressure line

Another effect generated by the rotor's rotation that must be kept into account is the centrifugal force acting on the reference pressure column of air.

The differential pressures between the probe's pressure and the hub reference pressure were reduced by the centrifugal force acting on the column of air in the pressure tubing caused by rotation of the blade (8).

The correction for this effect, has been taken from "Unsteady Aerodynamics Experiment Phase V: test configuration and available data campaign", and can be carried out as follows:

$$P_{cor} = P_{meas} + P_{cent}$$

<div align="right">**Eq. 4.7**</div>

$$P_{cent} = \frac{1}{2}\rho(r\omega)^2$$

<div align="right">**Eq. 4.8**</div>

The centrifugal force varies when the air's density changes, to give an idea of the order of magnitude of the correction Table 4.5 shows the effect of the centrifugal force on the pressure with a air density of 1.2 kg/m^3, the probe is positioned 0.9 m from the rotation centre.

Table 4.5 Effect of the centrifugal force on the column of air in the reference pressure line at different rotational speeds.

RPM	ω[rad/s]	P_{cent}[Pa]
0	0	0
50	5.23	13.4
100	10.47	53,3
200	20.93	212.9

The reference pressure is in the same order of magnitude as the pressure measurement itself, it is therefore crucial to apply this correction to the data collected.

Reference pressure correction has been applied during data post-processing.

Figure 4.22 shows a random sample of data after before and after being corrected to account for centrifugal force.
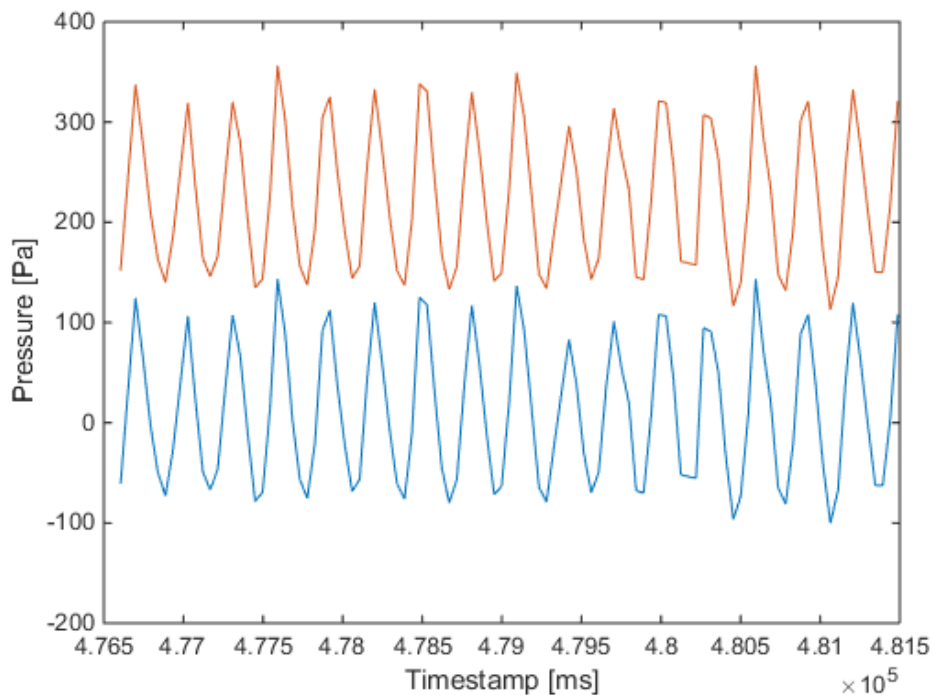
Figure 4.22 Random sample of data before and after the centrifugal force correction.

4.5 Data acquisition system

The data acquisition system used for the experiment can be conceptually divided in two sub-systems.

The first one is installed on the turbine's blade, this is directly connected to the five hole pressure probe and it's only functions are to read the analog signal from the pressure transducers, transform it to a binary digital signal that is then converted into a string and sent to the main computer through Bluetooth. This is exactly the same setup used during the calibration of the probe, for details on the hardware see section 2.3.

The second one is conceptually more complicated, but easier to assemble and run, since it is composed of standard National Instrument™ cards and can be easily run using LabView™, it's function is to retrieve every measurement, except for the pressure probe, to synchronize the entire system and store the data.

In this section the two parts of the data acquisition system will be analyzed with special attention on the software.

4.5.1 Pressure DAQ on the blade

As said the part of the Data Acquisition System used to read the pressures from the pressure transducers is installed on the blade, this is exactly the same instrumentation that was used for the probe's calibration.

The core of this part of the Data Acquisition System is and Arduino Uno Microcontroller. Figure 4.23 represents a schematization of the Arduino sketch written to measure and send pressures from five hole pressure probe.
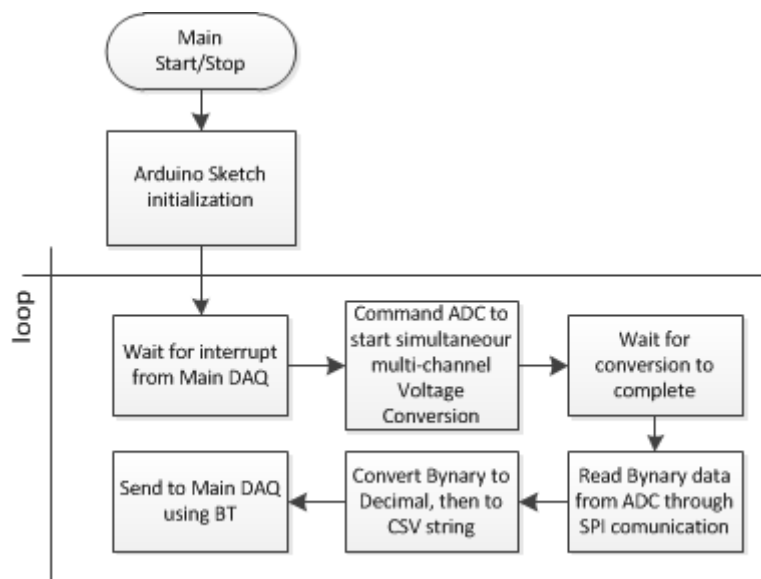
Figure 4.23 Flowchart representing the code uploaded on the Arduino

The sketch starts running when the Arduino is powered, after initializing a number of parameters necessary for communicating with the Analog to Digital Converter (ADC) and to prepare for the interrupt, Arduino enters into the loop. Here it waits until an interrupt is received, an interrupt is an external digital signal, in this case coming from the main DAQ, upon the reception of which Arduino stops doing whatever it was doing, in this case waiting, and calls a function specified in the setup.

Once the interrupt is received and the function is called, the microcontroller commands to the ADC to start the conversion of the analog signal, then waits for the conversion to be completed. Once the ADC has completed the conversion the number of digital counts is sent through SPI to the microcontroller in the form of a binary number. When the microcontroller receives the data this is converted it into a decimal number that is then inserted into a sting of comma separated values and sent to the main DAQ through the Bluetooth transreceiver that is also installed onto the blade.

4.5.2 Main DAQ

The most part of the Data Acquisition System is located in the wind turbine control room. The instrumentation control and synchronization is operated through a personal computer running on a Pentium4 processor, this computer is instrumented with a Nation Instrument™ data acquisition card, the PCI 6251 (29), that can easily be controlled using labview.
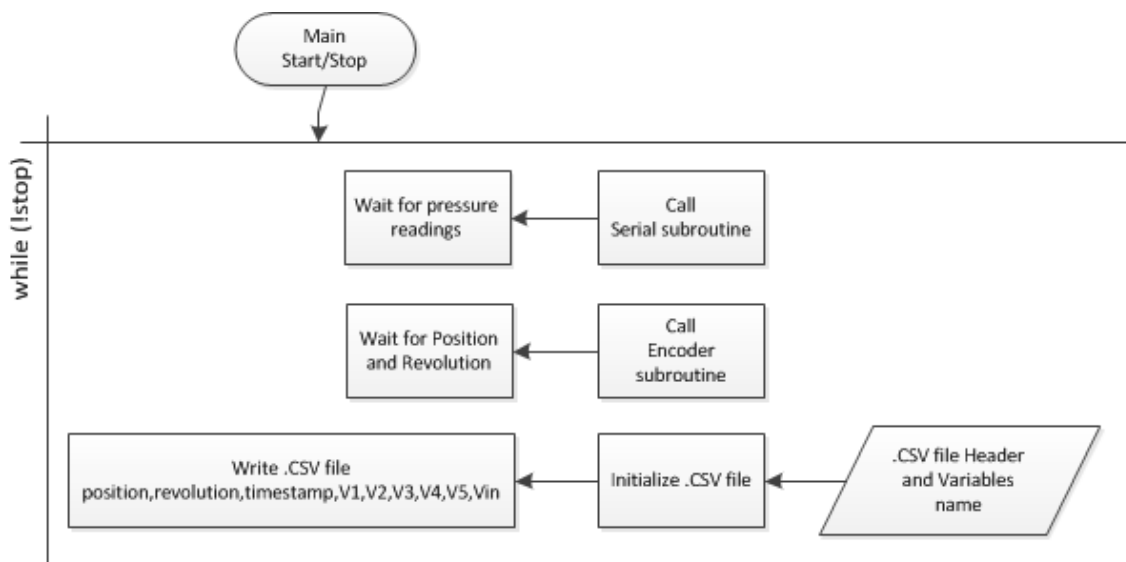
Figure 4.24 Flowchart representing the main section of the LabView™ code written to synchronize all the measurement performed on the wind turbine.

Figure 4.24 shows a block diagram that explains the LabView™ code written to coordinate the different measurement and instruments necessary for the experiment. After the code has been started it calls the 2 subroutines that are handling the encoder's position reading and the pressure measurements, everything it does then is simply waiting for to receive the position coming from the encoder and the pressure reading, once both these variables are available they are written into a .CSV file.
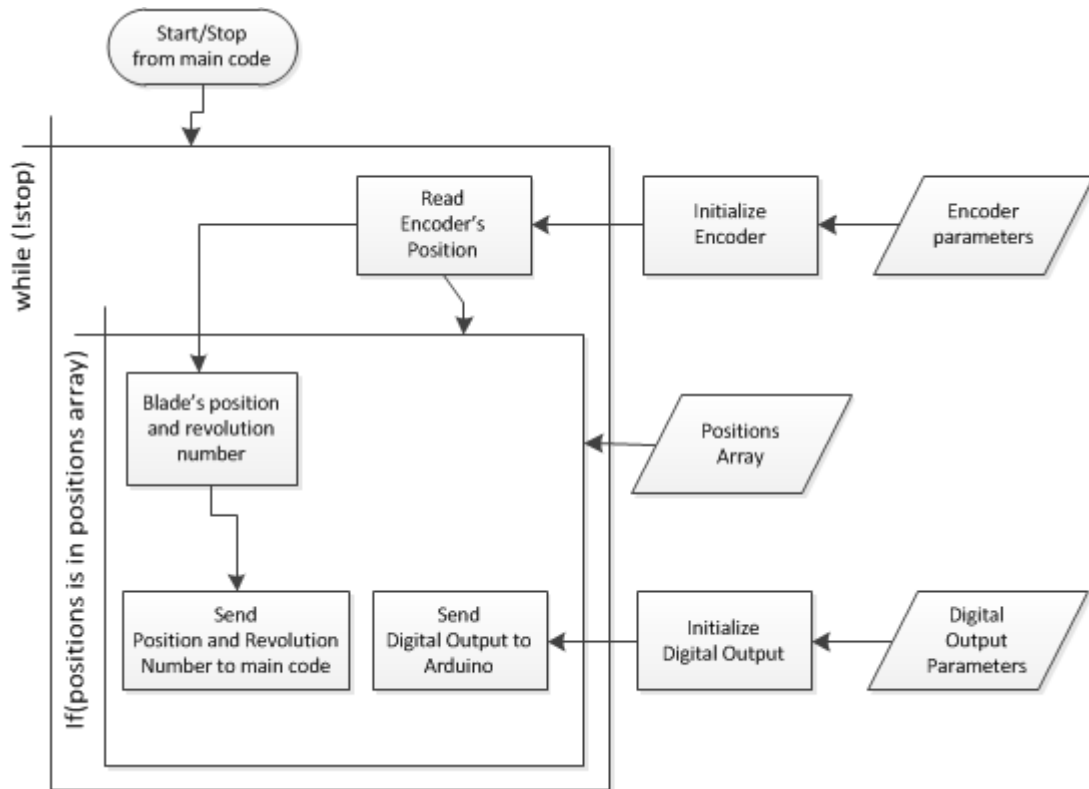
Figure 4.25 Flowchart representing the LabView™ code written to read the position encoder and trigger the pressure measurement.

Figure 4.25 shows a block diagram that explains the LabView™ code written to read the blade's position using the torque sensor's built in encoder. This code is a routine called by the main code that controls most the wind turbine instrumentation. First the routine initializes the sub routine that reads the encoder's signal (built-in in LabView™) after the user has set a series of parameter (channels to read, encoder's characteristics, etc...), likewise the digital output signal used to trigger the Arduino measurement is initialized.

Until the stop variable is turned to true the code keeps reading the blade's position, if the blade position is found into an array containing all the blade positions where the pressure must be read, a digital pulse is sent to the Arduino and blade position and revolution number is sent to the main code.
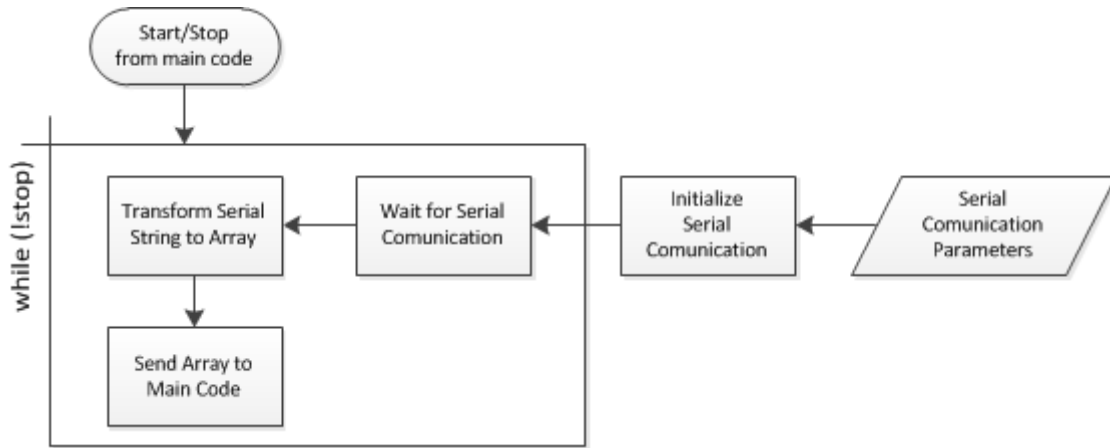
Figure 4.26 Flowchart representing the LabView™ code written to receive the pressure measurement from the DAQ installed on the blade.

Figure 4.26 shows a block diagram that explains the LabView™ code written to read the serial communication transmitted by the Arduino via Bluetooth, this serial communication includes the five voltages measured by the pressure transducers plus a timestamp. This code is a routine called by the main code that controls most the wind turbine instrumentation.

First the routine initializes the serial communication (built-in in LabView™) after the user has set a series of parameter (termination character, buffer size, etc..), when the serial communication is received, this is converted from a string of comma separated values to an array of values and then is sent to the main code to be written on a .CSV file.

4.5.3 Final instrumented test rig configuration

Figure 4.27 shows the configuration of the wind turbine instrumentation and the connections to the controlling computer after the five hole pressure probe was installed on the blade and the torque sensor on the main shaft.
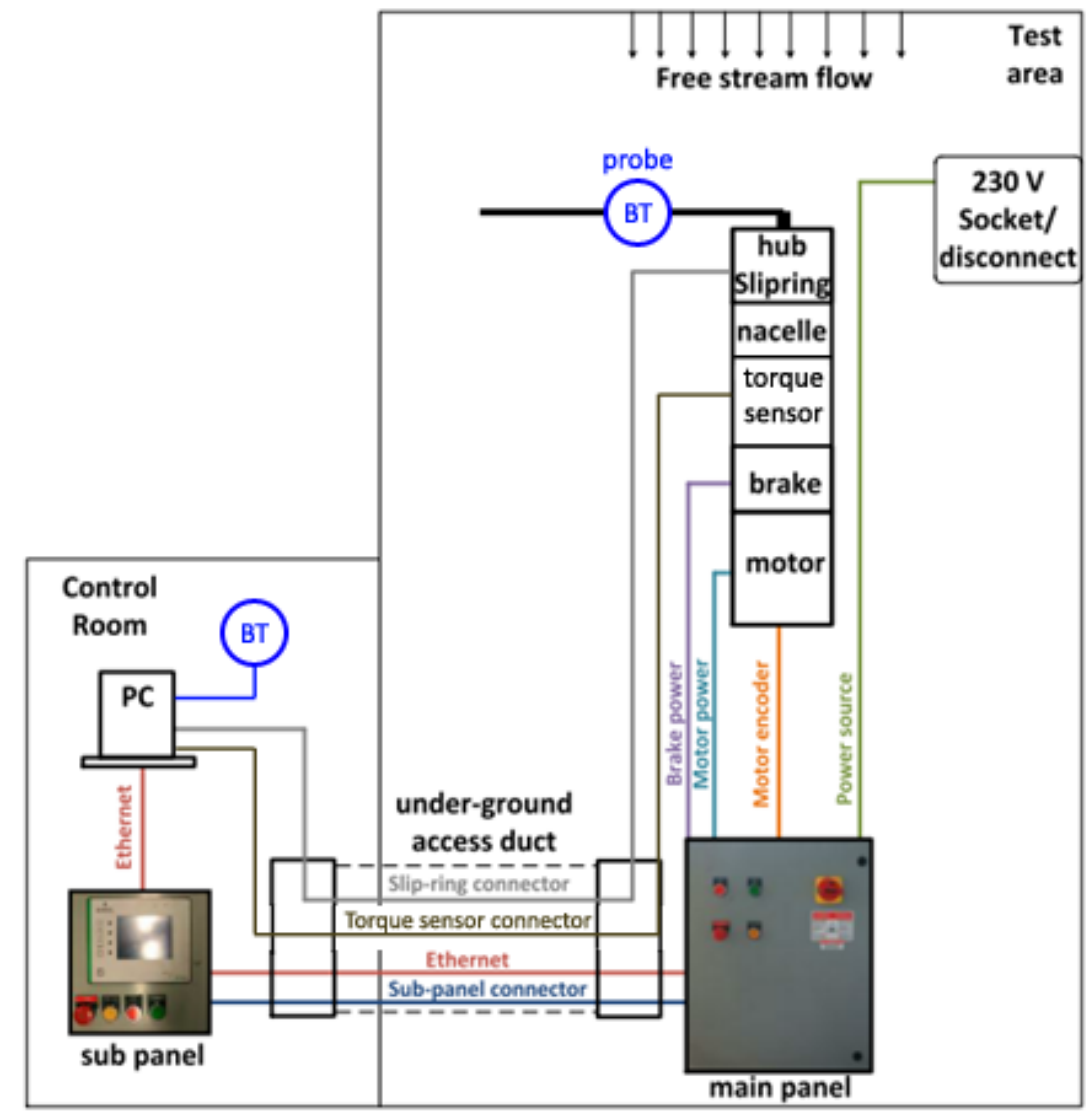
Figure 4.27 Schematics representing the test rig instrumentation and connections between the turbine and the control room, adapted from **(23)**.

Chapter 5   Results

After the installation on the wind turbine the correct functionality of the five hole pressure probe system will be tested. Finally the measurement points and the definitions of variables used for generating the result plots are indicated along with their sources and equations.

5.1 Testing goals and conditions

5.1.1 Objectives

The objective of this series of testing that the five hole pressure probe will be subject to is to test its correct functioning. To do so the probe will be used to measure pressures after its installation on the wind turbine blade and subject to a number of different flow conditions, turbine aligned with wind direction and not, different rotational speeds, different wind speeds, etc.

As anticipated above due to technical difficulties it has not been possible at this stage to measure an important parameter like rotor's azimuthal position. This is fundamental to be able to precisely assess the anomalies in the inflow to the blades due to phenomena like wind shear and turbine's yaw angle.

Therefore the current set of testing has been carried out with the sole purpose of testing the probe's correct functioning, the flow phenomena encountered will then de compared to the expected flow phenomena to see if the five hole pressure probe is actually working correctly.

5.1.2 Parameters and Measurements

The blade was instrumented with one five hole pressure probe, installed at 0.56 r/R (0.952 m) radial position, its measuring tip has been placed one chord (178 mm) upwind of the blade's leading edge to avoid flow disturbance. Extensive

details about the pressure probe and it's functioning principle can be found in section 2.1

Air temperature was measured at the facility with a digital thermometer, temperature was recorded between every set of experimental measurements. Atmospheric pressure was also recorded using a precision mercury barometer between measurements.

Table 5.1 Summary of measured parameters and their unit of measure.

Measurement	Instrument	Unit
Temperature	Digital thermometer	[°C]
Atmospheric pressure	Mercury barometer	[Pa]
Inflow speed	Five hole pressure probe	[m/s]
Inflow angles	Five hole pressure probe	[°]

The tests have been run varying a series of parameters, these include rotor's rotational speed, the turbine's yaw angle and wind speed.

Rotor's speed was controlled through the motor/generator variable frequency drive and continuously monitored through its built-in encoder, rotor's speed can be changed through the turbine main controller touch screen at any time.

The turbine yaw angle is adjusted manually between every data collection phase, even if it was not moved, correct alignment of the wind turbine was checked between every phase of data collection, this parameter is checked visually through a protractor built-in underneath the turbine's nacelle.

Wind speed could be indirectly controlled by varying the facility's fan frequencies, conversions between the fan's frequencies and the resulting wind speed is done accordingly to Ahmed (23), who, in his work, precisely measured wind speed at the location where the where the turbine is installed, resulting from different fan frequencies and therefore fan's rotational speeds.

Table 5.2 Summary of control parameters and how those can be controlled.

Parameter	Control instrument	Unit
Rotor's speed	Generator's encoder	[RPM]

Parameter	Control instrument	Unit
Turbine yaw angle	Protractor	[°]
Wind speed	Fans frequency	[Hz]

Another parameter that was varied during this first phase of data collection was the configuration of the reference pressure line. Four different reference pressure lines configuration have been tested with the scope to provides the steadies possible reference pressure level. Even if, as discussed in section 4.4.3, reference pressure theoretically does not influence the determination of inflow vector characteristics, having a steady reference pressure level positively influences pressure transducers hysteresis errors and acoustic distortion due to the tubing system.

5.1.3 Experimental procedure

The experimental procedure involved three stages, details about the three steps are given below:

1. **General facility warm-up.**
   The experimental facility (FireLab) had to be warmed-up, the frequencies of the 6 fans composing the fan's array of the wind gallery were gradually increased up to 60 Hz, once reached this frequency the fans were left running for at least 5 minutes. The blade section is installed into place, in this case the section's position is 0.56 r/R, the wind turbine is then run for at least two minutes, varying the rotational speed up to 200 RPM, to check for problems in the test rig.
2. **Experiment set-up.**
   This stage is about setting up the experimental parameters and is performed between every stage of the data collection campaign.
   - One of the reference pressure situation is chosen.
   - The turbine is set to the yaw angle chosen for the experiment.
   - The wind tunnel must be completely cleared out from any object and person.
   - The probe's Data Acquisition System and the Bluetooth for data transmission are powered.
   - Rotor's rotational speed is set to the desired value from the control panel.

- Finally temperature and atmospheric pressure are measured before starting the data acquisition.
3. **Data collection campaign.**
   The turbine's safety brake is released and the test rig is turned on to the desired speed, simultaneously the wind tunnel fans are turned on. The whole system is left running for at least one minutes to allow it to reach a stable functioning point before starting data collection. This step is repeated for every stage of the data acquisition campaign.

5.1.4 Experimental matrix

This series of test was designed mainly for two reasons, and therefore it can be divided in two groups. First, to investigate the influence of certain parameters (for example rotor's speed) on the results obtained with the five hole pressure probe and the newly built data acquisition system. Second, the probe has been tested in conditions that resemble possible future experiments, whose goal is to investigate different flow phenomena. These are identified by two letters P (preliminary) and F (flow).

Results of the first set of experiment have been presented throughout this work, while results of the second will be presented in the following sections.

Table 5.3 Summary of test sequences.

Group	Sequence	Seq. Code	RPM	Wind speed [m/s]	Yaw [°]	Notes
P	Structural integrity check		increasing, 0 to 200	0	0	
P	Vibrations and Centr. Force on PT		0,50,100,200	0	0	Blocked probe and ref. p.
P	Centr. Force on Ref. Pressure		50,100,200	0	0	
P	Different Ref. Pressure		100,200	0	0	4 Ref. pressure configuration
F	Turbine aligned	F1	100,200	0 and 11.5	0	

F	Turbine not aligned	F2	100,200	0 and 11.5	+30

Figure 1.4 shows the convection used for the turbine's yaw angle. This parameter is varied by rotating the turbine in the wind tunnel.

Data collected during the experiment has then been post processed using MatLab™ software.

5.2 Results and discussion

In this section results obtained during the probe's testing will be analyzed both from a qualitative and a quantitative point of view

5.2.1 Blade and probe structural integrity

Although the 3D printed blade section was the result of the assembly of various parts, this proved to have enough structural solidity to be able to withstand the toughest test condition obtainable at the facility. This has been tested in wind speeds ranging from 0 to 11.5 m/s, rotational speeds up to 200 RPM and for both axial and not axial wind conditions (with the latest being the heaviest duty condition, characterized by loads cyclically varying with the same period as the rotational speed).

The blade design proved to be practical, allowing to reach every piece of the equipment installed in it without the need to remove the blade section from the test rig. Also the particular design of the blade section allows to perform strain measurement without damaging the strain gauges installed on the spar during its installation.

3D printing proved to be a technique with enough precision to fabricate a very complex object without scarifying its structural integrity. It has been possible to print tiny elements like flaps and slots that made the blade section easy to assemble and with satisfying aerodynamic characteristics.

The probe clamping device, built in house, proved to be strong enough to firmly support the probe in all of the above cited operational conditions, so that the functioning of the probe was not influenced by the vibrations of the test rig. It also allowed to mount the probe on the spar without damaging the strain gauges attached to it.

The Data Acquisition System proved to be working fine and not to be influenced by the vibrations and centrifugal force generated by the test rig.

Overall the system proved to be working as hoped during the design phase. The most challenging problem, which was communication between the instrumentation on the blade and the control room, was successfully solved employing Bluetooth communication, also Arduino, a cheap and easy to use microcontroller, thanks to its modularity proved to have suitable characteristics for experimental wind turbine applications.

5.2.2 Expected results

Results from the preliminary group of experiments (P) were discussed throughout this work in this section and the next ones data collected during the Flow group of experiments (F) will be presented and discussed.

The flow (F) group of experiments can be subdivided in two groups as presented in Table 5.3.

A first sequence of experiments has been carried out in what can be called "normal operation" of the wind turbine, in this case the wind turbine axis was aligned with the main flow direction.

The second sequence has been carried out under the so called yaw loads, more details in section 0, this can be considered "non normal operation" even if in practice wind turbines are often subjected to this kind of conditions. One particular kind of yaw loads will be analyzed here, the case when the wind turbine is not aligned with the wind direction, or cross wind situation. Then the results will be comparatively evaluated with the case when the turbine is aligned with the flow of air.

Knowing the experimental conditions it is possible to make some forecast about the results that will be obtained, especially in the situation when the turbine is aligned to the flow direction.

In this case, knowing that the rotational speed of the blade is 200 RPM, the probe is located 0.952 m from the center of rotation, then the relative speed generated by the rotation (U) is 19.93 m/s; the wind speed (V) is 11.5 m/s, using velocity triangles, it is possible to make a rough estimation of the local incident velocity (W), around 23 m/s. Figure shows how this calculation was performed. It is also possible to make an estimation of what the angle of the flow compared to the rotor's plane should be, around 29.5°.
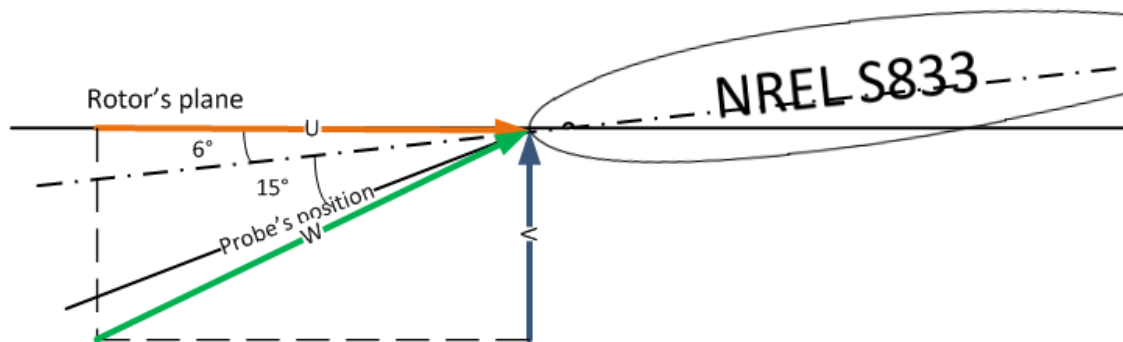
Figure 5.1 Wind turbine and velocity triangle

It is not possible to predict with so much accuracy the expected behavior in "non normal operation" conditions. Maeda and Kawabuchi (6), who employed a five hole pressure probe to measure incident flow characteristic on a wind turbine installed in the field can give an idea of how the incident velocity changes with the azimuthally angle. The result from their study is reported in Figure 5.2.

5.2.3 Turbine aligned with the wind direction

In this paragraph the results of results of the test sequence F1 will be presented and analyzed.

Table 5.4 shows the 4 testing conditions taken into consideration.

Table 5.4 Test subsequence of F1 test sequence.

Turbine Yaw [°]	Wind Speed [m/s]	Rotor Speed [RPM]	Sequence Code
0	0	100	F1a
0	0	100	F1b
0	11.5	200	F1c
0	11.5	200	F1d

Each sequence is made up of several hundreds of data points.

With the same methodology presented in the previous paragraph velocity and angle of attack have been estimated for each one of the cases, as presented in Table 5.5.

The parameters estimated are proposed in table   along with the measurements retrieved using the five hole pressure probe.

Table 5.5 Predictions and measured parameters for test sequence F1.

Seq.	Predicted Velocity [m/s]	Predicted Angle [°]	Measured Velocity [m/s]	Measured Angle [°]	Measured Slip Angle [°]
F1a	9.96	0	11.62	5.2	11,69
F1b	19.93	0	23.35	4.8	11,74
F1c	15.21	49.1	13.61	47,2	14,59
F1d	23.11	29.1	24.62	25.2	13,81

The results shown in table point out a discrepancy between the results that have been predicted using the simple velocity triangles and the actual measurements. This gap is actually the reason why this experiment has been done, to quantify the differences between the 2D models used to design wind turbines and the actual unsteady 3D behavior of the flow in such a complex system as an horizontal axis wind turbine.

For example the results obtained in sequence F1a and F1b, with the wind turbine rotating at 100 and 200 RPM, and the wind tunnel turned off, the predicted angle, with respect to the rotor's plane, with the 2D velocity triangles was of course 0°, while in practice this value is around 5° for both cases. This can be explained with the wind turbine drawing the flow, hence the velocity is considerably higher than the prediction, since the blade in moving in air that is not actually steady, but is drawn to the rotor's plane by the rotor itself.

Sequence F1c and F1d give a further confirmation of the difference between the 2D methods and the actual flow phenomena. The slip angle is considerably high, around 18° for both cases and therefore the flow cannot be accurately described with 2D methods. For example if the velocity vector measured in sequence F1d is projected on the blade's cross section plane, the same plane where the theoretical calculations are performed, the component of the velocity vector on that plan is 23.4 m/s, very close to the value obtained with the 2D velocity triangles methodology.

Results obtained in sequence F1d will be considered as a baseline for the following analysis.

5.2.4 Turbine out of alignment with the wind direction

As anticipated above, of course it is not possible to predict the expected behavior when the wind turbine is working under yaw loads conditions, in this case when it is not aligned with the wind's direction. The work by Maeda and Kawabuchi (6) can give a good idea of what the expected behavior should be.
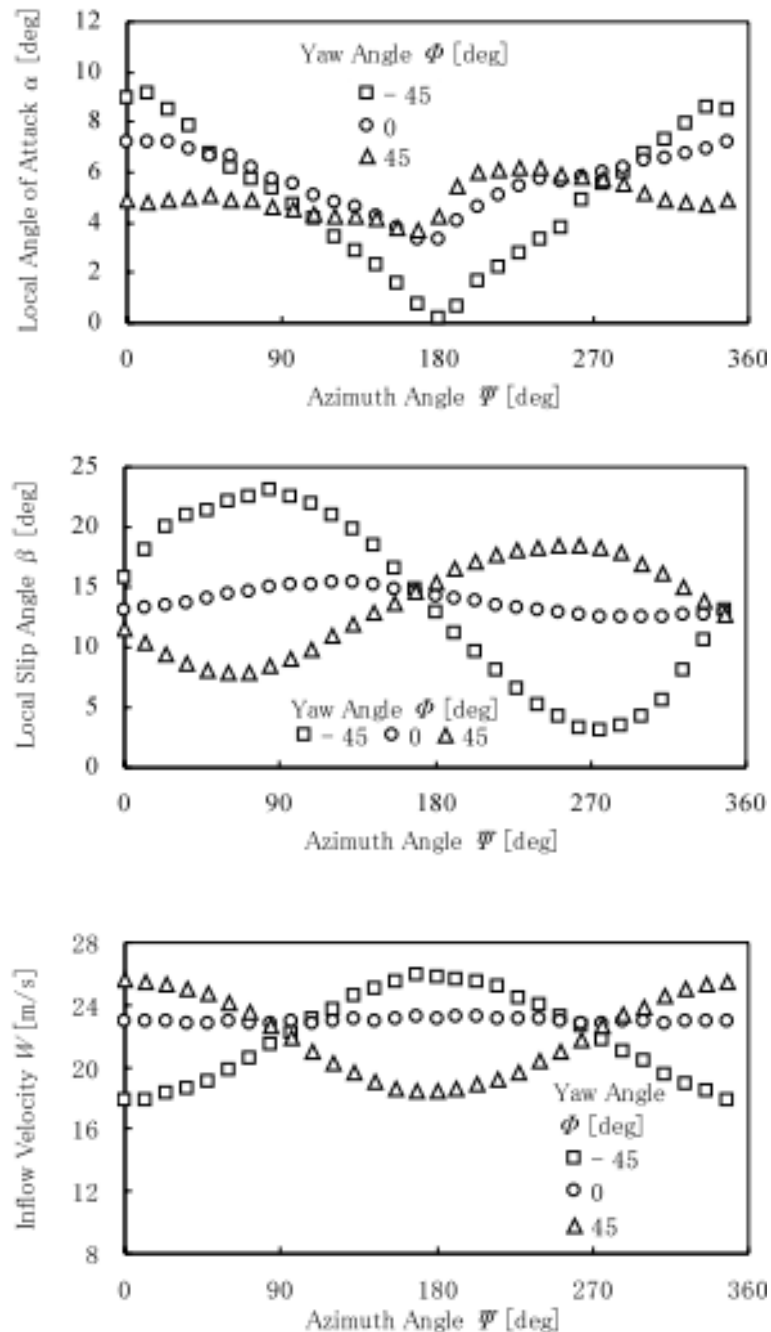
Figure 5.2 Local angle of attack change for yawed operational condition during one rotor's rotation (above), Local slip angle change for yawed operational condition during one rotor's rotation (middle), local inflow velocity change for yawed operational condition during one rotor's rotation (bottom) **(6)**.

What can be predicted is that the characteristics of the incident flow should cyclically change with a period that is the same as the period of the turbine's blade rotation.

Figure 5.2 shows that, if the pressure probe is working correctly, the inflow velocity should change with a sinusoidal behavior when the turbine is not aligned with the wind direction. Same thing can be said regarding the slip angle and the angle of attack.

Data has been collected at two different rotor's speed, for simplicity, here only the case, characterized by a rotors speed of 200RPM, will be taken into consideration. Everything said for the 200 RPM case can be considered valid also at different rotational speeds.

As mentioned in section 4.2.5 due to technical difficulties it hasn't been possible to retrieve information about the azimuthal position of the blade to couple with the pressure readings from the pressure probe. A different approach had then to be employed. This consists in performing the diametrically opposite operation, trying to infer the blade position from the measured pressure.
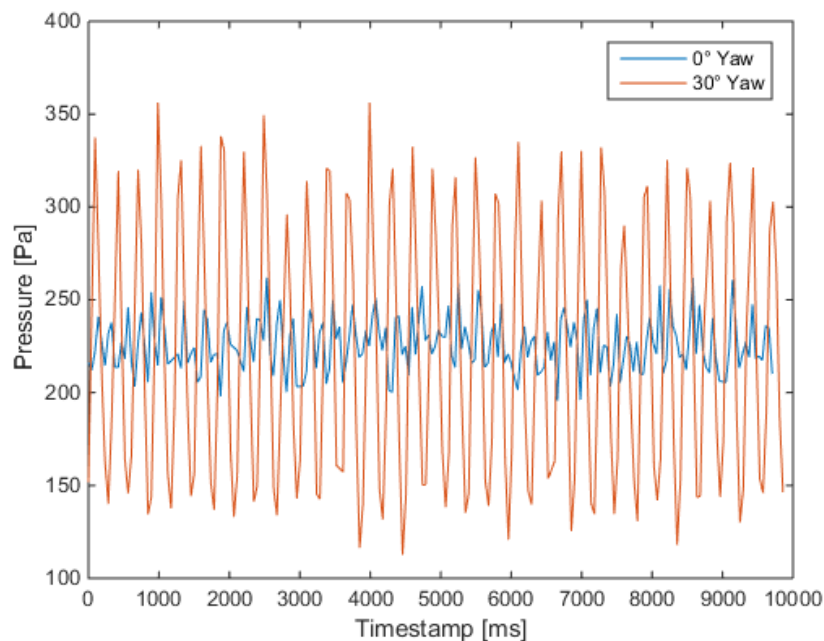
Figure 5.3 Exemplificative dataset showing the different pressure measurements for yawed and non yawed conditions.

Figure 5.3 shows an exemplificative set of data measured by one of the pressure transducers connected to one hole of the pressure probe. The blue line represents the measurement taken with the turbine aligned with the wind, while the red line

represents the case with the turbine positioned at a -30° angle compared to the wind direction.

The difference between the two cases is clearly visible, the measurement taken with the turbine at -30° present a clear periodicity.

The collected voltage values have then been converted to pressures, and using the technique explained in section 3.4, these are used to calculate the pressure coefficients that are then employed to infer velocity, pitch angle and slip angle. This process was done separately for each single line of data on the contrary of what was done with the other dataset sequences analyzed where the above mentioned parameters were obtained after the data had been averaged.
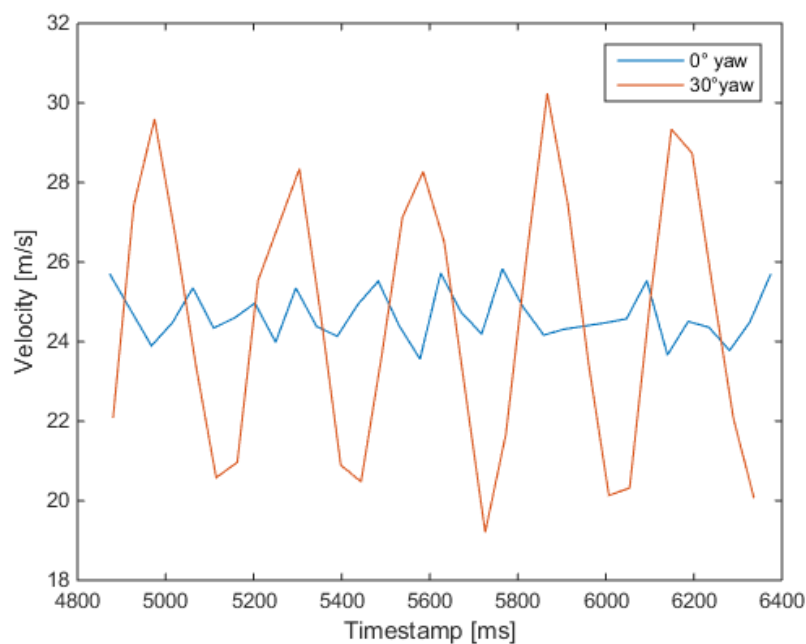
Figure 5.4 Short exemplificative dataset showing the different inflow velocity for yawed and non yawed conditions.

The variation in the signal has the same period as the blade's rotation as it can be observed in Figure 5.4. The data has been collected at 200 RPM, this means that the blade completes 3.33 rotation every second, exactly one rotation every 0.3 seconds. Figure 5.4 clearly shows that in one second the velocity presents a little more than three high peaks, it is possible therefore to conclude that these variation in the velocity are caused by different inflow conditions during one rotation of the blade.

The timestamp collected with the dataset has been manipulated to isolate the data taken from each rotation in bins, this was done by calculating the modulus of the

recorded timestamp divided by the time expected for one rotation. This results in data separated with a timestamp going from 0 to 300 ms.

$$NewTS = mod\left[\frac{(TS - TS_{start})}{300}\right]$$

The number of the rotation where the row of data was collected can be obtained as:

$$RotN = \frac{(TS - TS_{start})}{300}$$

Table 5.6 shows an example of a few lines of data with normalized timestamp and rotation number included.

Table 5.6 Example of a few lines of modified data.

Norm Timestamp [ms]	Timestamp [ms]	Velocity [m/s]	Total Pressure [Pa]	Static Pressure [Pa]	Pitch Angle [°]	Yaw Angle [°]	Rot N.
263	563	23,95	224,98	-31,09	1,28	1,94	1
10	610	19,86	151,27	-24,80	-5,60	4,02	2
57	657	20,95	165,96	-29,94	-5,78	20,13	2
103	703	25,70	256,25	-38,69	-3,99	22,63	2
150	750	29,28	345,29	-37,53	-1,59	18,20	2
197	797	27,93	305,81	-42,35	2,27	11,93	2
244	844	24,27	227,39	-35,62	0,11	4,30	2
291	891	21,89	187,80	-26,02	-2,18	4,80	2
39	939	19,21	134,27	-30,44	-7,78	14,45	3
85	985	22,60	192,63	-35,38	-2,71	24,24	3

Thanks to this process it is now possible to plot the data obtained with the five hole pressure probe grouped for every blade rotation. Figure 5.5 show a scatter

plot of the average variation of the pitch angle, inflow velocity and slip angle vary during one rotation, based on the New time stamp obtained as above.
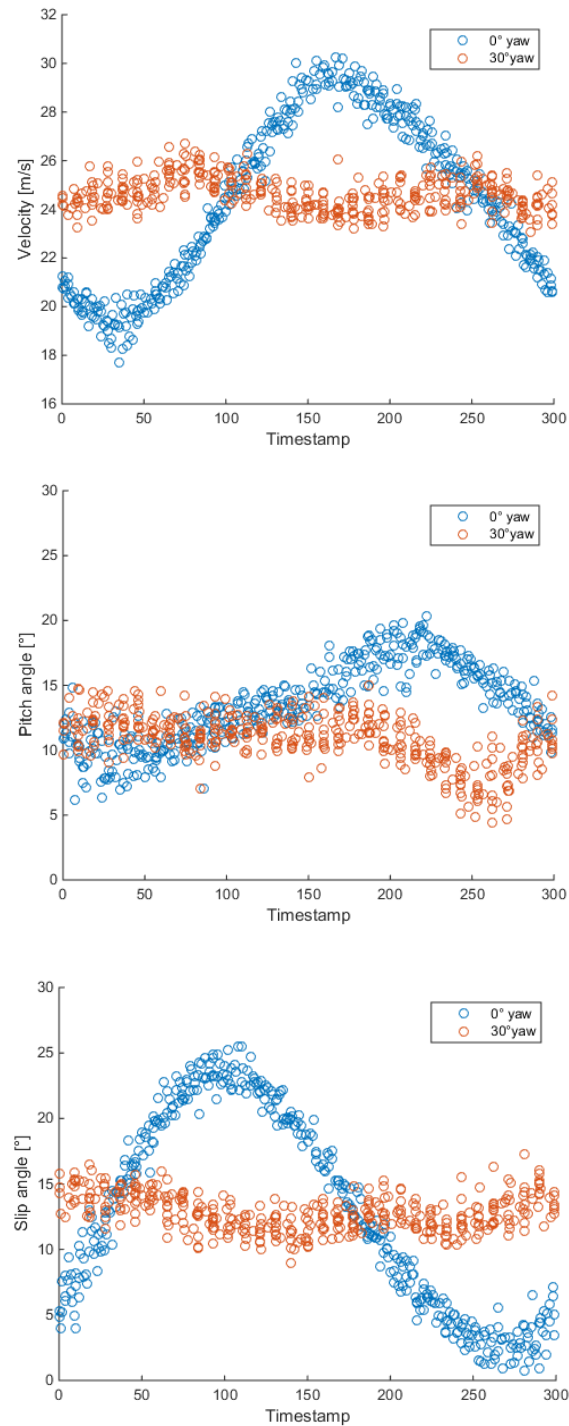
Figure 5.5 Scatter plot representing the variation of inflow velocity during one blade rotation (above), Scatter plot representing the variation of angle of attack during one blade rotation (middle), Scatter plot representing the variation of yaw angle during one blade rotation (top).

Data has then been subdivided in bins of 0.015 s (15 ms) each, based on the 0 to 300 ms timestamp, for a total of 20 bins for each rotation. Data that was contained in each bin has been averaged to be able to have a better visualization of how velocity, pitch angle and slip angle change. Figure 5.6 show the graphs obtained with this technique.
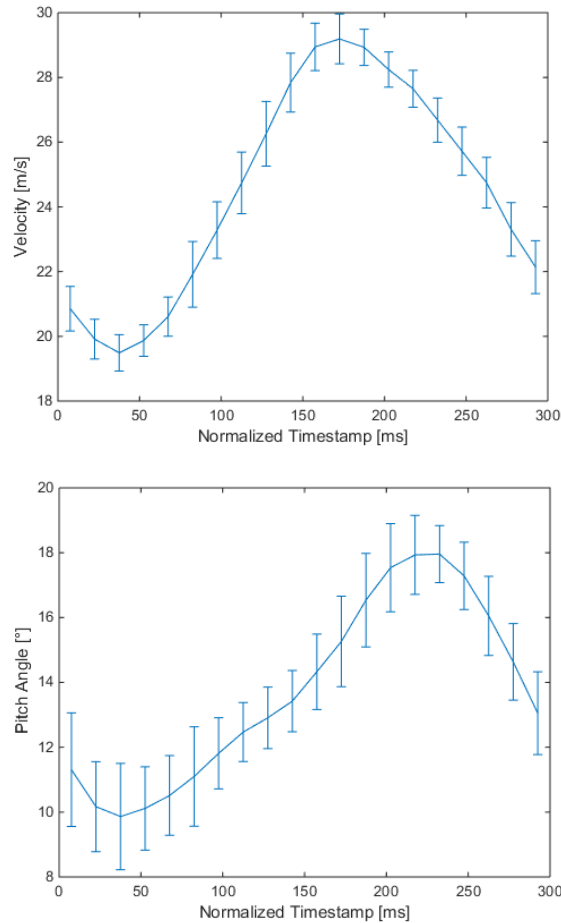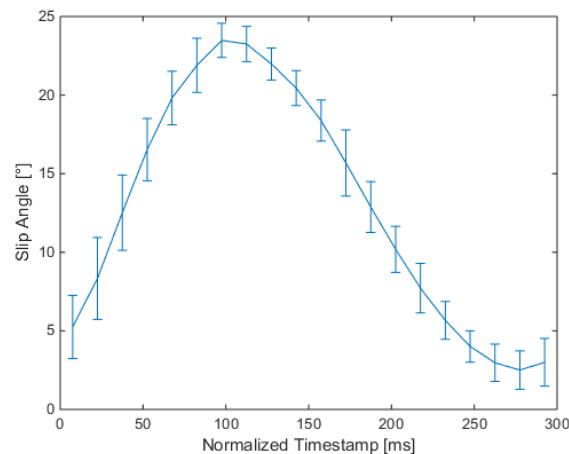
Figure 5.6 Plot representing the average variation and error bars of inflow velocity during one blade rotation (above), plot representing the average variation and error bars of angle of attack during one blade rotation (middle), plot representing the average variation and error bars of slip angle during one blade rotation (top).

From Figure 5.6 it is possible to identify the same behavior described by Maeda and Kawabuchi (6) and seen in Figure 5.2, is then possible to conclude that the five hole pressure probe setup is in working conditions and capable of determining local inflow characteristics to the test rig's blade.

5.2.5 Azimuthal angle prediction from data

Although it was not possible to record the blade's azimuth angle, using as a guide the work by Maeda and Kawabuchi (6) and making some simple reasoning on velocity triangle it is possible to make hypothesis on the azimuthal angle that corresponds to a particular velocity, pitch angle and slip angle situation.

Starting with the inflow velocity, knowing that the rotor is rotating in a clockwise direction, if observed from the front, and that the turbine's yaw angle is -30° (see **Errore. L'origine riferimento non è stata trovata.** for a reference), then it is possible to say that the blade is moving "towards" the wind when it is swiping the upper portion of the rotor, while it is moving "away" from the wind when it is in the bottom portion. Maximum relative wind speed happens when the tangential velocity of the blade is on the same plane as the undisturbed wind speed generated by the fan array. Therefore maximum inflow velocity point corresponds to the uppermost point reached by the blade during its rotation, 180° of azimuthal angle.

Pitch angle can be associated with azimuthal angle by thinking that when the blade sees a higher local inflow wind speed the angle of attack will be lower and vice-versa, this can be seen in Figure 5.7 showing two different velocity triangle, one with the blade moving toward the wind and another one with the blade moving

away from it. If observed carefully Figure 5.7 top, presents a lower angle of attack than Figure 5.7 bottom.
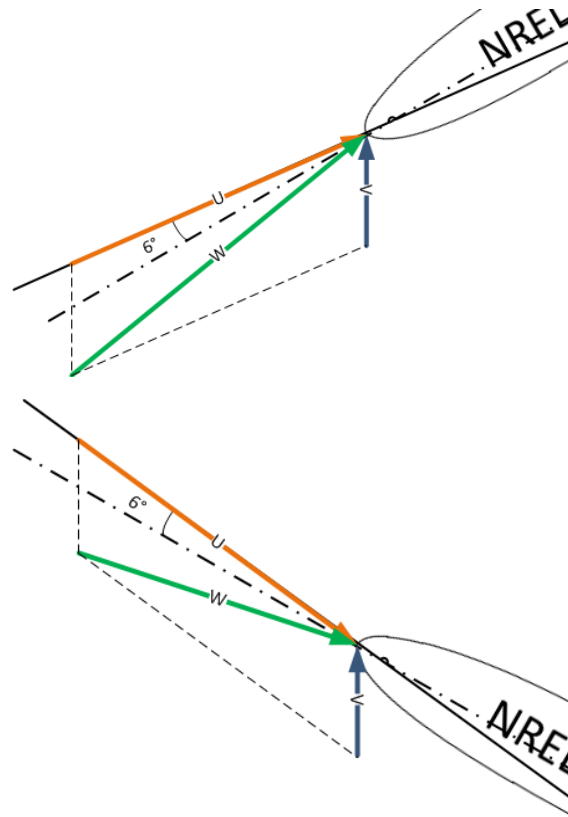
Figure 5.7 Velocity triangle for two different blade azimuthal locations, blade is moving towards the wind (top), blade is moving away from the wind (bottom).

Slip angle change can also be predicted, slip angle will be high when the blade is closest to be parallel to the wind direction, as the wind will be blown off the surface of the blade, in this case the slip angle is higher at 90° azimuth angle.

The above hypothesis find a confirmation in the work by Maeda and Kawabuchi (6). Velocity, pitch angle and slip angle change predictions during one rotor revolution as shown in Figure 5.8.
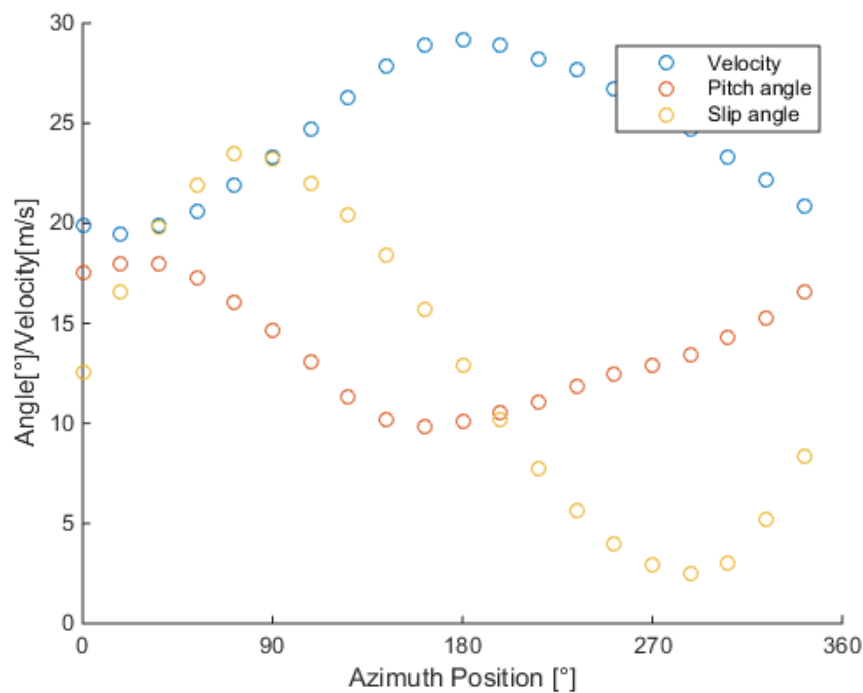
Figure 5.8 Velocity, pitch angle and slip angle prediction during one blade rotation.

5.3 Future developments

The five hole pressure probe and all the related instrumentation discussed in this work are only a part of a broader plan to have a test rig instrumented with a wide range of different instrumentations, and able to measure a number of fundamental parameters in order to understand the operation condition of a wind turbine in the field.

The installation of the five hole pressure probe will allow to extend this project in many directions. First fundamental step is to have the torque sensor working in order to be able to measure the blade position along with the generated torque, inflow conditions and other parameters

Once all the newly installed instrumentation will have successfully surpassed the testing and tuning phase, it will be possible to write LabView™ code that allows to collect loads on the blade and the turbine, generate torque and many other operational parameters (RPM, wind speed, etc…) along with the inflow characteristics collected with the five hole pressure. This will allow to make observations and try to correlate the different observed phenomena.

The next step to this wider data collection campaign will be to try to formulate and validate a model to predict loads and 3D flow phenomena on horizontal axis wind

turbine under yaw loads, this would be a great advance compared to the steady state and 2Dapproach employed to design wind turbines.

Conclusion

The scope of this thesis was to investigate the methodologies to use for the determination of local inflow characteristics to a small scale horizontal axis wind turbine. The applicability of five hole pressure probe for this kind of study has been assessed.

The importance of this study is related to the design stage of horizontal axis wind turbines. Those are generally designed with 2D steady approach. It has been however demonstrated, that inflow conditions around the turbine blades during field operation are highly 3D and unsteady. Sufficient field measurement is not available in order to create and validate new aerodynamics models to predict the effects of this 3D flow field on the turbine structure.

It is known that in field operation conditions a wind turbine operates for the majority of the time under yaw loads, a yaw load is any situation when the blade experiences a non-uniform inflow velocity and direction during its rotation. These are periodic loads and usually have a frequency that is the same as the rotation of the turbine's blade. Yaw loads must be kept into account during the design phase as the loads on the wind turbine structure can result to be very different than those estimated with 2D BEM methods. This is why large safety margins are usually adopted, meaning more material than what is actually necessary and therefore more expensive turbines.

There were two primary objectives to this thesis. First to study the five hole pressure probe as a solution for local inflow condition determination, successfully calibrating the instrument and assessing the best practices for the application of this apparatus to a small scale wind turbine. Second to design a new blade section along with the data acquisition system, install the five hole pressure probe on the wind turbine using this new section and test the correct functioning of the instrumentation.

Pressure probe calibration

Calibration of the five hole pressure probe has been successfully carried out in all its aspects.

In order to successfully perform this task a two axis traversing system has been designed and built, this allows to precisely traverse the probe on both pitch and yaw plane, while keeping the probe's tip in the same location throughout the whole calibration. To simplify the traversing of the probe and minimize the device's construction time it was chosen to manually move the probe in the yaw direction, while the probe's pitch was varied using a stepper motor automatically controlled by an Arduino microcontroller.

To accurately calibrate the pressure probe, considering the tight experimental schedule, some choices have been made about calibration conditions. As reported in literature (14) (11), Reynolds number has a small influence on the calibration of the probe, this influence can be minimized by performing the calibration at the expected Reynolds number that will be encountered during the actual employment of the probe, therefore calibration was performed at a unique Reynolds number (deriving from a calibration wind speed of 29 m/s). The probe has been traversed over a number of combinations of pitch and yaw angles included in the ±45° range, with steps between each calibration point of 5°, this forms a square matrix of calibration points to which the probe had to be moved, Figure 3.1. Due to the high turbulence present in the calibration wind tunnel a high number of samples had to be collected at each calibration position, this number was identified by studying the cumulative standard deviation of a 1000 pressure measurement samples, 400 was found to be the limit over which the standard deviation of the population of measurements tends to stabilize. The temporary setup of the calibration wind tunnel presented a 90° corner about 2.8 m upwind of its outlet, it was found during calibration that, due to this corner, the flow presented a 4° negative deviation from axiality, correction to this deviation in the flow has been applied during data post processing.

Calibration data was analyzed both numerically and visually, no anomalies have been found in it. The search for the most suitable method to interpolate the calibration data between each calibration point, led to cubic interpolation as the most precise and reliable method over direct linear interpolation and 4th order polynomials.

Three different data reduction methods, that implied the use of non dimensional pressure coefficients, have been taken into analysis. Experimental error analysis found that the multi-zone pressure coefficient approach gave the most accurate results over mono-zone pressure confidents and NREL pressure coefficients. This error has been quantified in 0.3° on pitch plane, 1° on the yaw plane (higher error due to manual traversing system) and 0.3% in velocity determination, Figure 3.22.

This approach presents two further advantages compared to the other two methods. First it allows to extend the measurable local inflow angles up to ±70° compared to the ±30° of the mono-zone method by excluding the hole on the lee side of the probe where flow separation occurs from the creation of the pressure coefficients.

Second, it doesn't need flow static pressure as the reference pressure for the five hole probe pressure readings retrieved with differential pressure transducers, as long as the scope is to measure velocity and the five pressure readings are referred to the same pressure level, any reference pressure is acceptable. This is a large improvement compared to the setup used in the NREL unsteady aerodynamic experiment (8), where a complex tubing system had to be developed to bring tunnel's static pressure level all the way to the rotor to be used as a reference.

Data Acquisition System

Application of a five hole pressure probe to a small scale wind turbine required to develop a customized data acquisition system. The main challenges to this task were the limited space on the wind turbine and the fact that no wired connection was available between the rotor and the main computer located in the wind tunnel control room. Both these challenges have been successfully overcome.

The unavailability of wired communication was solved with the choice of employing Bluetooth communication between the instrumentation installed on the turbine blade and the main computer. Bluetooth proved to be an adequate and relatively easy solution for wireless serial communication.

Space limitations have been solved by performing a selection of the smallest available pieces of equipment that satisfied the required accuracy characteristics. This resulted in a custom built data acquisition system of contained dimensions; 1.5 cm high, 7 cm wide and around 20 cm long. This equipment included 5 pressure transducers on a printed circuit board, an analog to digital converter chip, Arduino microcontroller, a built in power supply system based on a 9 V battery, micro SD for internal data storage and Bluetooth transreceiver to transmit the data to the main computer.

The exact same DAQ that has been employed for the five hole pressure probe calibration was also used to collect data after the instrument has been installed on the test rig, this choice has been made to improve the accuracy of the overall system.

Installation on the test rig

The instrumentation had then to be installed on the turbine's blade in order to be used for local inflow characterization. Thanks to the blade's modularity, only one of the five sections composing it had to be radically redesigned for this scope. This new section had to comply to a series of strict requirements.

The new blade section was designed in a way that the DAQ instrumentation contained inside it could be easily accessible in order to perform minor modifications or repairs. The interference with the airflow was minimized by fitting all the necessary instrumentation inside the blade section with the only exception of the five hole pressure probe whose tip has been placed one chord upwind of the blade's leading edge. The section was designed to be easy to install on the blade spar and not to interfere with the strain gauges measurement or damage them during installation.

A fundamental requirement for the new section was structural solidity, this has been achieved with and internal web of thin reinforcements and by providing the instrumentation access lid of three internal supports, those were also used to tightly join the access lid to the section's main body thanks to six screws accessible from the blade's pressure side, see Figure 4.11 and Figure 4.12.

Such a complex design could be possible only thanks to 3D printing, this proved to be the fastest and easiest prototyping technique for a model of such a high complexity.

The sole 3D printed new section was not strong enough to sustain the five hole pressure probe in an environment characterized by high centrifugal forces. The pressure probe was directly connected to the blade's spar with a custom designed clamp, see Figure 4.14. This inclines the probe 15° compared to the blade's chord, this is the nominal angle of attack at the location where the probe was installed (0.56 r/R, 0.956 m) with a wind speed of 8.5 m/s, the average wind speed that will be used during testing.

Probe testing

A series of test was conducted on the test rig in order to assess the correct functioning of the pressure probe system and how this responded to the harsh testing conditions.

First the influence of the centrifugal force and vibration on the pressure transducers has been assessed, it was found that, at 200 RPM, centrifugal force affects the pressure measurement by less than 1/1000 of the measurement itself,

while the test rig's increasing vibrations didn't show any clear effect on the standard deviation of the population of collected data. Since the reference pressure inlet for the differential pressure transducers is located in the hub, this is increased in level by the centrifugal force acting on the column of air in piping system. This effect has been quantified to be in the order on 210 Pa at 200 RPM and can slightly change due to air density and probe's radial position, this correction has been applied during data post processing that has been performed using MatLab™.

During this stage of the testing it was also important to assess the structural integrity of the newly designed blade section and the correct functioning of the DAQ system. No problems have been observed in the setup after running the first series of tests, pressures from the five hole pressure probe were measured and transmitted to the main computer via Bluetooth at a satisfying rate. Data acquisition on the main computer has been performed with LabView™, this was used to retrieve and time the pressure measurement along with the blade azimuthal position and, in prospective, it can be implemented to retrieve strain gauges readings as well as other measurements.

A second series of tests has then been conducted, its scope was to measure local inflow conditions with the turbine operating under yaw loads, this is the ultimate reason why the whole instrumentation has been designed and built. Results in yawed loads conditions have been comparatively evaluated to non yawed conditions. As expected the inflow measurement performed while the turbine was yawed showed a periodically oscillating inflow condition, the period of this oscillation was the same as the period of the rotor's rotation, see Figure 5.3. These oscillating measurements have been compared to the ones that were found in literature (6), and the same kind of results have been obtained.

It is therefore possible to conclude that the built instrumentation, comprising the five hole pressure probe, the DAQ, the new blade section and the code can successfully measure unsteady local inflow conditions to a wind turbine blade, therefore the initial objectives have been satisfactorily met.

Appendix A   Codes

MatLab code used for inferring inflow velocity vector with mono-zone approach:

```matlab
function [a] = fromPtoVectorOldPaper (Cal,Points)
    [m,n] = size(Points);
    a = (1:5);
    for i=1:m
        q = 1;
        Pmean = (Points(i,1) + Points(i,2) + Points(i,3) +
Points(i,4)) / 4;
        % pitch and yaw pressure coefficient
        Cpp = (Points(i,1) - Points(i,3))/(Points(i,5) - Pmean);
        Cpy = (Points(i,2) - Points(i,4))/(Points(i,5) - Pmean);
        aold = a;
        % functions to interpolate calibration data
        Yaw = griddata(Cal.Cpp,Cal.Cpy,Cal.Yaw,Cpp,Cpy,'cubic');
        Pitch = griddata(Cal.Cpp,Cal.Cpy,Cal.Pitch,Cpp,Cpy,'cubic');
        Cpt = griddata(Cal.Pitch,Cal.Yaw,Cal.Cpt,Pitch,Yaw,'cubic');
        Cps = griddata(Cal.Pitch,Cal.Yaw,Cal.Cps,Pitch,Yaw,'cubic');
        % estimate total and static pressures
        Ptot = Pref + Points(i,5) - Cpt * (Points(i,5) - Pmean);
        Pstat = Pref + Pmean - Cps * (Points(i,5) - Pmean);
        % velocity from total and static pressure
        v = sqrt(2*1.12*(Ptot-Pstat));
        % write results
        b = [v Ptot Pstat Pitch Yaw];
        a = [aold ; b];
    end
    a (1,:) = [];
end
```

MatLab code used for inferring inflow velocity vector with multi-zone approach:

```matlab
function [a] = fromPtoVectorZones (Cal,Points)
    [m,n] = size(Points);
    a = (1:6);
    for i=1:m
        aold = a;
        line5 = Points(i,1:5);
        % find maximum pressure hole
        [ma,p]=max(line5);
        toKeep = Cal.Max == p;
        CalZone = Cal(toKeep,:);
        % different PCs based on maximum pressure hole
        switch p
            case 5
                pMean = (line5(1)+line5(2)+line5(3)+line5(4))/4;
                den = line5(5)- pMean;
                Cpp = (line5(1)-line5(3))/den;
                Cpy = (line5(2)-line5(4))/den;
                Yaw =
griddata(CalZone.Cpp,CalZone.Cpy,CalZone.Yaw,Cpp,Cpy,'cubic');
                Pitch =
griddata(CalZone.Cpp,CalZone.Cpy,CalZone.Pitch,Cpp,Cpy,'cubic');
                Cpt =
griddata(CalZone.Pitch,CalZone.Yaw,CalZone.Cpt,Pitch,Yaw,'cubic');
                Cps =
griddata(CalZone.Pitch,CalZone.Yaw,CalZone.Cps,Pitch,Yaw,'cubic');
                Ptot = line5(5) - den*Cpt;
                Pstat = pMean - den*Cps;
            case 1
                pMean = (line5(2)+line5(5)+line5(4))/3;
                den = line5(1)- pMean;
                Cpp = (line5(1)-line5(5))/den;
                Cpy = (line5(2)-line5(4))/den;
                Yaw =
griddata(CalZone.Cpp,CalZone.Cpy,CalZone.Yaw,Cpp,Cpy,'cubic');
                Pitch =
griddata(CalZone.Cpp,CalZone.Cpy,CalZone.Pitch,Cpp,Cpy,'cubic');
                Cpt =
griddata(CalZone.Pitch,CalZone.Yaw,CalZone.Cpt,Pitch,Yaw,'cubic');
                Cps =
griddata(CalZone.Pitch,CalZone.Yaw,CalZone.Cps,Pitch,Yaw,'cubic');
                Ptot = line5(1) - den*Cpt;
                Pstat = pMean - den*Cps;
            case 2
                pMean = (line5(1)+line5(5)+line5(3))/3;
                den = line5(2)- pMean;
                Cpp = (line5(1)-line5(3))/den;
                Cpy = (line5(2)-line5(5))/den;
                Yaw =
griddata(CalZone.Cpp,CalZone.Cpy,CalZone.Yaw,Cpp,Cpy,'cubic');
                Pitch =
griddata(CalZone.Cpp,CalZone.Cpy,CalZone.Pitch,Cpp,Cpy,'cubic');
                Cpt =
griddata(CalZone.Pitch,CalZone.Yaw,CalZone.Cpt,Pitch,Yaw,'cubic');
                Cps =
griddata(CalZone.Pitch,CalZone.Yaw,CalZone.Cps,Pitch,Yaw,'cubic');
```

```matlab
                Ptot = line5(2) - den*Cpt;
                Pstat = pMean - den*Cps;
            case 3
                pMean = (line5(2)+line5(5)+line5(4))/3;
                den = line5(3)- pMean;
                Cpp = (line5(5)-line5(3))/den;
                Cpy = (line5(2)-line5(4))/den;
                Yaw =
griddata(CalZone.Cpp,CalZone.Cpy,CalZone.Yaw,Cpp,Cpy,'cubic');
                Pitch =
griddata(CalZone.Cpp,CalZone.Cpy,CalZone.Pitch,Cpp,Cpy,'cubic');
                Cpt =
griddata(CalZone.Pitch,CalZone.Yaw,CalZone.Cpt,Pitch,Yaw,'cubic');
                Cps =
griddata(CalZone.Pitch,CalZone.Yaw,CalZone.Cps,Pitch,Yaw,'cubic');
                Ptot = line5(3) - den*Cpt;
                Pstat = pMean - den*Cps;
            case 4
                pMean = (line5(1)+line5(5)+line5(3))/3;
                den = line5(4)- pMean;
                Cpp = (line5(1)-line5(3))/den;
                Cpy = (line5(5)-line5(4))/den;
                Yaw =
griddata(CalZone.Cpp,CalZone.Cpy,CalZone.Yaw,Cpp,Cpy,'cubic');
                Pitch =
griddata(CalZone.Cpp,CalZone.Cpy,CalZone.Pitch,Cpp,Cpy,'cubic');
                Cpt =
griddata(CalZone.Pitch,CalZone.Yaw,CalZone.Cpt,Pitch,Yaw,'cubic');
                Cps =
griddata(CalZone.Pitch,CalZone.Yaw,CalZone.Cps,Pitch,Yaw,'cubic');
                Ptot = line5(4) - den*Cpt;
                Pstat = pMean - den*Cps;
        end
        V = sqrt(2*1.12*(Ptot-Pstat));
        b = [V Ptot Pstat Pitch Yaw p];
        a = [aold ; b];
    end
    a (1,:) = [];
end
```

MatLab code used for inferring inflow velocity vector with NREL approach:

```matlab
function [a] = fromPtoVectorNREL (Cal,Points)
    [m,n] = size(Points);
    a = (1:5);
    for i=1:m
        aold = a;
        % initiate variables to check the error
        e=1;
        j=1;
        % first assumptions
        q=max(Points(i,:));
        Cpc = 1;
        % iterative process
        while j<100 || e<0.01
            Cpcold = Cpc;
            DCpp = (Points(i,1) - Points(i,3))/q;
            DCpy = (Points(i,2) - Points(i,4))/q;
            Cpcnew =
griddata(Cal.Cpp,Cal.Cpy,Cal.Cpc,DCpp,DCpy,'cubic');
            DCpc = Cpc-Cpcnew;
            Cpc = Cpc - (1/(2+j))*DCpc;
            q = Points(i,5)/Cpc;
            j = j + 1;
            e = abs(Cpcold - Cpc);
        end
        % find yaw, pitch and velocity from DCpp DCPy and q
        Yaw = griddata(Cal.Cpp,Cal.Cpy,Cal.Yaw,DCpp,DCpy);
        Pitch = griddata(Cal.Cpp,Cal.Cpy,Cal.Pitch,DCpp,DCpy);
        v = sqrt(2*1.12*(q));
        b = [v q Pitch Yaw j];
        a = [aold ; b];
    end
    a (1,:) = [];
end
```

Arduino code used to read pressure on the test rig:

```
//include SPI communication library
#include <SPI.h>
//pins for ADC shield
#define BUSY 3
#define RESET 4
#define START_CONVERSION 5
#define SHcs 10
//other variables
#define TOTAL_RAW_BYTES RESOLUTION
#define RESOLUTION 16
#define SCALE_FACTOR 0.000152587890625
int bytesToRead = TOTAL_RAW_BYTES;
byte raw[TOTAL_RAW_BYTES];
signed long parsed[8];
//variables shared in interrupts routines
volatile boolean flag = false;
//counters
int i;
int cn = 0;
//interrupt service routine
void Reading(){
  flag = true;
}
void setup() {
  //initializing Arduino pins
  pinMode(BUSY, INPUT);
  pinMode(RESET, OUTPUT);
  pinMode(START_CONVERSION, OUTPUT);
  pinMode(SHcs,OUTPUT);
  //initialize serial and SPI communication
  SPI.begin();
  Serial.begin(115200);
  //initialize and reset ADC
  digitalWrite(START_CONVERSION, HIGH);
  digitalWrite(SHcs, HIGH);
  digitalWrite(RESET, HIGH);
  delay(1);
  digitalWrite(RESET, LOW);
  // interrupt used to trigger the measurement
  attachInterrupt(0, Reading, LOW);
}
void loop() {
  //only if the flag has been turned to true by the interrupt
  if (flag == true)
  {
    flag = false;
    //start ADC conversion
    digitalWrite(START_CONVERSION, LOW);
```

```
    delayMicroseconds(10);
    digitalWrite(START_CONVERSION, HIGH);
    while (digitalRead(BUSY) == HIGH) {
    }
    //communicate data with SPI
    digitalWrite(SHcs, LOW);
    while (bytesToRead > 0) {
      raw[TOTAL_RAW_BYTES - bytesToRead] = SPI.transfer(0x00);
      bytesToRead--;
    }
    digitalWrite(SHcs, HIGH);
    //convert binary data to decimal
    bytesToRead = TOTAL_RAW_BYTES;
    parsed[0] = (raw[0] << 8) + (raw[1] >> 0);
    parsed[1] = (raw[2] << 8) + (raw[3] >> 0);
    parsed[2] = (raw[4] << 8) + (raw[5] >> 0);
    parsed[3] = (raw[6] << 8) + (raw[7] >> 0);
    parsed[4] = (raw[8] << 8) + (raw[9] >> 0);
    parsed[5] = (raw[10] << 8) + (raw[11] >> 0);
    parsed[6] = (raw[12] << 8) + (raw[13] >> 0);
    parsed[7] = (raw[14] << 8) + (raw[15] >> 0);
    for(i=0; i<8; i++) {
      if(parsed[i] & 0x8000) { // if reading is < 0 (stored as two's
complement)
          parsed[i] = parsed[i] | 0xFFFF0000; // set bits 31-16
      } else {
          parsed[i] = parsed[i];
      }
    }
    //send data via Bluetooth
    Serial.print(cn);
    Serial.print(",");
    Serial.print((float)parsed[1] * SCALE_FACTOR * 1000, 5);
    Serial.print(",");
    Serial.print((float)parsed[2] * SCALE_FACTOR * 1000, 5);
    Serial.print(",");
    Serial.print((float)parsed[3] * SCALE_FACTOR * 1000, 5);
    Serial.print(",");
    Serial.print((float)parsed[4] * SCALE_FACTOR * 1000, 5);
    Serial.print(",");
    Serial.print((float)parsed[5] * SCALE_FACTOR * 1000, 5);
    Serial.print(",");
    Serial.println((float)parsed[6] * SCALE_FACTOR * 1000, 5);
    cn = cn + 1;
  }
}
```

LabView block diagram of the code used to read the blade azimuthal position and trigger pressure measurement:

List of figures

List of tables

Nomenclature

v	Free stream wind velocity [m/s]
p	Pressure [Pa]
g	Gravity acceleration constant [9.81 m/s^2]
ρ	Density [kg/m^3]
z	Elevation [m]
u	Rotor tangential velocity [m/s]
w	Relative velocity [m/s]
p_r	Reference pressure [Pa]
P_T	Total pressure [Pa]
P_S	Static pressure [Pa]
P_{cent}	Centrifugal force pressure [Pa]
ω	Angular velocity [rad/s]
RPM	Revolutions per minute [rev/min]
R	Rotor radius [m]
r	Local rotor radius [m]
α	Angle of attack [°]
β	Twist angle [°]
ϕ	Turbine yaw angle [°]
ψ	Blade azimuth angle [°]

Acronyms

2D	Two-dimensional
3D	Three-dimensional
HAWT	Horizontal Axis Wind Turbine
MHP	Multi Hole Pressure Probe
FHP	Five Hole Pressure Probe
NREL	National Renewable Energy Lab
VFD	Variable Frequency Drive
DAQ	Data Acquisition System
Cpc	Center Hole Pressure Coefficient
Cpp	Pitch Pressure Coefficient
Cpy	Yaw Pressure Coefficient
Cpt	Total Pressure Coefficient
Cps	Static Hole Pressure Coefficient
SPI	Serial Peripheral Interface
ADC	Analog to Digital Converter
DC	Direct Current
IDE	Integrated Development Environment
SD	Standard Deviation

Bibliography

1. **Kobra, Gharali and Johnson, David A.** Effects of nonuniform incident velocity on a dynamic wind turbine airfoil. *Wind Energy.* 2014.

2. **IEA.** *Key World Energy Statistics.* Paris : IEA, 2013.

3. **BP.** *BP Energy Outlook 2035.* s.l. : BP, 2014.

4. **IRENA.** *Renewable energy technologies: cost analysis seres, Wind Power.* Abu Dhabi : IRENA, 2012.

5. **Government, Texas.** Wind Energy. *energyeducation.tx.gov.* [Online] http://www.energyeducation.tx.gov/renewables/section_4/topics/windmills_or_t urbines/e.html.

6. **Takao, Maeda and Kawabuchi, Hideyuki.** Surface Pressure Measurement on a Rotating Blade of Field Horizontal Axis Wind Turbine in Yawed Condition. *JSME International Journal.* B, 2005, Vol. 48, 1.

7. **Riso DTU.** *The DAN-AERO MW Experiments Final report.* Roskilde : Riso DTU, 2011.

8. **Hand, M.M., et al.** *Unsteady Aerodynamics Experiment Phase VI: Wind Tunnel Test Configuration and Available Data Campaigns.* Golden : NREL, 2001.

9. **Demetri, Telionis, Yihong, Yang and Othon, Rediniotis.** *Recent Developments in Multi-Hole Probe (MHP) Technology .* Gramado, BR : ABCM, 2009.

10. **G.L., Morrison, M.T., Schobeiri and K.R., Pappu.** Five-hole pressure probe analysis technique. *Flow Measurement and Instrumentation.* 1998, Vol. 9.

11. **A.L., Treaster and A.M., Yocum.** *The calibration and application of five hole probes.* s.l. : The Pennsylvania State University, 1978.

12. **Dudzinsky, Thomas J. and Krause, Lloyd N.** *Flow direction measuremnt with fixed-position probes.* Washington D. C. : NASA, 1969.

13. **L.J., Fingersh and M.C., Robinson.** *Wind Tunnel Calibration of 5-Hole pressure Probes for Application to Wind Turbines.* Golden, Colorado : NREL, 1997.

14. *Modeling, calibration, and error analysis of seven-hole pressure probes.* **Zillac, G. G.** 1993, Vol. 14.

15. **Gallington, R. W.** *Measurement of very larg flow angles with non-nulling seven-hole probes.* s.l. : Aeronautical digest, 1980.

16. **James D., Crawford.** *Design and calibration of seven hole probes for flow measurement.* Kingston, CA : Queen's University, 2011.

17. **Gerner, A.A., Maurer, C.L. and Gallington, R.W.** Non-Nulling Seven Hole Probes for High. *Non-Nulling Seven Hole Probes for High .* 1984, Vol. 2, 2.

18. **honeywell.** product page. *honeywell.com.* [Online] honeywell, 2014. http://sensing.honeywell.com/product-page?pr_id=141997.

19. **Devices, Analog.** AD7606 datasheet. *analog.com.* [Online] Analog Devices, 2012. http://www.analog.com/en/analog-to-digital-converters/ad-converters/ad7606/products/product.html.

20. **M.C., Gameiro Silva, C.A.C., Pereira and Cruz, J.M.S.** On the use of a linear interpolation method in the measurement procedure of a seven-hole pressure probe. *Experimental Thermal and Fluid Science.* 2003, 28.

21. **D. A., Johnson, A., Abdelrahman and D., Gertz.** Experimental Indirect Determination of Wind . *Wind Energy.* 2012, Vol. 36, 6.

22. **B., Gaunt and D. A., Johnson.** Wind turbine performance in controlled conditions: Experimental . *Int. J. Green Energy.* 2012.

23. **Ahmed, Abdelrahman.** *Development of a Wind Turbine Test Rig and Rotor for Trailing Edge Flap Investigation.* Waterloo, CA : University of Waterloo, 2014.

24. **M. K., Mcwilliam.** *Development of a Wind Tunnel Test Apparatus for Horizontal Axis Wind.* Waterloo, CA : University of Waterloo, 2008.

25. **Futek.** Futek TRS605. *futek.com.* [Online] http://www.futek.com/product.aspx?t=torque&m=trs605.

26. **NREL.** s833 airfoil. *wind.nerel.gov.* [Online] 2014. https://wind.nrel.gov/airfoils/Shapes/S833_Shape.html.

27. **D.T., Pham and R.S., Gault.** A comparison of rapid prototyping technologies. *Int. J. Mach. Tools Manufacture.* 1998, Vol. 38.

28. **Ltd., Stratasys.** Fortus 360mc Versatile machine. Durable parts. *Stratasys.com.* [Online] 2014. http://www.stratasys.com/3d-printers/production-series/fortus-360mc#content-slider-1.

29. **Instrument, National.** NI PCI-6251. *sine.ni.com.* [Online] 2013. http://sine.ni.com/nips/cds/view/p/lang/en/nid/14124.

30. *A novel calibration algorithm for five-hole pressure probe.* **Paul, Akshoy Ranjan, Upadhyay, Ravi Ranjan and Jain, Anuj.** 2, s.l. : MultiCraft, 2011, Vol. 3.